AD-A081 394 TEESSIDE POLYTECHNIC MIDDLESBROUGH (ENGLAND) DEPT O--ETC F/G 13/10
DETERMINATION OF SURFACE FRICTION COEFFICIENT OF A REPLICA OF S--ETC(U)
APR 79 D C AUGUSTSON N00014-78-G-0059

UNCLASSIFIED NL

1 OF 3
AD
A081 394

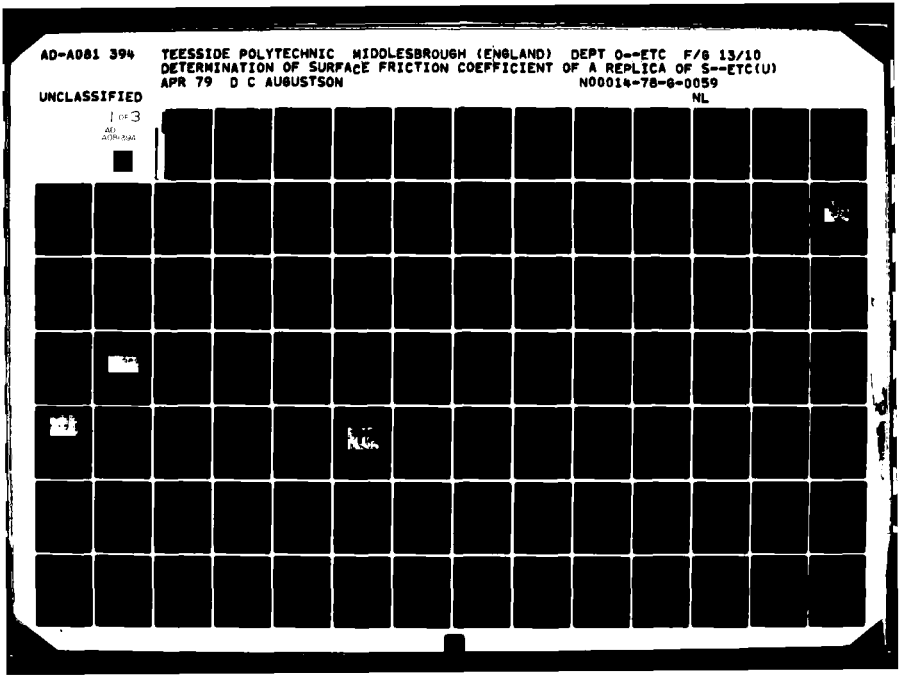

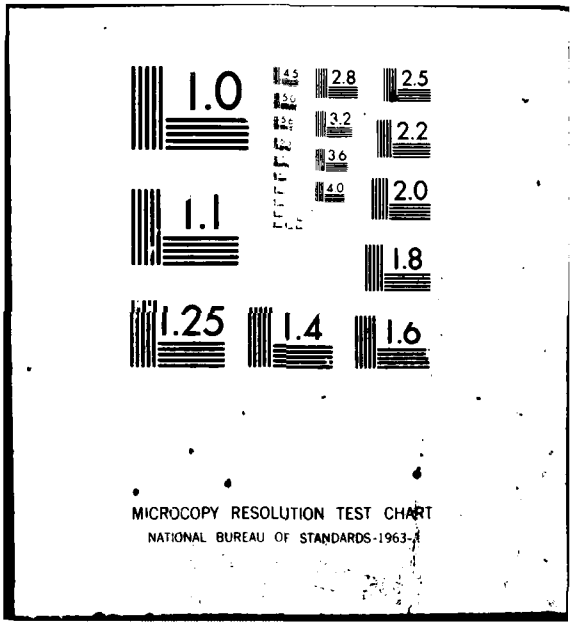
1.0
1.1
1.25
1.4
1.6
1.8
2.0
2.2
2.5
2.8
3.2
3.6
4.0
MICROCOPY RESOLUTION TEST CHART
NATIONAL BUREAU OF STANDARDS-1963-A

TEESSIDE POLYTECHNIC

DETERMINATION OF SURFACE FRICTION COEFFICIENT OF A REPLICA OF SHIPS-PLATE FROM BOUNDARY LAYER ANALYSIS IN AN OPEN CHANNEL

DAVID CHARLES AUGUSTSON

THIS PROJECT IS SUBMITTED AS PART OF THE FINAL YEAR REQUIREMENT FOR A B.Sc. HONOURS DEGREE IN MECHANICAL ENGINEERING

DEPT., MECHANICAL ENGINEERING

APRIL 1979

REPORT DOCUMENTATION PAGE

READ INSTRUCTIONS BEFORE COMPLETING FORM

1. REPORT NUMBER	2. GOVT ACCESSION NO.	3. RECIPIENT'S CATALOG NUMBER

4. TITLE *(and Subtitle)*

Surface friction coefficient of a ship's plate replica

See title of title page

5. TYPE OF REPORT & PERIOD COVERED

Interim Oct 1978-Apr 1979

6. PERFORMING ORG. REPORT NUMBER

7. AUTHOR(s)

D.C. Augustson

8. CONTRACT OR GRANT NUMBER(s)

N00014-78-G-0059

9. PERFORMING ORGANIZATION NAME AND ADDRESS

Department of Mechanical Engineering
Teesside Polytechnic
Middlesbrough ~~TS1 3BA U.K.~~ C.E.

10. PROGRAM ELEMENT, PROJECT, TASK AREA & WORK UNIT NUMBERS

NR 067-629

11. CONTROLLING OFFICE NAME AND ADDRESS

12. REPORT DATE

13. NUMBER OF PAGES

14. MONITORING AGENCY NAME & ADDRESS *(if different from Controlling Office)*

15. SECURITY CLASS. *(of this report)*

unclassified

15a. DECLASSIFICATION/DOWNGRADING SCHEDULE

16. DISTRIBUTION STATEMENT *(of this Report)*

Published

17. DISTRIBUTION STATEMENT *(of the abstract entered in Block 20, if different from Report)*

Approved for public release; distribution unlimi

18. SUPPLEMENTARY NOTES

Dissertation

19. KEY WORDS *(Continue on reverse side if necessary and identify by block number)*

surface friction; Prandtl law; boundary layer; replication; flow channel; friction plane; velocity profile; laser Doppler anemometry

20. ABSTRACT *(Continue on reverse side if necessary and identify by block number)*

One of the major problems in obtaining the surface friction coefficie[nt] is that accurate velocity measurements must be obtained in the boundary layer. There are several methods of achieving this and it is hoped that the following will give the reader a better understanding as to the applications and disadvantages of these techniques.

Continued over

One of the more modern approaches for evaluating the surface friction coefficient is use of the logarithmic inner law which has been used in, and the results verified, using the Prandtl power law technique.

INSTRUCTIONS FOR PREPARATION OF REPORT DOCUMENTATION PAGE

RESPONSIBILITY. The controlling DoD office will be responsible for completion of the Report Documentation Page, DD Form 1473, in all technical reports prepared by or for DoD organizations.

CLASSIFICATION. Since this Report Documentation Page, DD Form 1473, is used in preparing announcements, bibliographies, and data banks, it should be unclassified if possible. If a classification is required, identify the classified items on the page by the appropriate symbol.

COMPLETION GUIDE

General. Make Blocks 1, 4, 5, 6, 7, 11, 13, 15, and 16 agree with the corresponding information on the report cover. Leave Blocks 2 and 3 blank.

Block 1. Report Number. Enter the unique alphanumeric report number shown on the cover.

Block 2. Government Accession No. Leave Blank. This space is for use by the Defense Documentation Center.

Block 3. Recipient's Catalog Number. Leave blank. This space is for the use of the report recipient to assist in future retrieval of the document.

Block 4. Title and Subtitle. Enter the title in all capital letters exactly as it appears on the publication. Titles should be unclassified whenever possible. Write out the English equivalent for Greek letters and mathematical symbols in the title *(see "Abstracting Scientific and Technical Reports of Defense-sponsored RDT/E," AD-667 000)*. If the report has a subtitle, this subtitle should follow the main title, be separated by a comma or semicolon if appropriate, and be initially capitalized. If a publication has title in a foreign language, translate the title into English and follow the English translation with the title in the original language. Make every effort to simplify the title before publication.

Block 5. Type of Report and Period Covered. Indicate here whether report is interim, final, etc., and, if applicable, inclusi dates of period covered, such as the life of a contract covered in a final contractor report.

Block 6. Performing Organization Report Number. Only numbers other than the official report number shown in Block 1, such as series numbers for in-house reports or a contractor/grantee number assigned by him, will be placed in this space. If no such numb are used, leave this space blank.

Block 7. Author*(s)*. Include corresponding information from the report cover. Give the name*(s)* of the author*(s)* in convention orde: *(for example, John R. Doe or, if author prefers, J. Robert Doe)*. In addition, list the affiliation of an author if it differs from tha of the performing organization.

Block 8. Contract or Grant Number*(s)*. For a contractor or grantee report, enter the complete contract or grant number*(s)* unde which the work reported was accomplished. Leave blank in in-house reports.

Block 9. Performing Organization Name and Address. For in-house reports enter the name and address, including office symt of the performing activity. For contractor or grantee reports enter the name and address of the contractor or grantee who prepared the report and identify the appropriate corporate division, school, laboratory, etc., of the author. List city, state, and ZIP Code.

Block 10. Program Element, Project, Task Area, and Work Unit Numbers. Enter here the number code from the applicable Department of Defense form, such as the DD Form 1498, "Research and Technology Work Unit Summary" or the DD Form 1634, "Research and Development Planning Summary," which identifies the program element, project, task area, and work unit or equivale under which the work was authorized.

Block 11. Controlling Office Name and Address. Enter the full, official name and address, including office symbol, of the controlling office. *(Equates to funding/sponsoring agency. For definition see DoD Directive 5200.20, "Distribution Statements on Technical Documents.")*

Block 12. Report Date. Enter here the day, month, and year or month and year as shown on the cover.

Block 13. Number of Pages. Enter the total number of pages.

Block 14. Monitoring Agency Name and Address *(if different from Controlling Office)*. For use when the controlling or fundin office does not directly administer a project, contract, or grant, but delegates the administrative responsibility to another organization

Blocks 15 & 15a. Security Classification of the Report: Declassification/Downgrading Schedule of the Report. Enter in 15 the highest classification of the report. If appropriate, enter in 15a the declassification/downgrading schedule of the report, using the abbreviations for declassification/downgrading schedules listed in paragraph 4-207 of DoD 5200.1-R.

Block 16. Distribution Statement of the Report. Insert here the applicable distribution statement of the report from DoD Directive 5200.20, "Distribution Statements on Technical Documents."

Block 17. Distribution Statement *(of the abstract entered in Block 20, if different from the distribution statement of the report)*. Insert here the applicable distribution statement of the abstract from DoD Directive 5200.20, "Distribution Statements on Technical Do uments."

Block 18. Supplementary Notes. Enter information not included elsewhere but useful, such as: Prepared in cooperation with . . . Translation of *(or by)* . . . Presented at conference of . . . To be published in . . .

Block 19. Key Words. Select terms or short phrases that identify the principal subjects covered in the report, and are sufficiently specific and precise to be used as index entries for cataloging, conforming to standard terminology. The DoD "Thesaurus of Engineering and Scientific Terms" *(TEST)*, AD-672 000, can be helpful.

Block 20. Abstract. The abstract should be a brief *(not to exceed 200 words)* factual summary of the most significant informa- tion contained in the report. If possible, the abstract of a classified report should be unclassified and the abstract to an unclassified report should consist of publicly- releasable information. If the report contains a significant bibliography or literature survey, mention it here. For information on preparing abstracts see "Abstracting Scientific and Technical Reports of Defense-Sponsored RDT&E," AD-667 000.

TEESSIDE POLYTECHNIC

(6)

DETERMINATION OF SURFACE FRICTION COEFFICIENT OF A REPLICA OF SHIPS-PLATE FROM BOUNDARY LAYER ANALYSIS IN AN OPEN CHANNEL.

(9) Interim rept. Oct 78-Apr 79

(10) DAVID CHARLES AUGUSTSON

THIS PROJECT IS SUBMITTED AS PART OF THE FINAL YEAR REQUIREMENT FOR A B.Sc. HONOURS DEGREE IN MECHANICAL ENGINEERING

(15) N0014-78-G-0059

(12) 233

DEPT., MECHANICAL ENGINEERING

(11) APR 79

New

411 062

A

CONTENTS

INDEX TO PLATES

INDEX TO GRAPHS

INDEX TO TABLES

Acknowledgement.

The author wishes to extend his sincere and grateful thanks to his supervisor, Mr. S.T.Olszowski, for his help and guidance during the course of this project.

Also his thanks go to workshop technicians, Mr. J. Goodman and Mr. K. Huckle, for their help in the laboratory.

Finally, he cannot thank enough his wife, Barbara, for typing the original, hand written script, and for being a source of encouragement over the preceding years.

Summary.

One of the major problems in obtaining the surface friction coefficient is that accurate velocity measurements must be obtained in the boundary layer. There are several methods of achieving this and it is hoped that the following will give the reader a better understanding as to the applications and disadvantages of these techniques.

One of the more modern approaches for evaluating the surface friction coefficient is use of the logarithmic inner law which has been used in, and the results verified, using the Prandtl power law technique.

LIST OF SYMBOLS

English symbols.

a	overheating ratio Eq.(4.1); intercept Eq.(4.5).
A	outer law constant Eq.(8.26); distance of laser beams outside glass.
b	slope Eq.(4.5); thickness of glass channel sides.
B	inner law constant Eq.(8.25); distance of laser beams inside glass.
C	velocity of light Eq.(5.5).
$\hat{e}$	unit vector.
E	voltage.
f	frequency Eq.(5.4).
g	gravitational acceleration; function value.
G	form factor.
h	mean depth of flow.
H	shape factor δ^*/θ.
i	angle Eq.(7.1).
I	current.
k	average roughness height.
K	constant in Eq.(3.1); Von Karmens Constant; constant in Eq.(5.3).
l	length; dia of calibration tube; mixing length Eq.(8.19).
n	refractive index; variable in Eq.(3.1); Eq.(4.5); Eq.(4.7); power Eq.(8.12).

r	angle Eq.(7.1).
R	resistance.
t	time constant.
u	velocity within boundary layer.
$\bar{u}$	velocity vector.
u_*	friction velocity $\sqrt{\tau_0/\rho}$ Eq.(8.14).
u^+	u/u_* Eq.(8.31).
U	freestream velocity.
U^+	U/u_* Eq.(8.33).
v	mean velocity.
v_a	average velocity.
$\bar{v}$	velocity vector.
V	voltage; velocity vector.
W(%)	wake function Eq.(8.34); Eq.(8.36).
X	variable.
y	distance from surface.
y^+	yu_*/ν Eq.(8.32).
Y	variable.

Greek symbols.

β	Clausers parameter Eq.(8.28).
δ	boundary layer thickness.
δ^*	displacement thickness Eq.(8.4).
Δ	constant in Eq.(3.1); defect thickness Eq.(8.29).
θ	angle; momentum thickness Eq.(8.6).
λ	wavelength; local skin friction.
μ	absolute viscosity.
ν	kinematic viscosity. μ/ρ
π	3.1415927
Π	Coles wake parameter.
ρ	density.
τ	shear stress.
ω	angular frequency.

Dimensionless groups.

C_f	skin-friction coefficient.
F_r	Froude number Eq.(2.1.4).
R_e	Reynolds number Eq.(4.3).
R_{e_θ}	Reynolds number Eq.(8.10).

Subscripts.

∞	far field.
f	friction.
o	wall.
t	turbulent.
i	incident.
s	scattered.
D	Doppler frequency.

PRELIMINARY OUTLINE AND SURFACE REPLICA.

1.1 Introduction.

The aim of this project is to compare and critically analize the methods of deriving the surface friction coefficient of a replica of a badly corroded ships plate. The particular replica is attached to the bottom of a 20m flow channel which can simulate various flow situations.

The surface friction coefficient is obtained from the velocity profiles and use of analytical expressions. Boundary layer hot film anemometer probes were used for obtaining velocity profiles and the accuracy and reliability of such measurements were to be checked using a Laser Doppler Anemometer.

It is unfortunate that due to a delay outside the author's control that the Laser Doppler equipment was not obtained until March 1979 which will account for the results from the LDA being rather scanty.

The use of the LDA and HFA has the backing of SRC and also of the U.S.Navy.

Further investigation using LDA equipment is envisaged as a research project sponsored by the U.S.Navy, B.S.R.A. and Shell Research Co.

1.2 Replica of Ships Hull.

The replica of the ships hull was supplied by Shell Research Co. It is approximately 6.1 metres long by 30.5cm wide. Initially a polystyrene negative was cast on the side of a tanker which has been in continuous service for 25 years.

As is customary with the Shell tanker fleet, the ship has been dry-docked every three years and the hull shot-blasted and repainted at such regular intervals. The negative was taken after dry-docking but before any treatment was applied other than hosing down with clean water to remove slime.

The negative was then brought into the laboratory and a frame made the width of the channel. The negative was placed horizontally in the frame and a cast made from the negative in an Epoxy resin, care was needed so that the pouring of the resin did not in any way damage the surface profile on the negative.

Once the cast was dry the replica was removed from the mould. After the negative was removed, some imperfections in the casting were revealed, mainly at the edges. These were made good with glass-fibre resin after the replica was placed in the flow channel.

1.3 Installation of cast replica in the Channel.

The cast replica is approximately 25mm thick and therefore to eleminate any disturbing effects caused by the abrupt rise in the channel floor, an aluminium ramp was installed. Also to eliminate any effects from the end condition a similar ramp was attached at the rear of the model.

The model was now sealed along its edges using a plumber paste so as to obviate any disturbances caused by water passing between the edges of the model and the glass sides of the channel or the occasional liberation of trapped air bubbles.

This method of sealing also held the model in place on the bottom of the flow channel.

After carrying out certain flow tests over the model it was found that the initial method of securring the model to the base of the channel was totally unsatisfactory. This was due to the fact that even at moderate flow velocities of the order of 0.5m/s the model would be parted from the base due to the combined buoyancy effects and the viscous drag caused by the flowing medium. Once the model raised even slightly above the channel base the flowing stream lifted the model plate when the

dynamic force exceeded its apparent weight. Therefore a more secure method had to be employed.

The next method used was to wedge the model between the glass sides of the channel. Small wedges in hardwood were made, and this, for a time proved very successful. However, this method after a period of time again proved unsatisfactory, and it was therefore decided to bolt the model to the channel base. It should be remembered that the first two methods used were done so as to

a) not provide any obstructions to the flow so as to cause an interuption on the surface, and,

b) not to damage the surface profile in any way whatsoever.

For the third and final method it was decided to bolt the model to the base using 6-$\frac{1}{4}$inch BSF countersunk bolts spaced out and placed in areas where the surface was fairly smooth. See figs. 1.1. and 1.3.

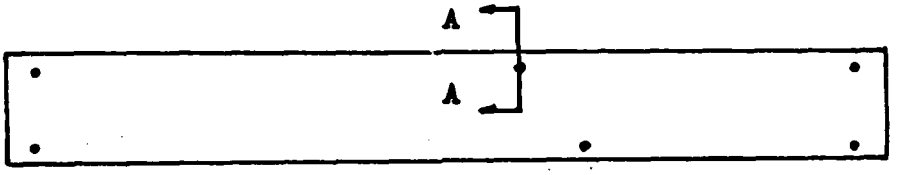

Fig. 1.1.
Showing positions of holes relative to model.

SECTION (A.A.)

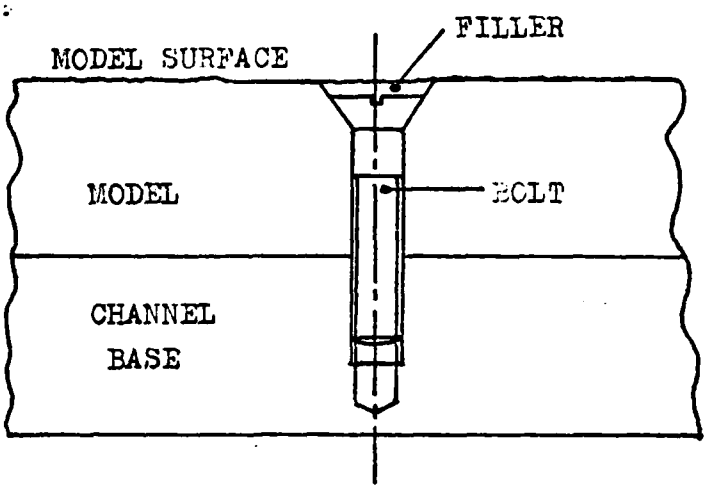

Fig.1.3.
Showing method of securing model to channel base.

The model and base were initially drilled using $\frac{1}{4}$inch Tapping drill, next the model, and only the model was drilled using a $\frac{1}{4}$inch dia. drill and the hole in the base tapped. The model was now countersunk so as to completely hide the head of the bolt from the surface. The remaining area between the bolt head and surface was then filled using plumbers paste. It should be noted that the fixing bolts were all placed away from the centre line as this is the main region in which velocity measurements were to be taken.

20m FLOW CHANNEL EQUIPMENT.

2.1 The Flow System.

The existing 20m flow channel, plate 1, is 30.5cm wide and 30cm deep.

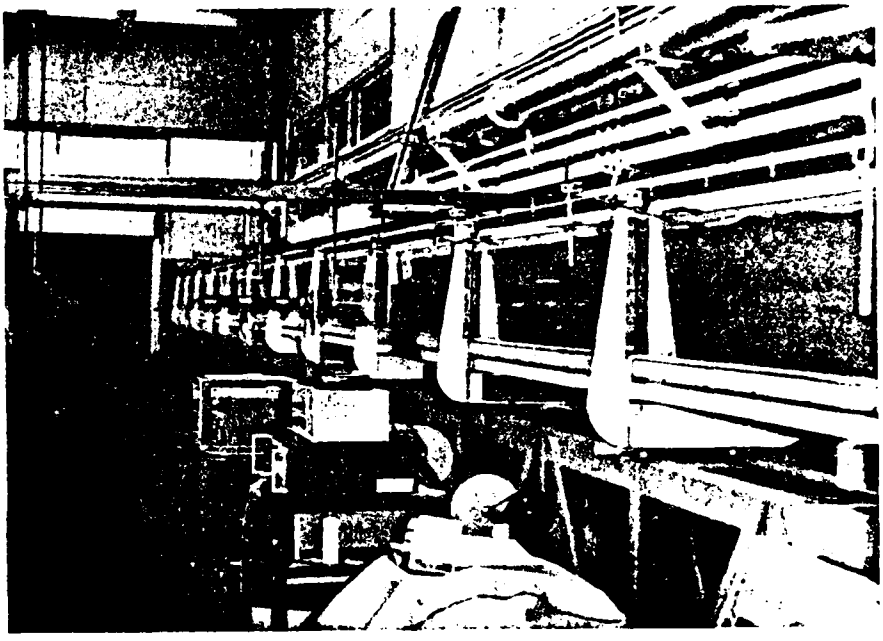

PLATE 1 SHOWING 20m FLOW CHANNEL.

The channel can be served using two main pumps, these will be referred to as P1 and P2 respectively. In these investigations the small-capacity axial-flow pump, P2 was never used due to faulty bearing, but it is enough to say that it has a much lower delivery than P1 and was the original pump that supplied this channel with water.

P1 however, is a fairly recent installation and has the advantage that it can be throttled in order to obtain very low flow rates; at its rated discharge it will give super-critical flow in the channel with a suitable slope.

The channel has the capability of being set at varying slopes by means of an electrically operated tilting apparatus. This ensures that the different type of flow modes can be obtained.

Sub-critical and super-critical flow are defined by the Froude number, F_r: For values of F_r less than one, the flow is sub-critical, and when F_r is greater than one, the flow is super-critical. The Froude number can be defined as the modulus of the inertia force divided by the modulus of the gravity force which gives the non-dimensional equation 2.1.1.

$$\text{Froude No.} = \frac{U^2}{lg} \qquad (2.1.1)$$

However, in practice it is often convenient to use the square root of the ratio so as to have the first power of the velocity.

This is quite permissible: equality of:-

$$\frac{U}{(lg)^{1/2}} \qquad (2.1.2)$$

implies equality of:-

$$\frac{U^2}{lg} \qquad (2.1.3)$$

Equation (2.1.2) is the more usual definition of Froude number F. Again this yields a non-dimensional equation.

In long, open channels the usual form of the Froude number is:-

$$F_r = \frac{U}{(gh)^{1/2}} \qquad (2.1.4)$$

Where U is the velocity of the flow, g is gravitational acceleration, and h is the mean depth of flow.

The mean depth of flow being defined as the cross sectional area of the stream divided by the width of the channel.

For the purpose of this investigation the flow was maintained below its critical value. This is to ensure that any flow instabilities are reduced to a minimum. Any misalignment of the glass panels which make up the sides of the channel, or undulations in the channel floor, would magnify any instabilities throughout the flow region at the critical and super-critical stage, whereas at tranquil (i.e.sub-critical) stage, the effects are not as serious.

Upon installation of the glass panels in the channel, care was taken to ensure that the glass plates were

perfectly aligned, and the two sides made parallel to very close limits. Any gaps in the joints are smoothed out using a sealing compound.

2.2 The Channel Apparatus.

As previously mentioned, the channel is approx. 20m long by 30.5cm wide and 30cm deep; therefore sufficiently long working plate models can be accommodated. However, allowances have got to be made for the inlet settling length and exit length respectively, bearing in mind the unsuitable disturbances propagating in the deturbulating tank at inlet and the action of a weir plate at the exit.

The channel is supplied with clean water from a pit whose capacity is approx. 7.5m by means of two pumps electrically driven, P1 and P2 arranged in parallel. P2 is an axial flow extraction pump, and the pump head is submerged in the water pit. The pump impeller is some 4ft. deep and is connected via a drive shaft housed in rubber water cooled bearings. This pump is capable of delivering 20 l/s at 2900 rev/min.

However, due to faulty bearings, this pump was not used in the following tests.
P2, which is the latest addition to the equipment, so that the flow in the channel can be operated in either the tranquil, critical or super-critical flow mode.
It is a rotor dynamic pump of the radial flow type.

This pump has been derated by reducing the impeller diameter and the reduced delivery rate is some 60 l/s at a rotational speed of 960 rev/min.

The pump delivers the flow to the channel through a 150mm bore header interconnecting pipe system, and manually operated flow control valves. The flow circuit incorporates a Dall tube meter with its pressure tappings connected to mercury-under-water manometers. Two manometers are connected in parallel: a vertical one for large flow rates and an inclined one for accurate measurement of low flow rate.

Water is delivered to a deturbulating tank, through a submerged inverted T-piece whose ends are blocked off; the water has to pass through a multiplicity of small diameter orifices drilled around the bottom leg of the T-piece. It then passes through a honey-comb type flow straightener laid horizontally over the supply section in order to minimise swirl and damp out large scale disturbances produced by the pipe work system.

The shape of the deturbulatory tank is such as to accelerate the flow before entering the channel. As the flow passes through the deturbulating tank into the channel it passes through another honey-comb flow

straightener whose purpose is to ensure flow approaching that of uniform potential at the channel inlet. Without the honey-comb sections, the swirl produced by the combination of bends in the pipe-line would be conveyed to the channel inlet and would persist for some distance downstream, thus causing non-uniform, grossly-disturbed flow in the working section of the channel. This situation would be unacceptable for taking meaningful velocity measurements. As the water passes around the system it must be ensured that there is an adequate reserve in the supply pit; if not, air entrainment and possibly cavitation may occur in the pump which would mar the experimentation.

The channel is piveted at the entry section and has two jacking points connected to an automated system, therefore the channel slope can be adjusted in order to give varying conditions in conjunction with the outlet weir which can be set to a suitable height to back up the flow as required.

It should be noted that if the channel exit is raised approximately two inches then the weight of water in the system i.e. channel and deturbulating tank, overloads the electric drive actuates the tilting jacks. The channel would not then be able to be lowered.

Excessive overload could cause serious damage to the torque motor. To relieve this condition the channel should preferrably be emptied and water released from the deturbulating tank through a drain valve at the base, before gross adjustments are made to the slope of the channel.

2.3 Filtration System.

When using this system it is important that the water is as clean and clear as possible. To achieve this, filtration is carried out on a by-pass principle; this entails a separate system whereby water is pumped, at a constant rate, from the pit through a small centrifugal pump, via a hose into a large cylindrical container. The water discharges by gravity back into the pit through a series of filters housed one on top of each other.

Filtration is vitally important since loosened rust and flakes of old paint from the pump, and accumulated grime in the pipe-line system cause discolouration of the water and the carry over of all sorts of debris; the resulting situation being such that the accuracy and reliability of measurements could not be depended on.

Also with equipment as delicate as the Boundary layer probes, serious damage can be caused; this however will be discussed later.

2.4 The Dall Flow Tube.

Situated approximately midway between the pump P1 and the deturbulating tank is a Dall Flow Tube measuring device. This unit is attached via two bolted flanges and connected in the main straight section of the interconecting pipe-line.

The Dall flow tube is a modified venture type meter which gives a measure of the water flow rate through the channel at any particular set of flow conditions.

The flow meter has two water-on-mercury manometers connected; one being vertical for large flow rates and the other inclined for accurate measure of low flow rates. Due to the working range used in these investigations, the inclined manometer was never used.

Once the pump P1 was running and water was flowing through the channel, before the manometer reading could be relied upon, the system required bleeding.

The procedure here is to firstly throttle the flow using the diaphragm valve at the deturbulating tank inlet in order to create a back pressure in the pipe-line. This is necessary because to ensure that air is not trapped in the Dall tube the two vent cocks must be

opened. These vent cocks are on the high pressure and low pressure side of the unit respectively, and if the flow is not throttled, then air could be drawn in through the low pressure vent. Once all the air was exhailed through the vent cocks, and water was coming out, these could be closed and the manometer bled to ensure that the system was working correctly.

The diaphragm valve could now be re-opened.
It is important to note that the diaphragm valve should always be fully opened when the system is started up, this is to ensure that the pressure exerted from the flow as it initially passes through the pipe system does not damage the diaphragm plate.

The Dall flow tubes main function is that it can be used to record the flow rate accurately for each particular set of measurements taken. This then makes it possible to reproduce the flow condition with the variable height weir plate and the channel slope, whereby repeat procedures can be carried out with accuracy.

2.5 Summing up of System.

From the preceeding passages it is evident that a range of varying conditions can be obtained by:

a) Control of valve at pump exit.
b) Channel slope.
c) Introduction of a weir plate at the exit of the channel.
d) Adjustment of diaphragm valve at entry to deturbulating tank.

Therefore not only can the conditions be controlled over a significent range, but also by using the Dall Tube flow meter a given set of flow conditions can be repeated thus ensuring that results can be checked and verified.

EQUIPMENT FOR MEASUREMENT OF VELOCITY PROFILES.

3.1 Measurement of Velocity Profiles.

Before any calculations can be carried out, it is necessary to obtain velocity profiles of the fluid as it passes over the replica of the ship's hull surface.

There are four possible methods for obtaining velocity profiles in the present flow system, and these are:

1) Pilot-static traverse.
2) Propellor type current meter (OTT meter)
3) The Constant Temperature Anemometer. (C.T.A.)
4) The Laser Doppler Anemometer. (L.D.A.)

3.1.1 Pilot-Static Traverse.

The pilot-static tube is connected to a water manometer which is open to the atmosphere. The difference in the static and stagnation pressures being measured in terms of height difference in the manometer reading.

The pilot-static tube can be connected to a carriage arrangement which allows the unit to move along the length of the channel, but also gives movement across the channel. The height of the pilot-tube can also be adjusted manually. Therefore this system allows pilot-static readings to be taken in three directions.

This particular piece of apparatus has several disadvantages, and these are:

a) Due to measurements being taken in a liquid medium, the time required for the manometer to settle to an equilibrium position is such that it renders the equipment far to inefficient. However, there will soon be a pressure transducer available in the department which, when connected to the pilot-static tube system, will give instantaneous readings.
At present the method employed to measure the manometer height is by means of a depth gauge or depth micrometer.

b) As previously mentioned the flow system incorporates a filtration unit in order to ensure the water is clean. This filtration unit however, will only filter the larger size debris and also the filtration is such that we cannot ensure that 100% of the water passes through the unit. Therefore the water still has impurities and rust deposits floating about, all of which tend to block up the pilot-static system. Thus, before this unit can be used successfully, a means of purging the pilot tube at regular intervals must be incorporated.

By the introduction of the Pressure transducer and a purging system, the pilot-static tube would be a reliable method for velocity measurement.

3.1.2 Laboratory Propeller Type Current Meter.

The propeller type current meter incorporates a propeller type unit which comprises the meter body and a propeller attached to the end.

PLATE 2 SHOWING PROPELLOR TYPE CURRENT METER.

The propeller is connected to a spindle which is situated in two ball bearings. Attached to the spindle are two contact springs, these in turn form the electrical connection to an electric contact unit. From the electrical contact unit a connecting cable is attached to an electrical counter which registers each

revolution of the propeller. The electrical counter unit is powered by 2 HP2 batteries connected in series giving an electrical potential of 3 volts.

The maximum voltage the unit should be subjected to is 6. When the unit is emersed in a flowing medium, the propeller revolves. The equation from which the mean flow velocity can be calculated is:

$$v = Kn + \Delta \qquad (3.1.)$$

Where v = mean velocity,
and n = number of revolutions of the propeller/sec.
K and Δ are constants depending upon propeller used. The propellers vary in size, i.e. diameter, helix angle, and the correct propeller must be chosen to cover the particular velocity range to be used.

In this particular project, the propeller used was No. 13569-2 type C1, and from the calibration charts for the unit, i.e. Calibration No. 2592 date of calibration 12.10.77.
The equation from which the velocity can be calculated directly is:

$$v = 0.102ln + 0.0206 \qquad (3.2.)$$

for the range: $1.677 < n < 11.827$.

The method employed in these measurements was to time the number of revolutions of the propeller using a stop watch, then by choosing the correct range of values for n the velocity of the fluid can be calculated directly using the equation above, (3.2). The period of test was 60 seconds.

This unit was mainly used to establish that there is a central working region in the channel. This can be seen from fig. D1 in appendix D

The propeller type meter, however, cannot be used with accuracy for velocity measurements near to a boundary because its size and operating characteristics interupt the flow within that boundary. Therefore this unit was mainly used so as to establish the working region across the channel and also the local velocity in the freestream.

3.1.3 Constant Temperature Anemometer.

The constant temperature anemometer used in the following tests is of the Disa Boundary layer hot film type. This anemometer consists of a thin electrically heated Nickel film fused to a gold plated quartz fibre for support. The fibre plus film has a thin insulating coat of quartz, and is held between two arms of the probe supports.

The probe traversing equipment consists of a guide tube system with a probe connection support attached to a mounting tube. The probe connection support is squeezed into position in the mounting tube and the cable from the probe connection runs through the mounting and guide tube system. The cable terminates at a B.N.C. plug at the top of the guide tube.

From the B.N.C. plug is connected the probe cable which is attached to the probe B.N.C. socket on the Disa 55M10.

Situated above the 55M10 is a 55M01 main unit. This unit consists of a meter for measurement of probe resistance; a decade resistance with a maximum value of 99.99 Ohms and various other facilities, i.e. probe type selector, square wave frequency, HF filter and gain control.

The 55M10 unit is now connected to a 55D15 linearizer so that the signal outputs from the probe when operating can be linearized to read $V_{out} = Kv$ with good approximation, where v = measured flow velocity.

The hot film probe forms one arm of a wheatstone bridge, the other arm consisting of a non inductive variable resistance box. The system operates whereby if the probe resistance is less than the resistance of the adjustable bridge arm, then an error voltage will be produced across the amplifier inputs. Therefore, this error voltage, when amplified causes the probe to heat up until its resistance is equal to that as previously set on the variable resistance box.
The bridge is now in balance again.

By placing the probe in a flowing medium, and switching to operate, the flow will try to cool the probe. This results in a small charge in the probe resistance which, as described previously, causes an error voltage across the probe.

A servo-amplifier connected inside the equipment feeds back a signal causing the bridge current to increase, and the probe temperature to return to its original value. The voltage which is fed to the bridge to

maintain the temperature of the probe can now be related to the fluid velocity by a suitable calibration. The calibration is carried out using a calibration tube which is attached to the side of the channel and will be discussed later.

3.1.4 Laser Doppler Anemometer.

The fourth and final method for measurement of flow velocity is by means of using the L.D.A. (Laser Doppler Anemometer.)

The main principle of operation is that a coherent source of laser light is split in a beam splitter to form two beams which cross some distance from the optical unit. This distance depends on the focal length of the lens system chosen. As the two beams intersect, the point consists of alternate light and dark fringes.

See fig. 3.1.

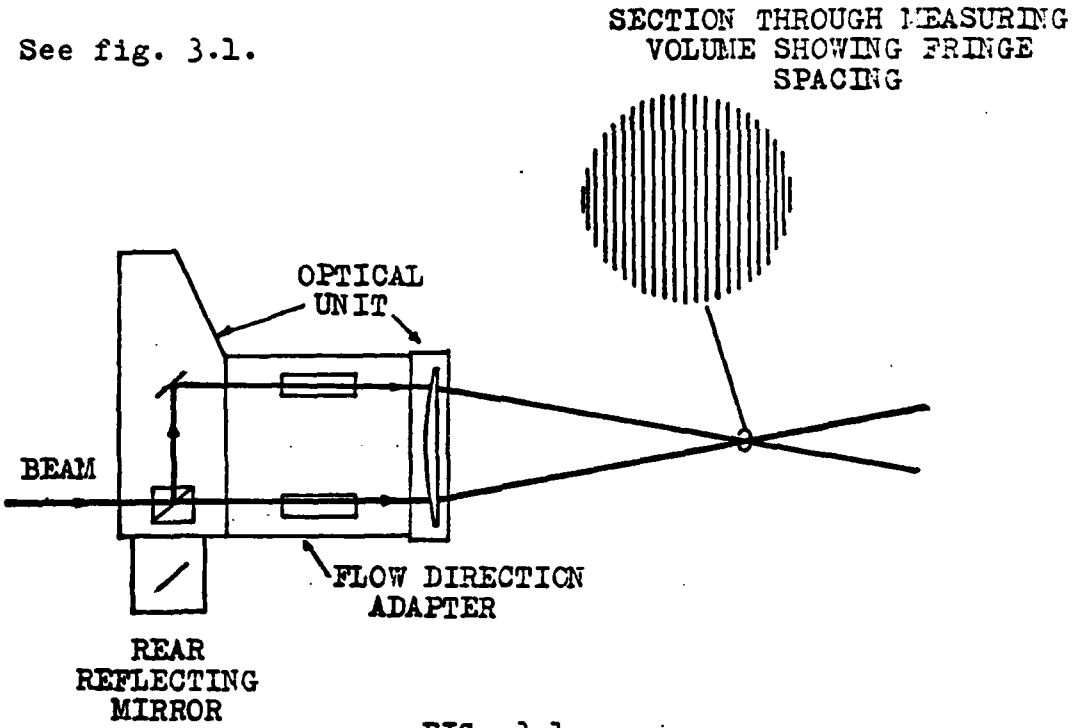

FIG. 3.1.

SCHEMATIC DIAGRAM OF OPTICAL UNIT AND FLOW DIRECTION ADAPTER.

Therefore any particle which passes through the fringe system will omit light pulses at a frequency which is dependant upon the particle velocity. This frequency is known as the Doppler frequency.

The scattered light is now detected on a Photomultiplier and the information relayed to the input of a Preamplifier. and then to a Frequency Tracker. The Frequency Tracker is an analoy instrument and 'tracks' the Doppler frequency. This is achieved by means of a voltage controlled oscillator in the feed back loop. The controlling voltage is directly proportional to the Doppler frequency and hence also the flow velocity.

The Doppler frequency can now be obtained from the analogue meter or by connecting a digital voltmeter where 0-10V corresponds to the full scale meter reading in all frequency ranges.

The L.D.A. will be explained in further detail later.

3.2 Summary of Velocity Profile Measurement Equipment.

From the preceding sections, 3.1.1 to 3.1.4 it is obvious that there are various methods available for measurement of the velocity profile. However, in order to obtain accurate velocity measurements from the surface in question, i.e. the replica of the ship's hull, to the mainstream, it is necessary to record velocities in the boundary layer. Therefore it is vital that the equipment to be used does not in any way disturb the flow.

Any disturbance of the flow regime will give rise to inaccuracies and irregularities in the values recorded. Therefore before any measurements can be taken, the correct equipment must be used and for these investigations the boundary layer hot film probes are small enough to cause minimum flow disturbance.

The pitot tube is adequate for fairly close boundary layer measurements, but the physical size of the unit causes disturbance of the flow between the pitot tube and the surface, therefore for close boundary layer work this type of equipment is not recommended.

The propeller type current meter, due to its physical size, restricts its use to anything other than free-

stream velocity measurements.

The boundary layer hot film probe is an ideal piece of equipment for velocity measurements close to the surface due to the physical size of the sensing element; therefore because of the advantages of the hot film probe over the other type of equipment, makes it ideal for velocity measurements and so was the equipment used in the investigations carried out.

The L.D.A. which was to be available December - January 1978 - 1979, did not arrive until March 1979. This equipment would have been the most accurate for velocity measurements because the two beams of Laser light passing through the flowing medium do not in any way disturb the flow. Therefore, had the equipment been available earlier, it would then have been possible to check the results obtained from the C.T.A.

USE OF THE CONSTANT TEMPERATURE ANEMOMETER. (CTA).

4.1 Constant Temperature Anemometer.

The constant temperature anemometer was the main item of equipment used for velocity measurements, however, before any measurements could be taken the probes working resistance had to be determined.

4.2 Initial Setting of Controls.

Before the equipment is switched on , and the probes working resistance calculated, the following procedure should be followed.

a) Check probe cable length is as indicated in the probe cable length window, i.e. 5, 20 or 100 metres.
b) Set Square Wave to off.
c) Set H.F Filter to 1.
d) Set Volts to 1.
e) Set Function switch to 'Stand By'.
f) Set Gain to 1.
g) Set Decade Resistance 00.00.
h) Set Probe type switch: depending on type of probe to be used, i.e. film or wire.

4.3 Determination of Probe Operating Resistance.

When the power has been applied, the pilot lamp on the main unit will show light. The meter needle will firstly deflect to the left to below zero and after about 90 seconds will move slowly to the right, indicating that the various internal circuits are ready for operation.

Before beginning any measurements, the instrument should be allowed to warm up for 15 minutes.

The probe cable can now be plugged into the probe socket and the cable and support terminated, (short circuited) using a shorting probe. By turning the Function switch to the Res. Meas position this causes a change in position of the meter needle which is then set to cover the red mid-scale mark by adjustment of the Zero Ohms potentiometer.

The functions switch is now returned to 'Stand By' and the shorting probe replaced by the probe to be used for measurements.

Plate 3 shows the boundary layer probe in position in the probe connection support.

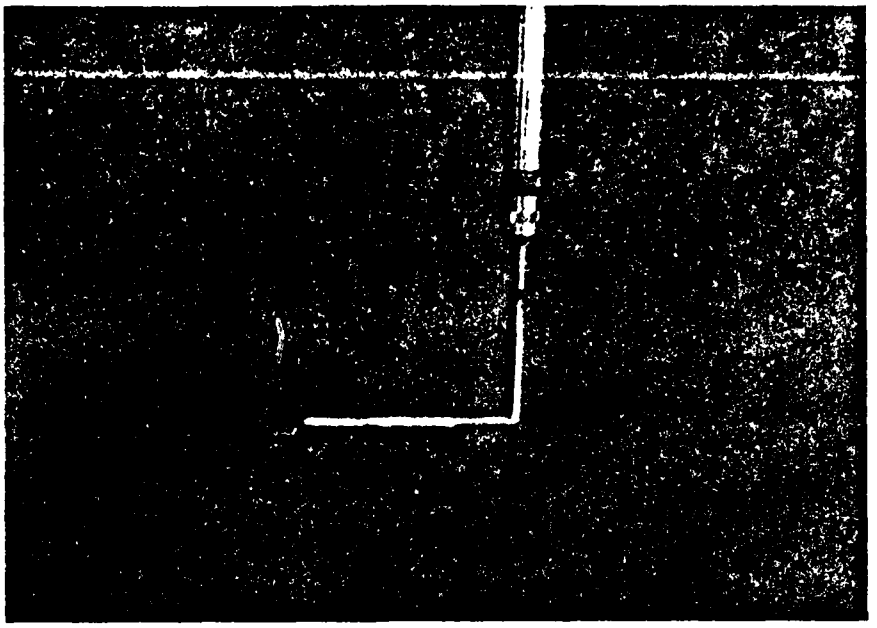

PLATE 3 SHOWING BOUNDARY LAYER PROBE

Now the probe is placed in the flowing medium and the function switch set to Res. Meas. (It is important to note here that if the function switch is adjusted without the probe being immersed, then serious damage to the probe or insulating quartz coating may result, hence destroying the probe.) Now by adjustment of the decade resistance box, the bridge circuit can be balanced. The resistance reading on the decade resistance box corresponds to the cold resistance of the probe.

The decade resistance box is now reduced by an amount corresponding to the probe-lead resistance, this,

however, causes the meter reading to change, which should then be brought back to cover the red mid-scale mark by adjustment to the Zero Ohms potentiometer. The function switch should now be re-set to 'Stand By'.

The constant-temperature anemometer employs a sensor which is kept at a pre-selected excess temperature by means of an electronic control circuit. The excess temperature is defined by the so-called overheating ratio: 'a'.

$$a = \frac{R - Ro}{Ro} \qquad (4.1.)$$

R = sensor hot resistance,

Ro = sensor cold resistance at ambient temperature.

Sensor hot resistance may therefore be calculated as

$$R = Ro\ (1 + a) \qquad (4.2.)$$

In this investigation, the overheating ratio was calculated to be 1.1, therefore by multiplying the resistance reading on the decade box by this factor, the decade box can be re-set so that the overheating ratio is provided automatically.

Now, by turning the Function switch to the 'operate' position, this closes the servo feed back loop and the anemometer is ready for operation.

4.4 Balancing The Bridge.

Before carrying out any measurements using the anemometer, it must be checked to ensure that the instrument is not oscillating due to inbalance of the bridge.

The frequency behaviour of the anemometer can be determined by producing a sudden change in the velocity of the flow acting on the probe. However, since it is difficult to produce accurately defined sudden velocity changes, the ideal way is by feeding a square-wave signal into the bridge.

By connecting an oscilloscope to one of the out sockets on the 55M01 and with the sensitivity set at approx. 0.1 V/cm it is possible to observe the impulse response without superimposed oscillation. However it is necessary during this test to expose the probe to a constant flow whose magnitude should at least equal the maximum velocity occuring during the measurement. Therefore this test was carried out in the calibration tube with the globe valve at inlet set for maximum flow, approx 1m/s.

The switch on the Square Wave Generator can be set to a desired frequency depending on the oscilloscope pattern. Both test frequency and oscilloscope frequency being

selected to give an easily readable pattern.

It is necessary to have a good, clear trace so that the changes caused by operating the controls give a clear indication of what is happening.

The Gain switch should now be increased until the response signal on the oscilloscope shows damped oscillations on the base line. By increasing the HF filter, the oscillations should reduce. Further adjustment should promote oscillations at the skirts of the signal.

The oscillations observed can however be compensated for by adjustment of the Cable Compensation settings Q and L. This adjustment should firstly start with L and as compensation proceeds it may be necessary to choose different settings of Q.

The Gain and HF Filter switches can now be increased and the compensation procedure repeated.

The above should be carried out until no further compensation can be accomplished, The Gain and HF filter can now be backed off until the oscillations disappear. The anemometer is now set for optimum frequency response.

4.5 Linearity.

In order to obtain results that follow a linear relationship, the 55M10 is connected to a 55D15 linearizer. By suitable adjustment of the gain and suppression controls, the unit can be adjusted to give full scale deflection at maximum flow velocity.

The full scale deflection represents 3 Volts DC output which can be transferred to a digital voltmeter if required.

4.6 Calibration of Boundary Layer Probe.

Before any velocity measurements in the channel can be recorded, it is necessary to calibrate the probe over the velocity range to be encountered. This is done by means of a calibration rig, as shown in Plate 4.

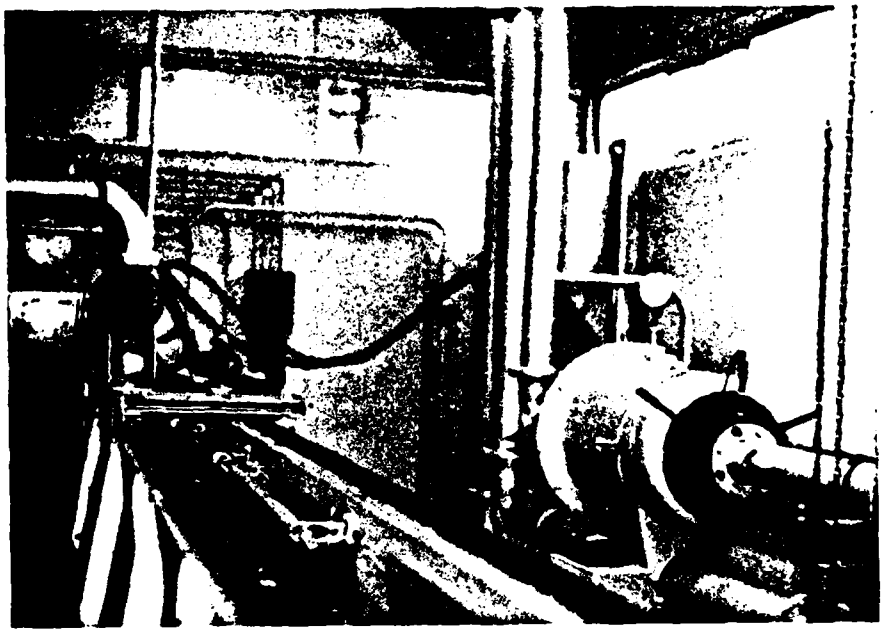

PLATE 4 SHOWING CALIBRATION RIG

The rig consists of a 2.15cm dia. calibration tube, 4.6m long. The length to diameter ratio is 213, therefore fully developed turbulent flow will be achieved at the pipe exit. (For fully developed turbulent flow, the length to diameter ratio must be greater than 50.)[1]

The calibration tube is connected to a constant head reservoir via a globe valve and hose system, the reservoir being supplied with water pumped from the channel. This ensures the same water is being used during both calibration and testing.

The calibration tube is attached to the side of the channel above the level of the water, and the probe inserted at the exit by means of the existing carriage support.

Calibration is carried out by adjusting the globe valve to give varying flow rates, and at each flow condition 3 separate sets of voltage readings are taken.

Due to turbulance and flow instabilities the recorded voltage at any one setting is not static but fluctuates. The degree of the voltage fluctuation depending on the level of turbulance. This fluctuation however, renders the analog meter on the linearizer inadequate for accurate voltage measurements. Therefore, the linearizer is connected to a Solartron Digital Voltmeter type LM 1420.2 which is connected into a paper tape data logging system.

By switching the Voltmeter to the record setting, this automatically samples the voltage readings at intervals

of 0.33 seconds. During a test period of 10 seconds, the total number of voltage readings recorded is 30.

The voltage results obtained can now be summed and the mean value calculated. This calculated value is taken as the true voltage for that particular valve setting.

4.7 Calculation of Centre-Line Velocity.

Once the experimentally recorded voltage and flow rate are obtained, it is necessary to calculate the actual velocity of flow to which the probe is subjected.

The probe was situated along the centre-line of the calibration tube, therefore the centre-line velocity must be calculated, (this being the actual velocity to which the voltage refers.) by first evaluating Reynolds number. Now by transferring the Re. number to fig. 4.1 or 4.2, whereby the ratio of Average velocity / Centre-line velocity can be obtained, so, the Centre-line velocity can be calculated directly.

$$\text{Reynolds No. (Re)} = \frac{\rho v_a l}{\mu} \qquad (4.3)$$

$$= \frac{v_a l}{\nu} \qquad (4.4)$$

where l = dia.of calibration tube,

and $\nu = \frac{\mu}{\rho}$

The Kinematic Viscosity (ν) varies with temperature, and therefore using fig. 4.3 or 4.4 (Ref. 1) this may be obtained at the required temperature.

The average velocity, v_a is calculated by dividing the

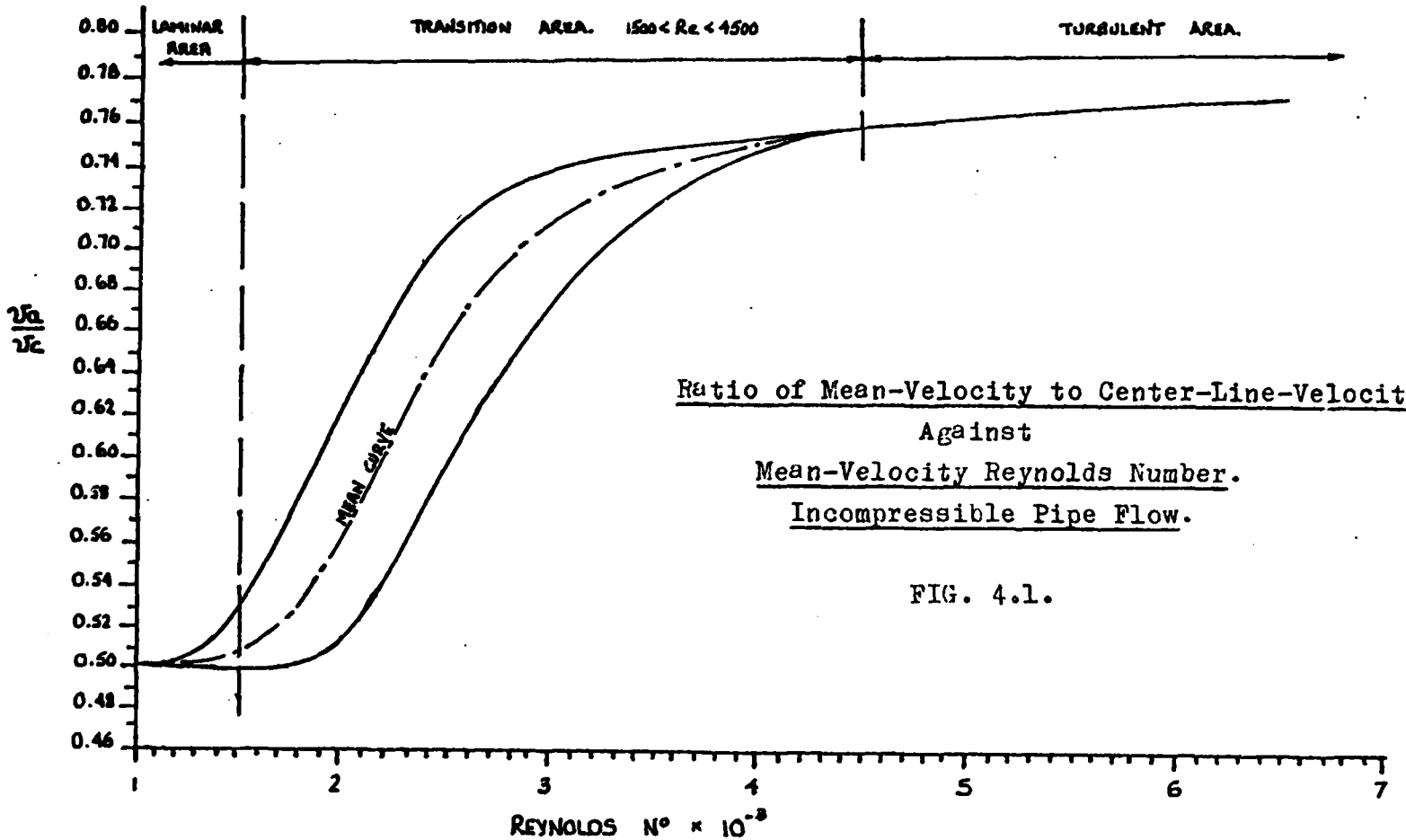

Ratio of Mean-Velocity to Center-Line-Velocity
Against
Mean-Velocity Reynolds Number.
Incompressible Pipe Flow.

FIG. 4.1.

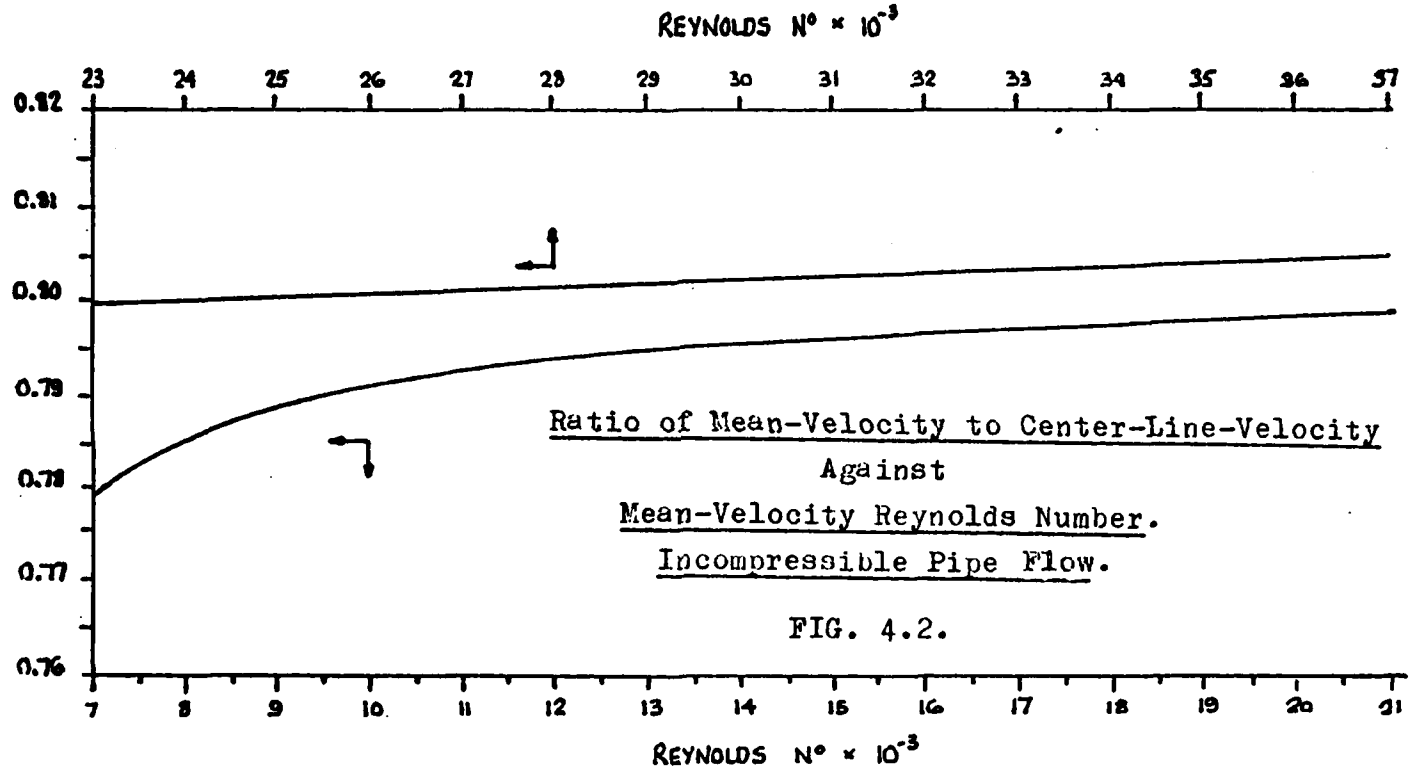

$\frac{u_a}{u_c}$

Ratio of Mean-Velocity to Center-Line-Velocity
Against
Mean-Velocity Reynolds Number.
Incompressible Pipe Flow.

FIG. 4.2.

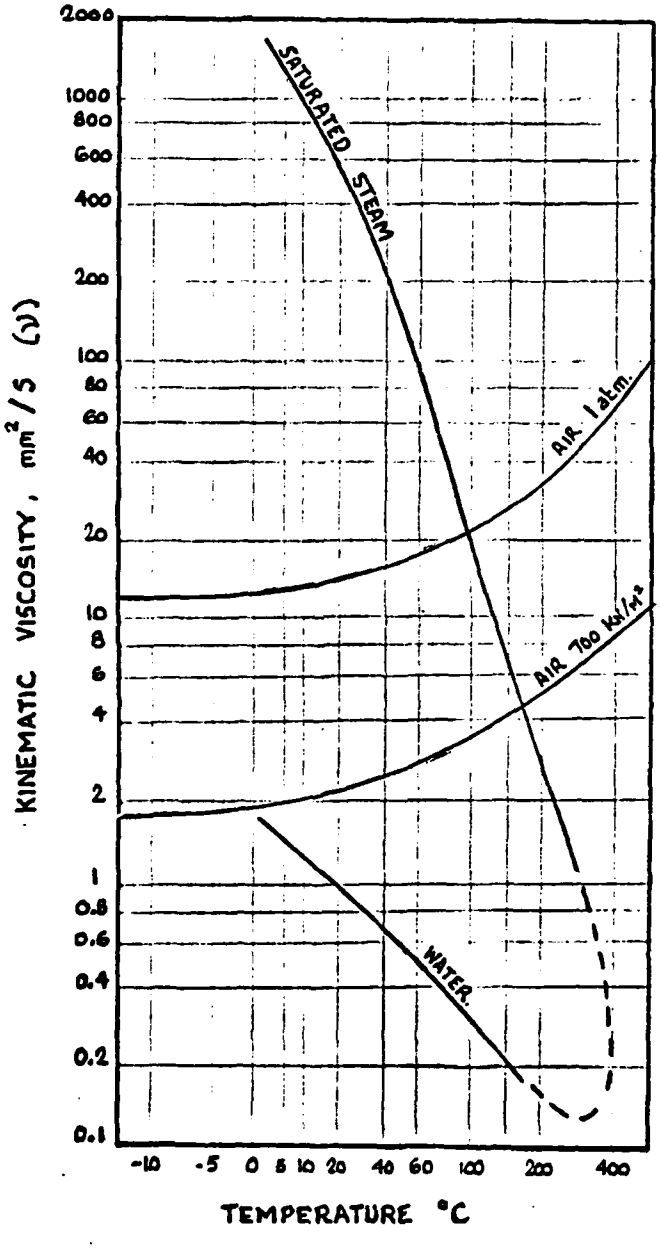

FIG. 4.3 Kinematic Viscosity of Fluids.

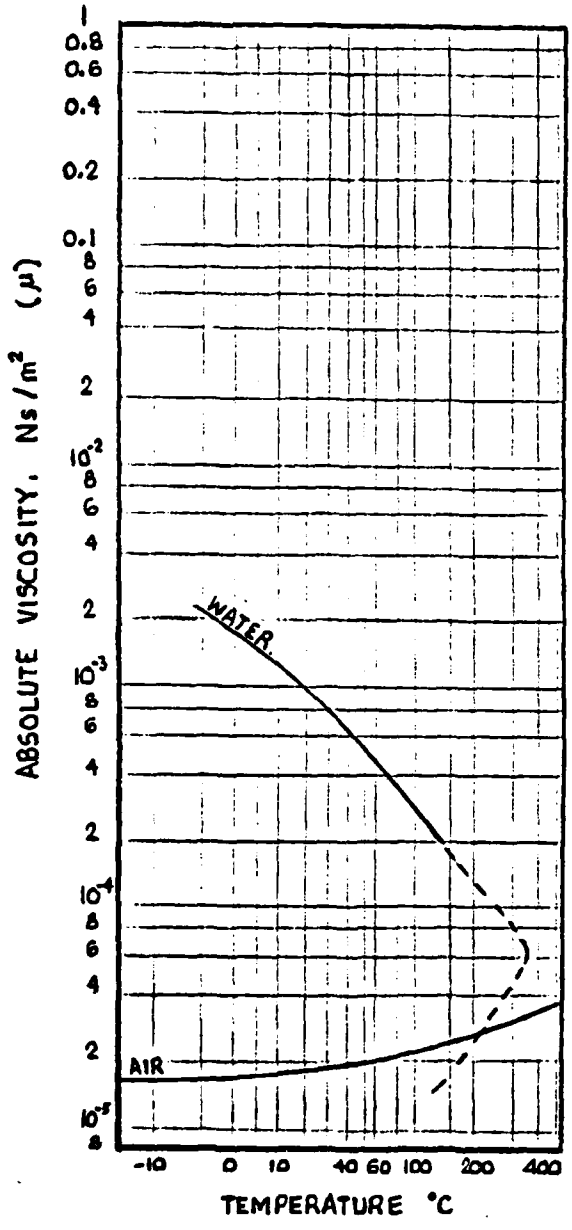

FIG. 4.4 Absolute Viscosity of Fluids.

average flow rate by the area of the calibration tube. During calibration of the probe, the fluid mode is always turbulent with Reynolds numbers greater than 2300. Therefore due to the shape of the velocity profile under turbulent conditions, it has been assumed that precise location of the probe along the centre-line of the calibration tube is not critical, and that for a small distance either side of the centre-line, the velocity difference will be approaching that of the centre-line velocity. However, location of the probe was carried out as accurately as possible.

It should be noted that for each valve setting, the probe was located in exactly the same position to enable uniformity in experimental procedure.

The calculated values of centre-line velocity and average voltage can be seen in tables A3 and A4 Appendix A.

4.8 Probe Calibration Graphs.

To obtain a relationship between the voltage and centre-line velocity, it is necessary to graph the results: Tables A3 and A4 Appendix A which refer to probe 1 and 2 respectively.

These graphs indicate that the plotted points exhibit a linear relationship governed by the law $y = bx + a$, where 'y' and 'x' are the variables, and 'b' and 'a' are the slope and intercept respectively.

In order to obtain the best straight line to be drawn through the experimentally obtained data, it is necessary to use the 'Method of Least Squares' analysis, initially developed by Gauss.[24]

For this analysis there are 3 basic equations which are:

$$n\,a + b\lesssim X = \lesssim Y \qquad (4.5)$$

$$a\lesssim X + b\lesssim X^2 = \lesssim XY \qquad (4.6)$$

$$\frac{n\lesssim XY - \lesssim X\lesssim Y}{\sqrt{(n\lesssim X^2 - (\lesssim X)^2)(n\lesssim Y^2 - (\lesssim Y)^2)}} = \lesssim 1 \qquad (4.7)$$

where (4.7) indicates whether or not statistically the

line gives a good fit to the plotted experimental data.

In the previous equations, 'a' and 'b' are constants, and 'X' and 'Y' refer to the experimentally obtained results.

For the calculations using the afore said equations, 'X' is usually designated as the value from which 'Y' relies upon, therefore, in this investigation the values of recorded voltage rely upon the centre-line velocity, thus 'X' refers to the centre-line velocity, and 'Y' to the recorded voltage readings.

(4.5) and (4.6) are the two main equations for establishing the law that fits the best straight line, whereas (4.7) gives an indictation as to whether or not statistically the straight line obtained is a good fit to the experimental data. The value obtained from this equation should be approximately: 0.98 - 1 for good fit.

For the two Boundary Layer probes used, the straight line relationships obtained are:

<u>Probe 1</u>

$$v = 0.301263V + 0.1392472 \qquad (4.8)$$

Probe 2.

$$v = 0.303719V + 0.2643 \qquad (4.9)$$

where v = velocity

and V = recorded voltage reading.

4.9 Probe Traversing.

Once the probe had been calibrated and calibration data obtained, i.e. equations (4.8) and (4.9) for probe 1 and 2 respectively, it is now possible to obtain velocity profiles from the surface under investigation.

The method employed here required the probe to be traversed across the flow from the surface in question and voltage data obtained at pre-determined positions. Initially probe 1 was located in the centre of the channel at a position of 0 Ft. along the test surface, (total distance from channel entry 9ft. 6inches.) using the carriage support assembly.

The probe was now positioned as close to the surface as possible without actually touching it, this being so as not to damage the delicate probe sensing element. The vernier measuring system attached to the probe traversing carriage assembly was now set to zero and

this taken as the probes datum position, the initial setting being within 0.5mm from the surface.

By turning the function selector on the 55M10 unit to 'operate' this meant that the probe was working and experiencing a cooling effect due to the moving fluid. The voltage required to balance the bridge circuit was indicated on the digital voltmeter.

The data logger could now be switched on and sampled voltages recorded for a test period of 10 seconds, whereby the total number of results obtained was 30.

After this test, the function switch was returned to the 'stand by' position and the probe removed from the flowing regime. Inspection of the probe could now be carried out to ensure no damage had occured.

This procedure was repeated for probe positions of: 0,1,2,3,4,5,6,7,8,9,10,15,20,25,30,35,40,45,50,75,100, 150 and 200mm above the surface in question. The recorded voltages at each probe position are as indicated in appendix B.

The reference (1.1),(2.1) etc. refers to probe traverse 1 using boundary layer probe 1 and probe traverse 1 using boundary layer probe 2 respectively.

4.10 Probe Contamination.

Before any measurements were taken using the boundary layer probe it was gently brushed using a dilute solution of acetic acid, this removed any impurities from its surface which may alter the heat transfer characteristics of the sensing element.

Because the probe operates on the amount of heat removed from the element, it is extremely important that the conductivity from the element is not impeded in any way.

Conductivity impedance will result in irregularities taken hence making them invalid.

THE LASER DOPPLER ANEMOMETER. (LDA).

5.1 Introduction.

The 36th European Mechanics Colloquium, which was held at Imperial College between the 17th and 19th of April 1972, was the first such meeting to be devoted entirely to Laser Anemometry. This colloquium was the first of its kind whereby researches from all over Europe interested in Physics, Electronics and Fluid Mechanics with the sole purpose of trying to communicate their theoretical knowledge, exchange experience in the use of and demonstrate contributions made in the principles and use of Laser Anemometry as a means for velocity measurements in fluid flow.

5.2 Basic Principles.

The optical heterodyne detection of the Doppler shift is basic to the operation of the velocity meter. The fundamental concept of a frequency shift in radiation received from a moving body by a stationary detector has been understood, and used in communications and astronomy, for example, for many years.

One of the first suggestions that mixing of two signals of different frequencies to generate a difference or beat frequency, was made by A.T.Forrester[12] in 1947 and 1948. This he published in the Physics Rev., Volume 73

page 922 in 1948.

If we consider a situation whereby two incident monochromatic plane light beams are superimposed on the surface of a detector, i.e. photocathode, and we assume their angular frequencies are ω_1 and ω_2. The electric fields will be:

$$E_A = E_1 \cos \omega_1 t \qquad (5.1)$$

$$E_B = E_2 \cos \omega_2 t \qquad (5.2)$$

The output current from the photomultiplier tube, I, is proportional to the square of the electric field incident upon it, i.e.

$$I = (E_A + E_B)^2 \times K \qquad (5.3)$$

where K = constant.

However, the photomultiplier will not follow frequencies greater than several hundred megahertz, therefore terms in the expansion of (5.3) involving ω_1, ω_2, or $\omega_1 + \omega_2$ will give rise only to a d.c current proportional to the time average of those terms. If however, $(\omega_1 - \omega_2)/2\pi$ is below about 100MHz there will be an a.c signal of frequency $\omega_1 - \omega_2$.

With the more conventional light sources, the optical heterodyne process was only marginally effective due

to the relatively large band widths (10^9 Hz). The low intensity per unit bandwidth gave extremely poor signal-to-noise ratios, and therefore ruled out detection of Doppler shifts smaller than 10^9 Hz.

However, the major difficulties encountered above using monochromatic light were later overcome with the advent and development of the Laser.

The Laser, (light amplification by stimulated emmission of radiation) emits a continuous coherent wave of plane polarized light, this due to very high power levels being contained within a very narrow bandwidth makes the laser ideal for use as the source of light.

5.3 The Doppler Effect.

The Doppler effect is named after Christian Doppler who gave an explanation in 1842 of the higher frequency of a train whistle as it approached an observer, and the lower frequency as the train went away from the observer.

An observer on a particle moving away from a fixed source of light would see the light at a lower frequency than the source frequency, and to a stationary observer, the light scattered from the particle would also appear to have a different frequency.

The geometry of the situation is shown FIG. 5.1.

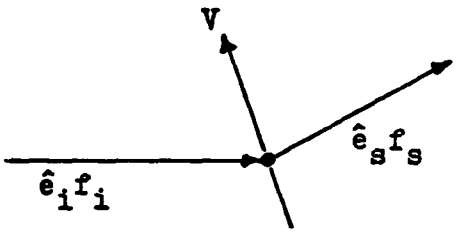

FIG. 5.1.

Light of frequency f_i is incident upon a moving scattering center. An oscillating field will be induced in the scattering center by an electric field of the incident radiation.

The frequency of this oscillation e_i is given by the relationship:

$$f = f_i \left\{ 1 - \frac{V\hat{e}_i}{C} \right\} \qquad (5.4)$$

where C = velocity of light.

f = frequency of oscillation.

f_i = frequency of incident light.

$\hat{e}_i$ = unit vector in incident direction.

V = velocity vector of the scattering center.

Also $C = \lambda f$ (5.5)

where λ = wavelength of light.

To any observer at the position of the photomultiplier tube this frequency of scattered radiation is shifted because of the Doppler Effect.

The frequency f_s (frequency of scattered light) observed at the photomultiplier tube is

$$f_s = f \left\{ 1 + \frac{V\hat{e}_s}{C} \right\} \qquad (5.6)$$

Where $\hat{e}_i$ and $\hat{e}_s$ are the unit vectors in the incident and scattering direction respectively.

By eliminating f from equations (5.4) and (5.6) we have:

$$f_s = f_i \left(1 - \frac{V\hat{e}_i}{C} \right)\left(1 + \frac{V\hat{e}_s}{C} \right)$$

$$f_s = f_i \left(1 + \frac{V\hat{e}_s}{C} - \frac{V\hat{e}_i}{C} - \frac{V\,\hat{e}_i\hat{e}_s}{C} \right)$$

$V^2 \ll C^2$ therefore the last term in the bracket can be ignored.

from equation (5.5)

$$\frac{f}{C} = \frac{1}{\lambda}$$

therefore:

$$f_s = f_i + \frac{1}{\lambda}V.(\hat{e}_s - \hat{e}_i)$$

$$f_s - f_i = \frac{1}{\lambda}V.(\hat{e}_s - \hat{e}_i) \qquad (5.7)$$

where:

$$f_s - f_i = f_D = \text{Doppler frequency.} \qquad (5.8)$$

therefore from equation (5.7) we can see that the Doppler frequency is directly proportional to the particle velocity.

5.4 Early Developments.

One of the first uses of Laser Anemometry for the measurement of fluid velocity flow was by Y.Yeh and H.Z.Cummins (1964)[13], who measured velocity in a fully developed laminar pipe flow. Foreman (1965-1966) later refined the techniques and applied them to the measurement in gases.

Following on from the initial work done, R.J.Goldstein[17] and D.K.Kreid (1967) used the method to measure the flow developed in rectangular ducts and also to study turbulence intensity.

One of the most commanding attributes of Laser Anemometry is that unlike the hot-wire, hot-film anemometers calibration is not necessary, also equation (5.7) indicates that the Doppler shift $f_s - f_i$ is directly proportional to the component of velocity in the direction $\hat{e}_s - \hat{e}_i$. This does give one major advantage, and that is that the anemometer can be used to study and take measurements in situations of high turbulance without the complication of non linear characteristics.

The earlier developed systems did however, have major drawbacks, and these were mainly associated with the

types of optical system used.

The units, as used by Yeh, Cummins, Foreman, George etc, all required several optical components such as mirrors and beam-splitters with the resulting situation that alignment was critical, hence necessitating the equipment being mounted on large lathe beds.

Goldstein and Kreid refined the original systems to the one as shown FIG. 5.2.

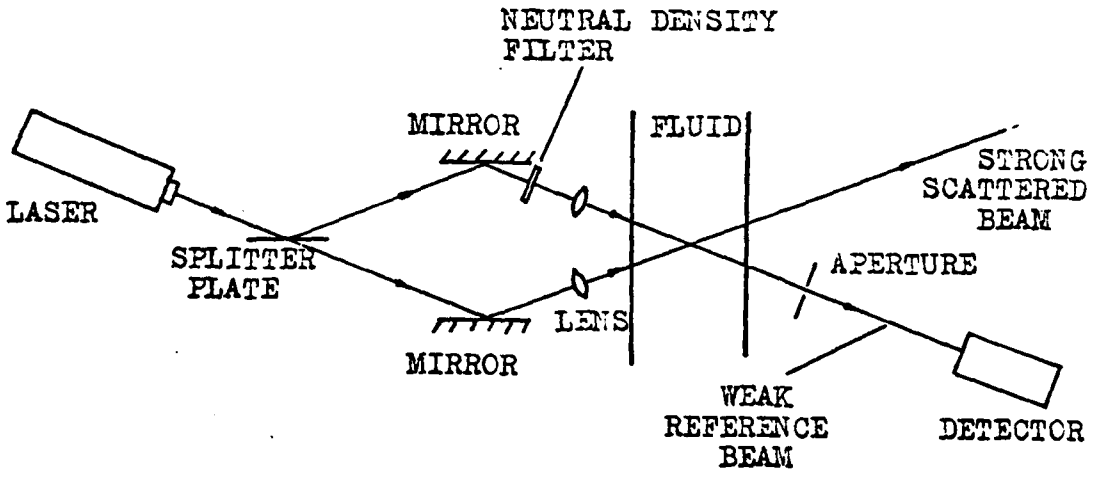

FIG. 5.2 GOLDSTEIN-KREID SYSTEM.

This system, however, had several disadvantages in that alignment was critical, also a distinct encumbrance was encountered when adjustments were required, i.e. traverse across a pipe channel etc.

Rudd, however, refined the system even further, whereby the initial laser beam passed through a lens system to produce a wide spread of coherent light. This light was then masked to produce two single beams.
The major fault with this system was that due to the masking much of the laser power was lost, thus necessitating lasers of very high intensity to be used, e.g. 25-50 mW.

Traversing of the units was again made difficult due to the complexity of the system.

5.5 The Optical System.

In all such systems previously discussed, the critical factor is the optical unit. Basically there are three main types which are shown in FIG. 5.3, 5.4, and 5.5.

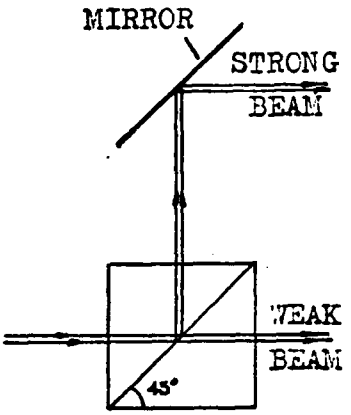

FIG. 5.3

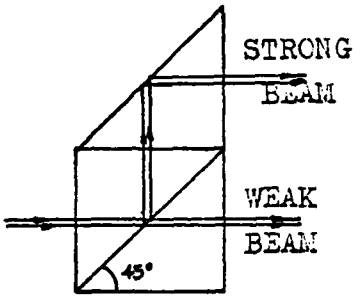

FIG. 5.4

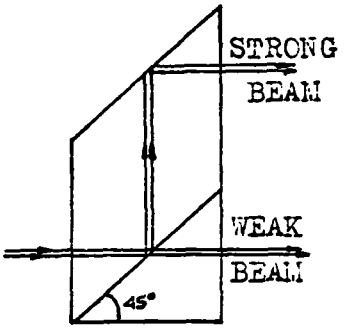

FIG, 5.5

FIG. 5.3 shows two right angle prisms and a reflecting mirror. Partially reflective surfaces are made so that about 4-5% of the incoming light is transmitted through and the rest, about 95% is reflected and brought parallel to the former by a reflecting mirror.

FIG. 5.4 and 5.5 shows alternative design using three right angled prisms, and one right angled prism with a rhomboid respectively.

FIG. 5.5 is typical of the system used at The National Engineering Laboratory, although the laser beam entered from the base and not as indicated in the FIG.

FIG. 5.3 is typical of the unit to be used by the author in the preceding investigations.

The main advantage of this type of beam-splitter arrangement, is that it can be housed in a unit which permits the change in direction of velocity measurement without disturbing the optical unit. The Disa 55L01 type system is basically that of FIG. 5.3, and the whole optical unit can be rotated about its own axis, thus always ensuring that the optics are aligned.

5.6 Modes of Operation.

In order to utilize the measuring principle based on the Doppler effect, there are three main modes of operation, these are:

1) Reference-Beam Mode. FIG. 5.6.
2) Differential Doppler Mode. FIG. 5.7.
3) Dual-Beam Mode. FIG. 5.8.

5.6.1.

In the reference-beam mode, FIG. 5.6, the laser light is split up into two beams which are directed at the place of measurement in the flow.

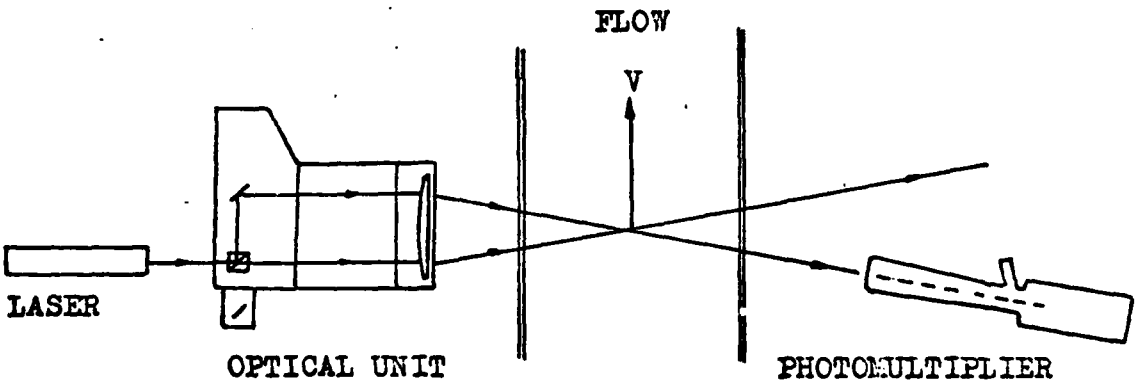

FIG. 5.6

The place of beam intersection forms the measuring volume. The intensity of the reference-beam can be reduced by introducing a neutral density filter to

optimise the signal picked up from the photomultiplier. The photomultiplier receives two signals, one with frequency shift and one without. The photomultiplier then emits an alternating current with a beat frequency, f_D equal to that of the Doppler frequency, equation (5.7)

5.6.2.

The Differential-Doppler Mode FIG. 5.7 is also known as the 'fringe mode' because the beams form a fringe system in the volume of intersection.

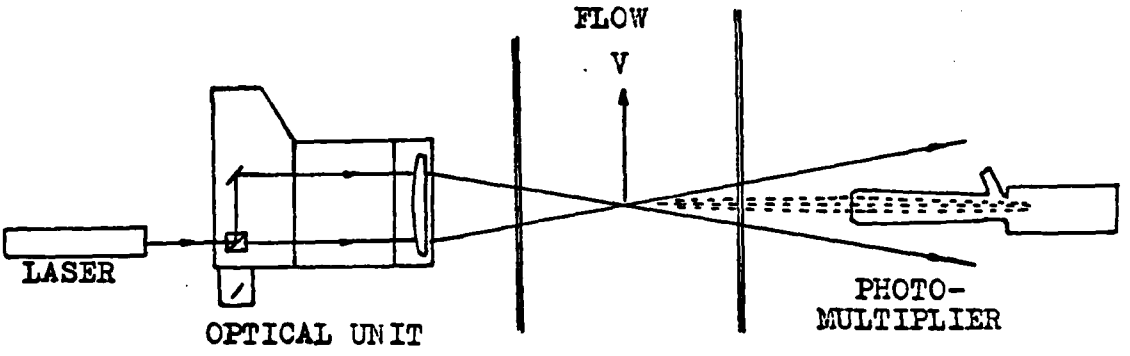

FIG. 5.7

This system is best used where the intensity of scattered light is low and, therefore the scattered light can be picked up over a wide angle since the differential Doppler frequency is independent of direction and detection.

In this mode the photomultiplier picks up scattered light signals from the same direction from two incident beams. Each scattered beam therefore has a frequency shift relative to the incident beam that it originates from.

The differential-Doppler mode can also be used with backscattering, however, even with high concentrations of scattering particles, the system necessitates the use of an extremely powerful laser. e.g.25mW.

In this mode, the equipment is located on one side of the flow only, hence the name 'backscatter'. One useful method whereby the 'backscattering' mode can be used is when the equipment is mounted inside the hull of a ship, and measurements are being taken of the velocity profile of the ship, relative to the water it passes through.

5.6.3.

The Dual-Beam mode, FIG. 5.8, is where the laser is situated on one side of the measuring volume and the Optical unit and photomultiplier are on the other.

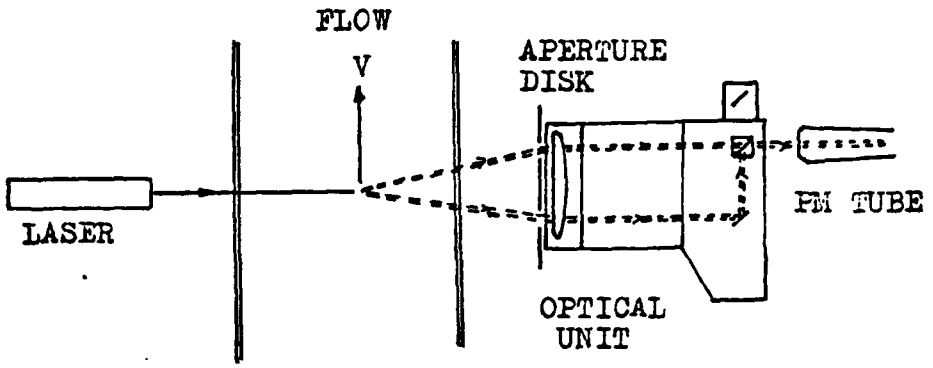

FIG 5.8

In this mode the aperture disks supplied with the optical unit are used by attaching the disk required to the front of the beam-splitter. The twin holes allow only two scattered beams to pass through the lens which are combined into one beam to be picked up by the photomultiplier.

The photomultiplier receives two light signals, each of which are scattered in a different direction from the same incident beam. Both signals, however, will have frequencies shifted with respect to the frequency of the incident beam. Again the output from the photomultiplier

will be of a signal equal to the beat frequency.

Due to the relative magnitude of the laser power, the dual-beam mode is not to be used in these investigations. The velocity measurements are to be confined to Reference-beam mode and differential-Doppler mode with forward scattering.

The systems as described previously, can also be modified whereby the introduction of extra beam-splitters and photomultipliers give the added advantage that both two and three dimensional flow measurements can be investigated.

5.7 Velocity Measurement.

The laser anemometer measures the Doppler frequency, f_D obtained from a frequency shift, due to particles in the flow. The advantage of this system is that particles may therefore be as small as the wavelength of the laser light, i.e. 632.8×10^{-9} m (0.0000006328m)[19] in diameter.

With particles as small in diameter as that shown, it is assumed that they have the same velocity as that of the flowing medium, even in regions of very high turbulence.

For all the modes of operation to be used in this investigation, the flow velocity can, therefore, be calculated from the equation:

$$V = \frac{f_D \times \lambda}{2 \sin \frac{\theta}{2}} \qquad (5.9)$$

where V = local flow velocity,

f_D = Doppler frequency,

λ = wavelength of laser light,

and θ = Beam intersection angle.

5.8 Light Scattering Particles.

The presence of particles in the fluid under investigation is essential to laser anemometry. Water however, normally contains an ample concentration of suitable particles, whereas atmospheric air and gases do not. Seeding must therefore be introduced of suitable size and quantity.

In general the particles must be small enough to be able to follow high frequency turbulence situations with accuracy better than 1%, also the concentration of such particles is of grave importance.

The particles, although small enough to follow the turbulence fluctuations, must be large enough to cause detectable scattering. The correct concentration amount varies depending on the mode of operation.

In forward fringe mode, the scattering particles are less than that for the reference-beam mode, whilst backscattering requires very much higher concentrations.

Due to the existing system, i.e. flow channel,and the conditions as previously mentioned with respect to rust particles etc., transported around the system, seeding of the flow is not required.

5.9 Equipment Supplied.

The Laser anemometer to be used to verify results obtained from the hot film anemometer was purchased from Disa, and represents Disa 55L Laser Anemometer Mark 1 system. This basically consists of six separate items:

1) 10mW maximum intensity Hughes Laser class 3B. with exciter.
2) 55L01 Optical Unit.
3) 55L02 Flow Direction Adapter.
4) 55L10 Photomultiplier.
5) 55L15 High Voltage Supply.
6) 55L20 Doppler Signal Processor.

These will be discussed separately.

5.9.1.

Laser.

The Laser recommended to fulfill our requirements was a 10mW maximum intensity Hughes Helium-Nean type class 3B. The usual recommended laser intensity for operating in the forward scatter modes is 5mW, therefore, the above should give good performance results.

The Laser, before being used, was checked for intensity and was found to be 6mW, therefore this unit is not

powerful enough to be used in the backscattering mode of operation.

5.9 (2&3)

Optical Unit including Flow Direction Adapter.

The main function of the optical unit is to produce two coherent beams of light from the initial single source. This type of optical unit is exceptionally versatile and can be used in all the modes of operation as discussed in section 5.6, except 2-Dimensional as this requires a supplementary unit.

Three focal length lenses are also supplied which give working ranges of 13cm, 30cm and 60cm respectively, thus allowing the intersection angle of the two laser beams to be continuously adjusted within a 1:3 range, e.g. between 8 and 24 degrees beam angle for a working distance of 13cm.

In the investigations of the velocity profile, the lens used has a focal length of 30cm. This was necessary because of the channel width, i.e. 30.5cm. The lens used also had minimum and maximum beam angles of 3.4 to 10.3 degrees respectively.

The biprism and adjustable surface mirror inside the housing, constitutes the beam-splitter. The mirror can be moved 25.5mm in a direction 55° to the system axis by means of a micrometer screw. The position of the mirror is indicated in a small window, and by this adjustment, the beam separation can be varied between 18 and 54mm respectively.

The two beam adjusters located on top of the unit, enable perfect intersection of the beams at the point of measurement. These beam adjusters are 2 glass wedges with wedge angles of 3° .These are positioned next to each other, but their tapers are at 90° to each other.

Now, by adjusting the micrometer screws, this permits rotation of the wedges, ensuring a high resolution of beam-adjustment for perfect beam intersection.

The unit also comes complete with an aperture disk for measurement in the dual-beam mode on forward scattering, however, it was the authors intention not to use this mode of operation.

FIG. 5.9 indicates a schematic diagram of the optical and flow direction adapter.

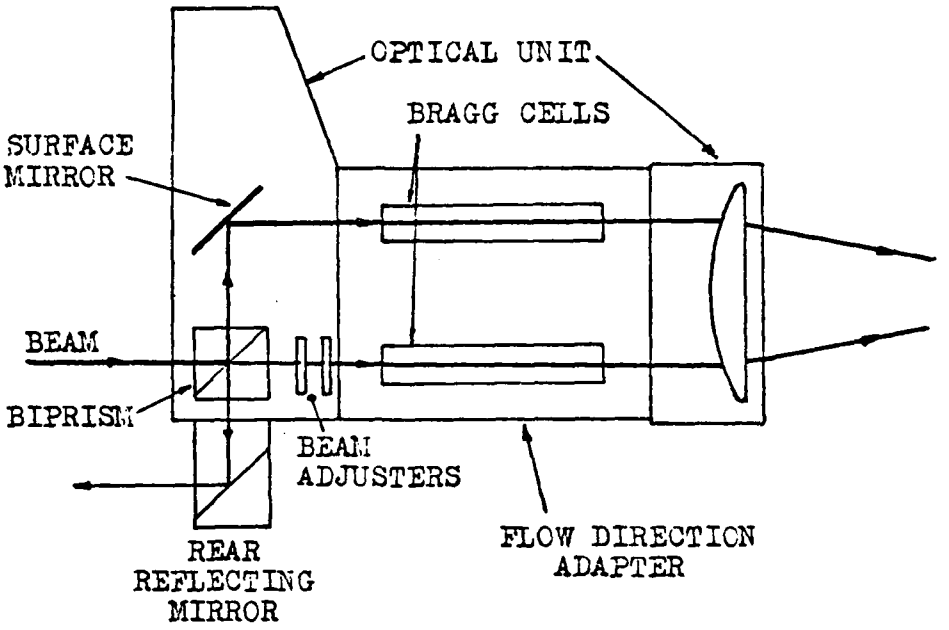

FIG. 5.9

The flow direction adapter is connected to the optical unit and contains two optical Bragg cells mounted in parallel. These cells are in a fixed position but their angular position may be adjusted to allow the laser beams to pass through undisturbed.

The Bragg cell consists of a block of acousto-optic material. Along one side of each of these blocks is bonded a series of piezoelectric transducers. Upon the application of an RF-voltage across the tranducers a train of plane acoustic waves is created in the material moving through the cell with the velocity of sound.The moving waves are absorbed by a damping material on arrival to the other side of the block. The acoustic wave fronts in the cell constitute a thick moving optical grating which diffracts the light passing through

AD-A081 394 TEESSIDE POLYTECHNIC MIDDLESBROUGH (ENGLAND) DEPT O--ETC F/G 13/10
DETERMINATION OF SURFACE FRICTION COEFFICIENT OF A REPLICA OF S--ETC(U)
APR 79 D C AUGUSTSON N00014-78-G-0059

UNCLASSIFIED NL

2 OF 3
AD
A081 394

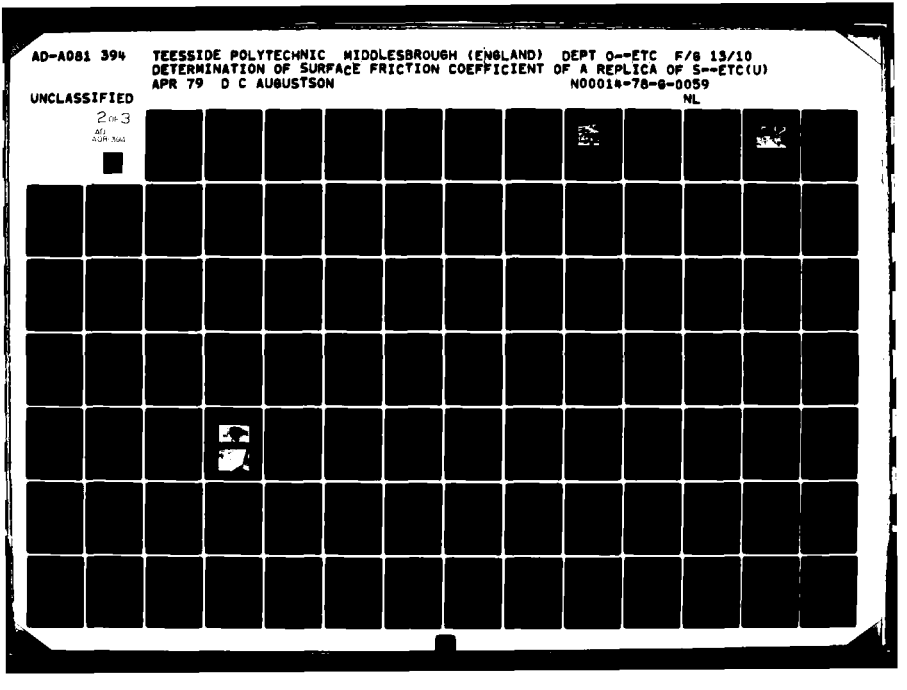

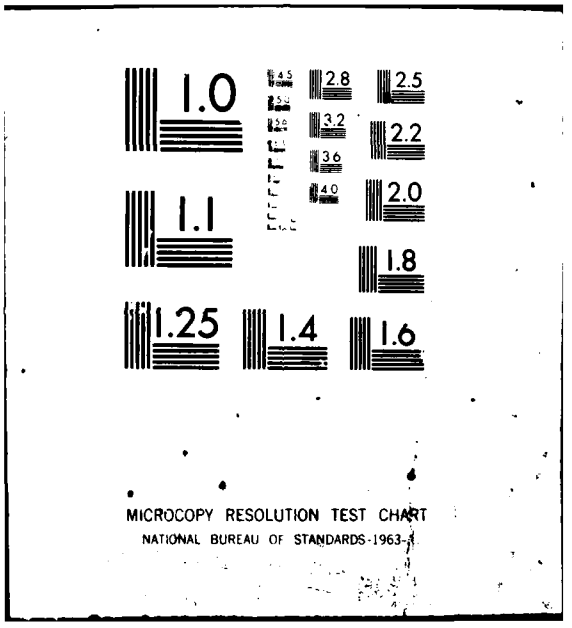
1.0
1.1
1.25
1.4
1.6
1.8
2.0
2.2
2.5
2.8
3.2
3.6
4.0
MICROCOPY RESOLUTION TEST CHART
NATIONAL BUREAU OF STANDARDS-1963-A

the cell. One cell shifts one input beam by a reference f_R plus an increment ($f_s/2$) and the other by a reference minus an increment ($f_s/2$), therefore the net frequency shift is f_s. This frequency shift may be used to measure highly turbulent velocities, and since the Doppler frequency fluctuation caused by the turbulent motion do not change, therefore the relative frequency range is reduced as the zero shift, f_0 is increased.

The effect of the frequency shift is thus to produce a detector current of frequency f_0 when measuring a particle at rest in the measuring volume, whereas the frequency is increased if the particle moves to one side and decreased when it moves to the other.

By means of the switch on the front of the flow direction adapter driver, seven frequency values f_0 may be selected, each of these frequencies corresponds to the midscale value on the 55L35 frequency tracker unit.

If a digital voltmeter is connected to the output from the meter unit without frequency shift the scale reading on the analog meter corresponds to 0-10V dc in all frequency ranges. However with frequency shift then 5V corresponds to zero velocity, also the sign on the unit,

+ or - indicates flow direction.

5.9.4.

Photomultiplier.

The photomultiplier detects the Doppler shifted light scattered from the point of measurement. FIG. 5.10 shows a diagramatic view of the unit.

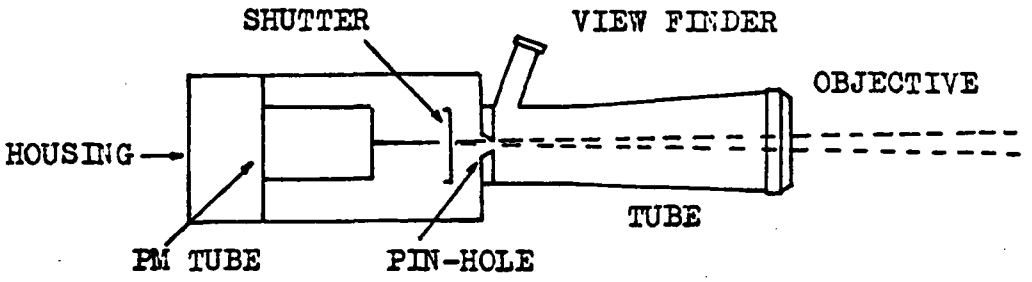

FIG. 5.10

The photomultiplier is located in the main housing and is protected from light by a built-in shutter controlled from a knob at the side.

A pin-hole aperture in front of the shutter prevents undesired light from hitting the PM. tube during measurement thereby optimizing the signal quality. Two

sprung adjusting screws enable the pin-hole aperture to be accurately centred on the scattered light, thus allowing adjustment for maximum possible quality and minimum possible ambient unwanted light.

The unit consists mainly of a tube section and focusing optics, and three close-up lenses are also supplied with focal lengths of 200, 333 and 600mm respectively.

It is important that the correct close-up lens is attached to the photomultiplier to match that as installed in the beam-splitter. Correct lens installation ensures optimum performance from the photomultiplier and allowing use of the same pinhole and aperture for all ranges of focal lengths.

Situations which occur whereby the photomultiplier is placed differently to that of the laser, will result in the pinhole requiring to be changed.

5.9.5.

<u>High Voltage Supply</u>.

The high voltage supply is the driving unit for the photomultiplier and supplies a continuously adjustable D.C. voltage.

Located on the front panel are two meters which indicate photomultiplier tube anode current and high voltage supplied respectively. The supply can be adjusted from 0 - 2000V dc, and has an accuracy range of 25%, whereas the anode current meter range is 0 - 100μA.

With this unit care must be taken that the correct high voltage cable is connected from the supply to the rear of the photomultiplier tube. This cable has modified BNC sockets, and is denoted with a red covering at its ends. This modified BNC connector is to prevent interchanging of the high voltage and signal cable connections thus causing grave damage to the photomultiplier tube.

5.9.6.

Signal Processor.

The Doppler Signal Processor consists of the following main circuits:

a) 55L30 Preamplifier.

b) 55L35 Frequency Tracker.

c) 55L40 Meter Unit.

a) Preamplifier.

The preamplifier input socket is connected to the output of the high voltage supply unit. As the name implies

the unit amplifies and filters the signal received from the photomultiplier tube. Upon setting of the frequency range on the Frequency Tracker, the built-in filters in the preamplifier are automatically switched for top and bottom signal cutting.

b) The Frequency Tracker can be both manually and automatically controlled. The manual control is utilized during the initial setting of the equipment and then by switching to 'auto' the unit tracks the Doppler frequency automatically.

This unit contains the electronics for optimising the signal to noise and ratio and also has the frequency range selector which gives seven frequency ranges 2.25 K Hz to 15 M Hz.

c) The last piece of equipment is the Meter Unit. This has 2 BNC output sockets located in parallel and the Meter indicates the Doppler frequency. The meter gives an analog reading of accuracy 1% f.s.d., however, by connecting one of the BNC sockets to a digital voltmeter then 0-10V refers to full scale deflection in all frequency ranges. This voltage therefore provides an instantaneous indication of the Doppler frequency and hence the flow velocity.

DESIGN OF LDA SUPPORT.

6.1 Design Considerations of LDA Support System.

Before the equipment as described in sections 5.9 could be used, it was necessary to design a support system whereby the laser, beam-splitter and photomultiplier could be mounted.

With regards to the existing channel and bearing in mind that it was hoped to take velocity measurements from the replica of the ships hull to the mainstream of the flow, as with the CTA unit, some means of traversing had to be allowed for.

Initially there were two possible design routes:

1) The support for the units could be attached to the existing channel main-frame. This was, however, decided against because of the restriction imposed from the ancillary channel leveling equipment. Supporting the units in this manner would have restricted the traversing along the channel to approximately 1 meter.
2) The second alternative was to mount the main support onto one of the existing traversing carriages.

Plate 5 indicates the final designed support system, drawings of which can be seen in Appendix F.

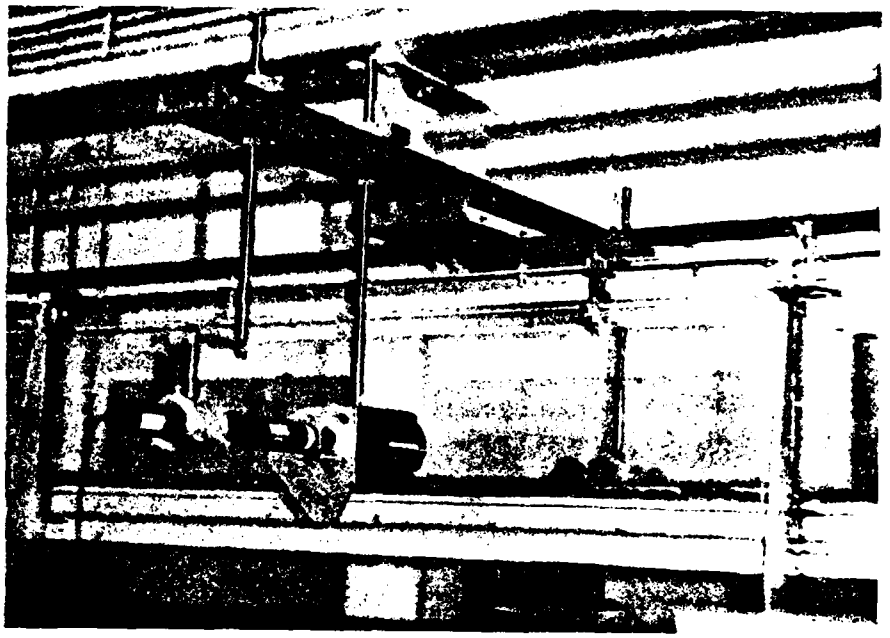

PLATE 5 SHOWING LASER SUPPORT

6.2 Design of LDA Support System.

It had been initially intended to mount all three units separately, whereby the brass support rods would pass through the main and sliding supports respectively. These would then be clamped into position using a cap screw at the side. Upon final receipt of the equipment this is how the LDA was initially set up.

From this initially set up the design progressed whereby the brass rods were threaded and six brass adjusting nuts were made. This enabled traversing in the vertical plane to be controlled and made with accuracy.

The critical alignment between the laser and the beam-splitter was not fully realised until the equipment was working, whereby it was decided that if the laser was attached to the beam-splitter, then the critical alignment between the two would no longer be necessary. Also by having the laser and beam-splitter attached resulted in the system being much more stable, and during traversing the unit moves as one.

Drawings of the designed frame including optical unit back plate etc., are as noted in appendix F.

To enable measurements to be taken in both the vertical and horizontal plane, the beam-splitter must be capable of being rotated through 90°. However, for vertical measurements this presented no problem, but in the horizontal plane the laser is not in line with the central axis of the optical unit. Therefore the laser support bar had to be cut and an adjusting bar made to account for the eccentricity between the two units.

In the investigation to be carried out, it was envisaged that only velocities in the horizontal plane would be obtained, therefore, once the laser / beam-splitter was set then this would not be moved other than for vertical traversing.

Plate 6 shows the laser and beam-splitter attached and positioned for measurement in the horizontal plane.

PLATE 6

REFRACTION.

7.1 Laws of Refraction.

The flow velocity can be calculated from the equation (5.9) of section 5.7.

$$\text{i.e. } V = \frac{f_D \times \lambda}{2 \sin \frac{\theta}{2}}$$

where V = local flow velocity.

f_D = Doppler frequency.

λ = wavelength of He-Ne Laser = 632.8×10^{-9} m.

θ = Beam intersection angle, degrees.

However, before any measurements are taken, it is necessary to take into consideration the fact that the laws of refraction must be strictly adhered to.

There are two basic laws of refraction, and these are:

1) The incident ray, refracted ray and normal are all 'coplaner' at the point of incidence.
2) For any two substances.

$$\frac{\sin i}{\sin r} = \text{constant } {}_1n_2 \qquad (7.1)$$

where n = refractive index of medium (2) with respect to (1).

This is more commonly known as 'Snells Law'.

FIG. 7.1 indicates the equation (7.1)

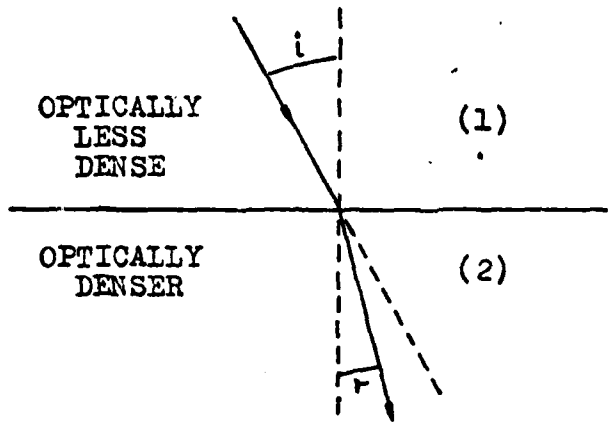

FIG. 7.1

If we consider FIG. 7.2.

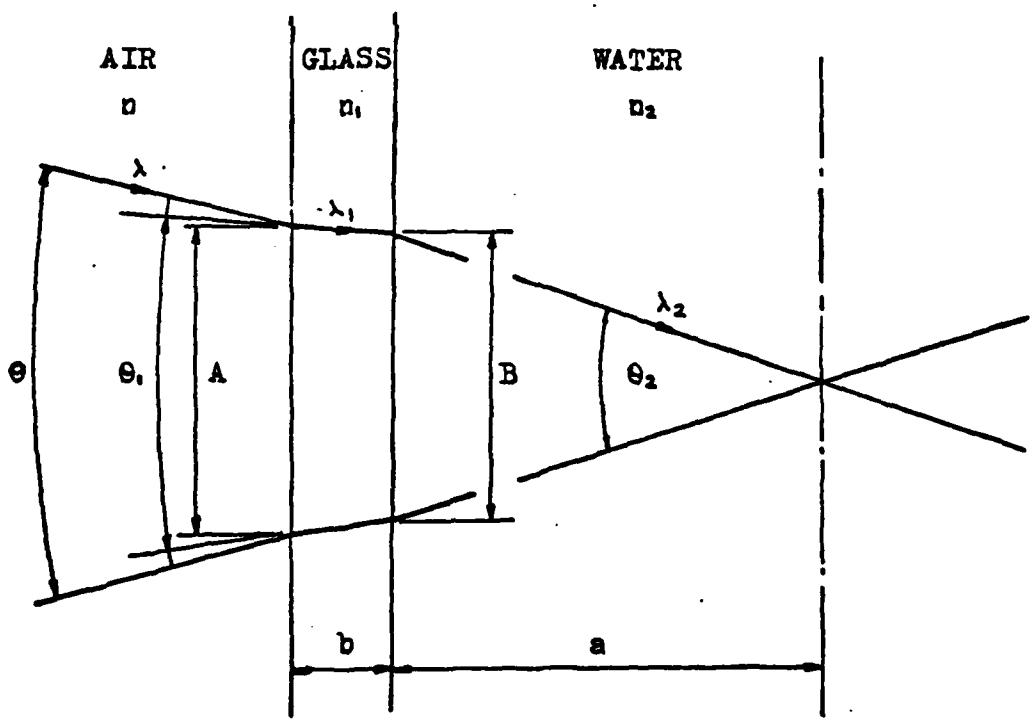

FIG. 7.2.

Now by considering the laws of refraction and from equation (7.1)

If we consider a beam of light passing from air to water, then the wavelength of the light will slow down as it travels through the various mediums.

$$\lambda_1 = \frac{n}{n_1} \lambda \qquad (7.2)$$

where λ_1 = wavelength of laser light in glass,

and $\lambda = 632.8 \times 10^{-9}$ m.

also,

$$\lambda_2 = \frac{n_1}{n_2} \lambda_1 \qquad (7.3)$$

therefore,

$$\lambda_2 = \left(\frac{n_1}{n_2}\right)\left(\frac{n}{n_1}\right) \lambda$$

$$\lambda_2 = \left(\frac{n}{n_2}\right) \lambda \qquad (7.4)$$

now,

$$\sin \frac{\theta_1}{2} = \frac{n}{n_1} \sin \frac{\theta}{2} \qquad (7.5)$$

and,

$$\sin \frac{\theta_2}{2} = \frac{n_1}{n_2} \sin \frac{\theta_1}{2}$$

therefore,

$$\sin \frac{\theta_2}{2} = \left(\frac{n_1}{n_2}\right)\left(\frac{n}{n_1}\right)\sin \frac{\theta}{2}$$

therefore,

$$\sin \frac{\theta_2}{2} = \left(\frac{n}{n_2}\right)\sin \frac{\theta}{2} \qquad (7.6)$$

From equations (7.4) and (7.6) it has been shown that both the angle of intersection and wavelength of laser light are independant of the glass sides of the channel.

In order to establish the actual position of the beam intersection within the flow, this can be done by measuring the width of the two beams at the initial point of entry on the glass side of the channel.

therefore,

$$\tan \frac{\theta_2}{2} = \frac{B}{2 \times a} \qquad (7.7)$$

where a = half the width of the channel.

also,

$$\tan \frac{\theta_1}{2} = \frac{(A-B)}{2 \times b} \qquad (7.8)$$

when b = thickness of glass side.

therefore $A = B + (A-B)$ (7.9)

where A equal to the distance apart of the two laser beams at entry into the channel.

Therefore it is possible to establish the intersection point within the flowing regime by fairly accurate measurement of the beam distance 'A'.

Therefore from the forgoing conclusions and using the initial equation (5.9)

$$V = \frac{f_D \times \lambda}{2\sin\frac{\theta}{2}}$$

This equation can be modified to take into account the laws of refraction whereby V can be calculated.

therefore,

$$V = \frac{f_D \times \lambda_2}{2\sin\frac{\theta_2}{2}} \qquad (7.10)$$

In atmospheric air the refractive index 'n' at 760mm Hg at 20°C [19]

$$= \underline{1.000277}$$

If however the flow medium is water as in these investigations, then, [19]

$$\underline{n_2 = 1.334 \text{ at } 0^\circ C}$$

The temperature dependance of 'n' in water is approx.

$$\underline{\Delta n = 0.0001/^\circ C} \quad [19]$$

Therefore if we assume that the water temp. is 10°C, then,

$$n_2 = 1.334 + 10(0.0001)$$

$$\underline{n_2 = 1.335}$$

where n = new refractive index at 10° C.

Therefore from equation (7.4) the wavelength of laser light in the flowing medium can be calculated:

$$\lambda_2 = \left\{\frac{n}{n_2}\right\} \lambda$$

$$\lambda_2 = \frac{1.000277}{1.335} \times 632.8 \times 10^{-9}$$

$$\lambda_2 = \underline{474.13879 \times 10^{-9} \text{ m.}}$$

BOUNDARY LAYER THEORY.

8.1 The Boundary Layer.

FIG. 8.1 illustrates a real fluid flowing past a surface or solid boundary.

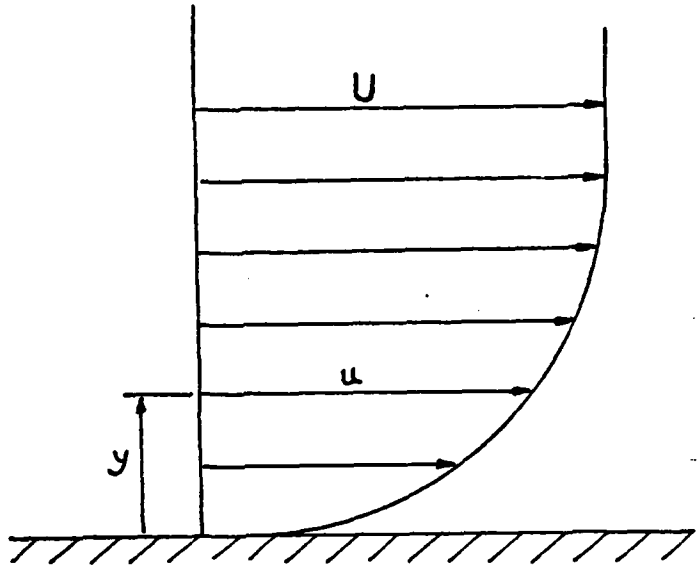

FIG. 8.1

At the boundary there is a very thin layer of fluid that adheres to the surface and therefore has a zero velocity with respect to the surface.

Some distance away in the mainstream, however, there is a region normal to the surface in the 'y' direction where the fluid has a constant velocity 'U'.

Near to the wall there is a region normal to it in which there is a velocity gradient where 'u' varies from zero to 'U', this region in which there is a

velocity variation is known as the 'boundary layer', and is usually designated δ (delta).

The concept of a boundary layer was first introduced in 1904 by the German engineer, Ludwig Prandtl, (1875-1953). He suggested that the flow may be considered in two parts:

1) That in the boundary layer where the shear stresses are of prime importance.
2) Beyond the boundary layer where (in general) velocity gradients are small, therefore the effect of viscosity is negligible.

If we consider the boundary layer in laminar flow, the fluid can be said to move in layers with one layer tending to slide with respect to its neighbour.

The shear stress is τ N/m^2

therefore $\tau = \mu \frac{du}{dy}$

where $\frac{du}{dy}$ is the velocity gradient and μ is the absolute viscosity.

Shear in laminar flow is caused by internal friction due to the molecular interaction between adjacent layers. There is however, no transfer of fluid between these

layers.

Linear Momentum.

The term 'linear momentum' of a body is defined as the product of the mass of the body multiplied by its linear velocity. In laminar flow, the momentum transfer between the adjacent layers is molecular, however, if the flow is 'turbulent' there is molecular friction plus an additional interaction due to the momentum transfer of fluid masses between adjacent layers.

The term 'turbulance' implies 'irregular fluctuations', not a regular motion.

The region close to the wall or surface may be classed as a 'turbulent boundary layer'. Close to the wall, however, there is a region in which the velocity approaches zero and the action between layers is purely molecular rather than turbulent. Therefore, although the whole layer may be classed as turbulent, the small laminar region close to the wall is termed the 'laminar sublayer'. This laminar sublayer may have an appreciable thickness, or it may be so thin that the molecular viscous action is extremely small in comparison with the turbulent mixing of the central region.

8.2 Thickness of a Boundary Layer δ (delta).

Because the velocity within the boundary layer increases to the velocity of the main-stream asymptotically some arbitary convention must be adopted to define the thickness of the layer.

One such possible definition of the thickness is that distance from the surface, whereby the velocity reaches 99% of the freestream velocity 'U'. In these investigations, to enable this distance to be identified clearly, the boundary layer has been taken to extend to 98% of the freestream velocity 'U'.

8.3 Displacement Thickness.

If we consider flow over a flat plate, the fluid will shear against the plate due to no-slip conditions causing a frictional drag. The velocity distribution will show a smooth drop-off to zero at the wall. If we consider the boundary layer thickness as that defined above, which is the thickness of the shear layer, then streamlines outside the shear layer will deflect amount δ^* 'the displacement thickness'.

Consider FIG. 8.2.

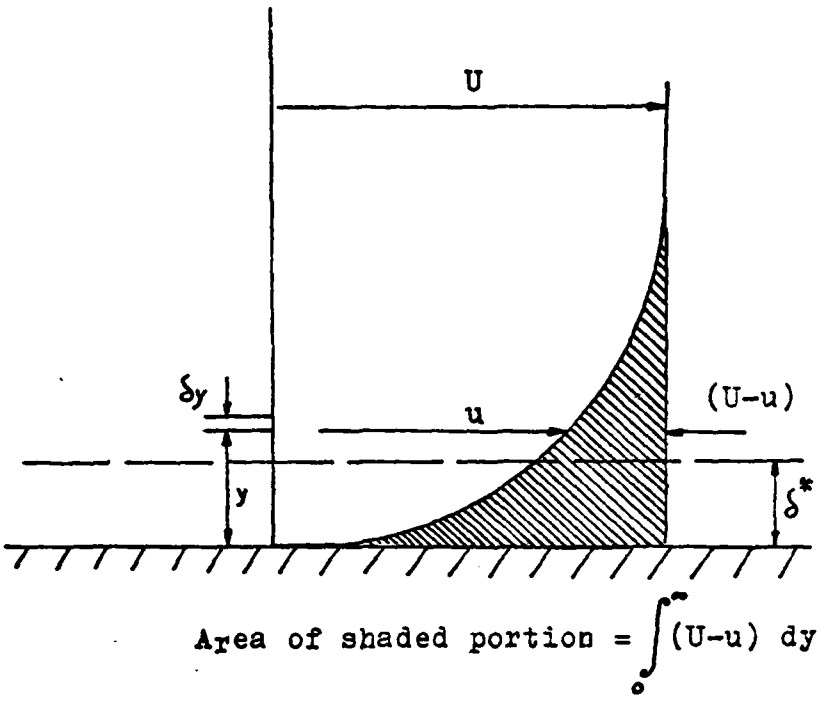

FIG. 8.2.

If we consider the velocity 'u' parallel to the surface at a distance 'y' from it, then the volume flow per unit width through an element y in two-dimensional flow is:

$$u\,\delta y \qquad (8.1)$$

If however there had been no boundary layer the flow would have been:

$$U\,\delta y \qquad (8.2)$$

Therefore the total reduction of flow caused by the

boundary layer is:

$$\int_0^\infty (U-u)\, dy \qquad (8.3)$$

Now to reduce the total flow of a frictionless fluid by that of equation (8.3) then this may be equated to $U\delta^*$,

Therefore,

$$U\delta^* = \int_0^\infty (U-u)\, dy$$

$$\delta^* = \frac{1}{U} \int_0^\infty (U-u)\, dy$$

$$\delta^* = \int_0^\infty \left(1 - \frac{u}{U}\right) dy \qquad (8.4)$$

Equation (8.4) is the formal definition of the boundary layer displacement thickness δ^* and holds true for any incompressible flow, whether laminar or turbulent, constant or variable pressure, constant or variable temperature.

8.4 Momentum Thickness θ (theta).

If we again consider the previous fig., the fluid passing through an element of the boundary layer carries momentum at a rate

$$(\rho u\, \delta y)\, u \text{ per unit width.}$$

whereas in frictionless flow the same mass of fluid would have momentum

$$(\rho u\, \delta y)\, U$$

Therefore for constant density the total reduction in momentum

$$= \int_0^\infty \rho(U-u)\, u\, dy \qquad (8.5)$$

Equation (8.5) represents the momentum flow under frictionless conditions through a thickness, θ

therefore,

$$(\rho U \theta)\, U = \int_0^\infty \rho(U-u)\, u\, dy$$

$$\theta = \int_0^\infty \frac{u}{U}\left(1-\frac{u}{U}\right) dy \qquad (8.6)$$

Equation (8.6) is the defining relation for a second parameter, the momentum thickness θ .

The definition holds true for any arbitrary incompressible boundary layer, but if we are not assuming that of a flat plate, θ is not equal to the drag divided by ρU^2. Therefore, this means that momentum thickness, although

useful in certain empirical correlations is by no means as fundamental a quantity as δ^*.

The equations(8.4) and (8.6) are illustrated by FIG. 8.3.

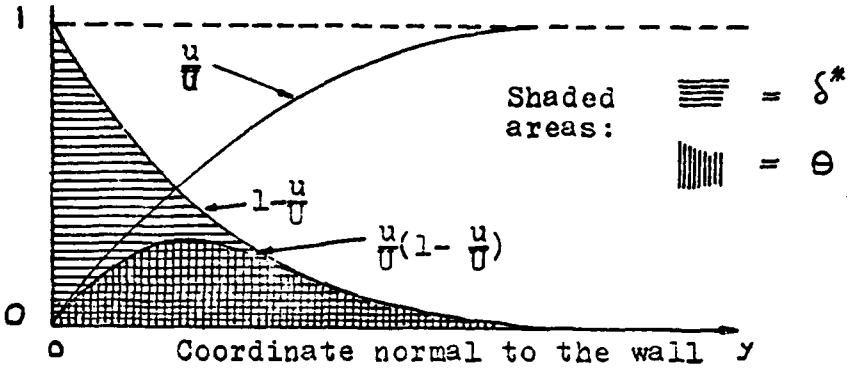

FIG. 8.3.

It should be noted that θ must always be less than δ^* and the ratio δ^*/θ is called the 'shape factor' and usually is denoted by H.

The value of H is always greater than unity and in turbulent flow varies from about 1.3 to 2.5.[5]

8.5.

The Two-Dimensional Turbulent Boundary Layer Equation.

There are three basic laws of conservation:

1) Conservation of Mass (Continuity)

2) Conservation of Momentum.

3) Conservation of Thermal Energy.

If by definition a boundary layer is one in which there are large lateral changes and slow longitudinal changes in flow properties,

and $\bar{v} \ll \bar{u}$ and $\frac{\partial}{\partial x} \ll \frac{\partial}{\partial y}$

then the equation for continuity and Momentum are:

continuity, $$\frac{\partial \bar{u}}{\partial x} + \frac{\partial \bar{v}}{\partial y} = 0 \qquad (8.7)$$

Momentum, $$\bar{u} \frac{\partial \bar{u}}{\partial x} + \bar{v} \frac{\partial \bar{u}}{\partial y} = U \frac{dU}{dx} + \frac{1}{\rho} \frac{\partial \tau}{\partial y} \qquad (8.8)$$

By integration of equation (8.8) across the boundary layer this yields the ordinary differential equation:

$$\frac{d\Theta}{dx} + (2 + H) \frac{\Theta}{U} \frac{dU}{dx} = \frac{\tau_w}{\rho U^2} = \frac{C_f}{2} \qquad (8.9)$$

The equation (8.9) is known as the Kármán momentum

integral relation.

At the minimum, two additional relations are required to supplement the Kármán integral relation, e.g. (8.9). This was first demonstrated by Ludwig and Tillmann in 1949, who correlated experimental skin-friction data from a wide variety of flow conditions. It was found that an effective algebraic correlation existed between the three variables θ , H and C_f and derived the empirical relationship:

$$C_f = 0.246\ Re_\theta^{-0.268} \cdot 10^{-0.678H} \qquad (8.10)$$

$$C_f = 0.246\ \left(\frac{u\theta}{\nu}\right)^{-0.268} \cdot 10^{-0.678H}. \qquad (8.11)$$

8.6 Use of Momentum and Displacement Thickness.

Once the velocity distribution has been obtained, then θ and δ^* can be calculated. From the velocity profile for probe traverse (2.1) and (2.2) the velocity at each distance 'y' from the base was obtained and divided by the freestream velocity 'U'. By assuming the velocity distribution follows that suggested by Prandtl whereby:

$$\frac{u}{U} = (y/\delta)^n \qquad (8.12)$$

various values of n were chosen whereby the value ob-

tained from $(y/\delta)^n$ gave the best agreement to u/U at that particular value of 'y'. The results of which can be seen in table E_1 and E_2 in appendix E.

It is now possible to obtain accurate values of θ and δ^* by integrating the velocity distribution from $0 \rightarrow \delta$ using the summation of the various power law profile. (Calculations of which are on the following pages.)

Now by substitution of the value θ and H (shape factor) into the empirical relationship proposed by Ludwig and Tillmann in 1949,[3] whereby C_f may be obtained directly:

$$C_f = 0.246 \left(\frac{U\theta}{\nu}\right)^{-0.268} . 10^{-0.678H.} \qquad (8.11)$$

8.7.

Calculation of C_f Using the Ludwieg-Tillman Empirical Equation.

To calculate the Momentum thickness θ for probe traverse (2.1) it can be seen from table E1 in appendix E that the velocity profile follows the 1/5th power law to 0.0425m. and the 1/4th power law to the edge of the boundary layer. Therefore, θ can be calculated by the evaluation of two integrals, from equation (8.6).

$$\theta = \int_0^{\delta} \left(\frac{y}{\delta}\right)^{1/n} \left(1 - \left(\frac{y}{\delta}\right)^{1/n}\right) dy$$

$$\theta_1 = \int_0^{0.0425} \left(\frac{y}{\delta}\right)^{1/5} \left(1 - \left(\frac{y}{\delta}\right)^{1/5}\right) dy$$

$$\theta_2 = \int_{0.0425}^{0.052} \left(\frac{y}{\delta}\right)^{1/4} \left(1 - \left(\frac{y}{\delta}\right)^{1/4}\right) dy$$

$$\theta_T = \theta_1 + \theta_2$$

$$\theta_T = \left[\frac{5}{6}\frac{y^{6/5}}{\delta^{1/5}} - \frac{5}{7}\frac{y^{7/5}}{\delta^{2/5}}\right]_0^{0.0425} + \left[\frac{4}{5}\frac{y^{5/4}}{\delta^{1/4}} - \frac{4}{6}\frac{y^{6/4}}{\delta^{2/4}}\right]_{0.0425}^{0.052}$$

$$\theta_T = \underline{0.006232} \text{ m.}$$

The displacement thickness δ^* can now be calculated using equation (8.4)

$$\delta^* = \int_0^{\delta} \left(1 - (y/\delta)^{1/n}\right) dy$$

$$\delta_1^* = \int_0^{0.0425} \left(1 - (y/\delta)^{1/5}\right) dy$$

$$\delta_2^* = \int_{0.0425}^{0.052} \left(1 - (y/\delta)^{1/4}\right) dy$$

$$\delta_T^* = \delta_1^* + \delta_2^*$$

$$= \left[y - \frac{5}{6}\frac{y^{6/5}}{\delta^{1/5}}\right]_0^{0.0425} + \left[y - \frac{4}{5}\frac{y^{5/4}}{\delta^{1/4}}\right]_{0.0425}^{0.052}$$

$$= 0.008484 + 0.0104 - 0.010172$$

$$\delta_T^* = \underline{0.008712} \text{ m.}$$

Shape Factor $H = \delta^*/\theta = \frac{0.008712}{0.006232} = 1.39795$

Using equation (8.11) C_f can be calculated

(8.11)

$$C_f = 0.246 \ (u\theta/\nu)^{-0.268} \ 10^{-0.678H}$$

$$C_f = 0.246 \left(\frac{0.565 \times 0.006232}{0.0000013}\right)^{-0.268} \cdot 10^{-0.678 \times 1.39795}$$

$$C_f = \underline{0.00334}$$

$$C_f = \frac{\tau_o}{\frac{1}{2}\rho U^2} \qquad \rho = 1000 \text{ Kg/m}^3$$

$$\tau_o = 0.00334 \times \tfrac{1}{2} \times \rho \times 0.565^2$$

$$\tau_o = 0.533 \text{ N/m}^2$$

$$u_o = \sqrt{\frac{\tau_o}{\rho}} = \sqrt{\frac{0.533}{1000}} = \underline{0.023 \text{ m/s}}$$

To calculate the momentum thickness θ for probe traverse (2.2) using the results in table E2 appendix E
From these results the velocity profile follows that as shown

$\left(\frac{y}{\delta}\right)^{1/5.6}$ from y = 0 to 1.5 mm.

$\left(\frac{y}{\delta}\right)^{1/5}$ from y = 1.5 mm to 17.5 mm.

$\left(\frac{y}{\delta}\right)^{1/5.6}$ from y = 17.5 mm to 42.5 mm.

$\left(\frac{y}{\delta}\right)^{1/5}$ from y = 42.5 mm to 52.5 mm.

$\left(\frac{y}{\delta}\right)^{1/4}$ from y = 52.5 mm to 65 mm.

Therefore, to completely evaluate θ and δ^* we require the addition of five integral equations respectively:

$$\theta_1 = \int_0^{0.0015} \left(\frac{y}{\delta}\right)^{1/5.6} \left(1 - \left(\frac{y}{\delta}\right)^{1/5.6}\right) dy$$

$$\theta_2 = \int_{0.0015}^{0.0175} \left(\frac{y}{\delta}\right)^{1/5} \left(1 - \left(\frac{y}{\delta}\right)^{1/5}\right) dy$$

$$\theta_3 = \int_{0.0175}^{0.0425} \left(\frac{y}{\delta}\right)^{1/5.6} \left(1 - \left(\frac{y}{\delta}\right)^{1/5.6}\right) dy$$

$$\theta_4 = \int_{0.0425}^{0.0525} \left(\frac{y}{\delta}\right)^{1/5} \left(1 - \left(\frac{y}{\delta}\right)^{1/5}\right) dy.$$

$$\theta_5 = \int_{0.0525}^{0.065} \left(\frac{y}{\delta}\right)^{1/4} \left(1 - \left(\frac{y}{\delta}\right)^{1/4}\right) dy$$

$$\theta_T = \theta_1 + \theta_2 + \theta_3 + \theta_4 + \theta_5$$

$$\theta_1 = \left[\frac{56}{66} \frac{y^{66/56}}{\delta^{10/56}} - \frac{56}{76} \frac{y^{76/56}}{\delta^{20/56}} \right]_0^{0.0015}$$

$$\theta_1 = \underline{0.0003616}\ m$$

$$\theta_2 = \left[\frac{5}{6} \frac{y^{6/5}}{\delta^{1/5}} - \frac{5}{7} \frac{y^{7/5}}{\delta^{2/5}} \right]_{0.0015}^{0.0175}$$

$$\theta_2 = \underline{0.0034708}\ m$$

$$\theta_3 = \left[\frac{56}{66} \frac{y^{66/56}}{\delta^{10/56}} - \frac{56}{76} \frac{y^{76/66}}{\delta^{20/56}} \right]_{0.0175}^{0.0425}$$

$$\theta_3 = 0.0334258 - 0.0269068 - 0.0117468 + 0.0080702$$

$$\theta_3 = \underline{0.0028424}\ m$$

$$\theta_4 = \left[\frac{5}{6} \frac{y^{6/5}}{\delta^{1/5}} - \frac{5}{7} \frac{y^{7/5}}{\delta^{2/5}} \right]_{0.0425}^{0.0525}$$

$$\theta_4 = 0.0419206 - 0.0344294 - 0.0325314 + 0.0256125$$

$$\theta_4 = \underline{0.0005723}\ m$$

$$\theta_5 = \left[\frac{4}{5} \frac{y^{5/4}}{\delta^{1/4}} - \frac{4}{6} \frac{y^{6/4}}{\delta^{2/4}} \right]_{0.0525}^{0.065}$$

$$\theta_5 = 0.052 - 0.0433333 - 0.0398163 + 0.0314551$$

$$\theta_5 = \underline{0.0003055}\ m$$

$$\theta_T = \underline{0.0075526}\ m$$

Similarly:

$$\delta_T^* = \delta_1^* + \delta_2^* + \delta_3^* + \delta_4^* + \delta_5^*$$

$$\delta_1^* = \int_0^{0.0015} \left(1 - \left(y/\delta\right)^{1/6.6}\right) dy$$

$$\delta_2^* = \int_{0.0015}^{0.0175} \left(1 - \left(y/\delta\right)^{1/5}\right) dy$$

$$\delta_3^* = \int_{0.0175}^{0.0425} \left(1 - \left(y/\delta\right)^{1/5.6}\right) dy.$$

$$\delta_4^* = \int_{0.0425}^{0.0525} \left(1 - \left(y/\delta\right)^{1/5}\right) dy.$$

$$\delta_5^* = \int_{0.0525}^{0.065} \left(1 - \left(y/\delta\right)^{1/4}\right) dy.$$

$$=$$

$$\delta_1^* = \left[y - \frac{56}{66}\frac{y^{11/56}}{\delta^{10/56}}\right]_0^{0.0015} = 0.0008507 \text{ m}$$

$$\delta_2^* = \left[y - \frac{5}{6}\frac{y^{6/5}}{\delta^{1/5}}\right]_{0.0015}^{0.0175} = 0.0053711 \text{ m}$$

$$\delta_3^* = \left[y - \frac{56}{66}\frac{y^{11/56}}{\delta^{10/56}}\right]_{0.0175}^{0.0425} = 0.003321 \text{ m}$$

$$\delta_4^* = \left[y - \frac{5}{6}\frac{y^{6/5}}{\delta^{1/5}}\right]_{0.0425}^{0.0525} = 0.0006108 \text{ m}$$

$$\delta_5^* = \left[y - \frac{4}{5}\frac{y^{5/4}}{\delta^{1/4}}\right]_{0.0525}^{0.065} = 0.0003163 \text{ m}$$

$$\delta_T^* = \underline{0.0104699} \text{ m}$$

$$\text{Shape Factor } H = \frac{\delta_T^*}{\theta_T} = \frac{0.0104699}{0.0075526}$$

$$= \underline{1.386264}$$

Using equation (8.11)

$$C_f = 0.246 \left(\frac{0.565 \times 0.0075526}{0.0000013}\right)^{-0.268} \cdot 10^{-0.678 \times 1.386264}$$

$$C_f = \underline{0.00323}$$

$$\tau_o = C_f \times \tfrac{1}{2} \rho U^2$$

$$\tau_o = \underline{0.5155} \text{ N/m}^2$$

$$U_o = \sqrt{\frac{\tau_o}{\rho}} = \sqrt{\frac{0.5155}{1000}} = \underline{0.0227} \text{ m/s}$$

8.8 Distribution of Velocity in Turbulent Flow.

Prandtl is credited with introducing (in 1925) the concept of a 'mixing length'. For molecular motion there is defined a term, mean free path of the molecule, which means the average distance a molecule travels between collision. Mixing length is analogous to 'mean free path'. This concept of a mixing length states that in the turbulent exchange the fluid masses displaced perpendicular to the mean flow carry momentum over a certain length perpendicular to the flow.

The mixing length is defined as the average distance perpendicular to the mean flow covered by the mixing particle. The turbulent shear stress τ can be taken as a function of,

$$f(\rho, du/dy, l) \qquad (8.13)$$

where l = mixing length.

du/dy = velocity gradient.

ρ = density.

The ratio τ/ρ has units of m^2/sec^2 and usually the expression $U_* = \sqrt{\frac{\tau}{\rho}}$ (8.14)
is used where U_* has units m/s.

Prandtl related the local r.m.s. fluctuations to the local velocity gradients through a turbulent length scale.

$$\sqrt{u'^2} \approx \ell_1 \frac{\partial \bar{u}}{\partial y} \qquad (8.15)$$

and,

$$\sqrt{v'^2} \approx \ell_2 \frac{\partial \bar{u}}{\partial y} \qquad (8.16)$$

Where ℓ_1 and ℓ_2 are called the mixing lengths which are analogous to the molecular mean free path but much larger.

In practice the particle does not move a distance ℓ and then suddenly changes velocity, but undergoes a gradual change. However, on the assumption that the change in velocity $\Delta\bar{u}$ experienced by the particle in moving a distance 1 in the y direction is $1\,\partial\bar{u}/\partial y$ and proportional to both u' and v' as described previously in equations (8.15) and (8.16).

$$\text{Now } \tau_t \text{ (turbulent shear)} = \frac{\text{Force}}{\text{Area}} = -\rho\overline{u'v'} \qquad (8.17)$$

Prandtl then deduced that $u'v' \propto l^2 (\partial\bar{u}/\partial y)^2$

Now by absorbing the coefficient of proportionality into the l^2 and accounting for the sign of τ_t with $\partial\bar{u}/\partial y$ using equation (8.17)

$$\tau_t = \rho l^2 \left|\frac{\partial \bar{u}}{\partial y}\right| \frac{\partial \bar{u}}{\partial y} \qquad (8.18)$$

Equation (8.18) is known as the Prandtl mixing length theory. It is however, dimensionally correct and realistic physically. The mixing length l is strongly dependant upon the distance from the wall y and the following empirical approximations have been suggested.

Very near the wall. (inner layer)	$l \sim y^2$	Suggested by (Reichardt 1951)
Fairly near the wall. (overlap layer)	$l = Ky$ where $K = 0.41$	(Karman 1930)
Far from the wall. (outer layer)	$l \sim$ constant.	(Prandtl 1942)

Karman in 1930 introduced a further concept by means of similarity, he suggested that the mechanism of turbulent friction can be fully characterized by a single length l only for the case in which the flow pattern in the neighbourhood of every point in similar.

Karman presented the following expression in terms of

the mean flow where:

$$l = K \left| \frac{\partial \bar{u}/\partial y}{\partial^2 \bar{u}/\partial y^2} \right| \qquad (8.19)$$

where K = The internationally accepted constant 0.41. This analogy however, does have loop holes, one of which is with regards to pipe flow.

The velocity profile across a turbulent boundary layer can be split into three regions; the 'inner', or wall layer where viscous shear dominates, the 'outer', or wake layer where turbulent shear is dominant and an 'overlap' layer where both types of shear are significant.

Prandtl deduced that the mean velocity must depend upon the wall shear stress, the fluid properties and the distance y from the wall, therfore the inner law can be expressed as:

$$u = f(\tau_o, \rho, \mu, y) \qquad (8.20)$$

and therefore,

$$u/U_o = f(y U_o/\nu) \qquad (8.21)$$

where $U_o = \sqrt{\frac{\tau_o}{\rho}}$ m/s

For the outer layer Karman deduced that the wall tends to act merely as a source of retardation reducing the local velocity u below the freestream velocity U independently of viscosity μ but dependant upon the wall shear stress and the distance y over which its effect has diffused. Therefore the outer, or velocity defect law,

$$U-u = f(\tau_o, \rho, y, \delta) \qquad (8.22)$$

$$U-u/U_o = g(y/\delta) \qquad (8.23)$$

where f and g refer to function off respectively.

For the overlap region it is possible to merge the two functions together because these two laws are valid.

This is the overlap region:

$$u/u_o = f((\delta u_o/\nu)(y/\delta)) = U/u_o - g(y/\delta) \qquad (8.24)$$

For the equation above to be true it can only be so if both f and g are logarithmic functions,

where, $u/u_o = \frac{1}{K}\log_e(\frac{yu_o}{\nu}) + B$; inner variables (8.25)

and $U-u/u_o = -\frac{1}{K}\log_e(\frac{y}{\delta}) + A$; outer variables (8.26)

In the equations (8.25) and (8.26) K,A and B are purely dimensionless constants.

where K = 0.41 Von Kármán constant.

B = 5.0 Coles constant (1955)

and, A varies depending on whether or not the flow is boundary layer flat plate or Pipe or channel flow, therefore for a smooth flat plate,

$$u/u_\circ = \frac{1}{K}\log_e\left(\frac{y u_\circ}{\nu}\right) + 5.0$$

$$u/u_\circ = 2.439\log_e\left(\frac{y u_\circ}{\nu}\right) + 5.0 \qquad (8.27)$$

The constant A varies from 2.35 for boundary layer flow (flat plate) to 0.65 for Pipe or channel flow. If in the case A = 0 this would mean that the outer layer has completely vanished so the logarithmic overlap extends all the way to $y = \delta$. Therefore for A = 2.35 means that there is a small overlap layer and for A = 0.65 means that a negligibly small overlap exists.

The validity of the inner law can be seen by plotting $u/u_\circ$ against $\log_e\left(\frac{y u_\circ}{\nu}\right)$ or $\left(\frac{y u_\circ}{\nu}\right)$ for probe traverse (2.1) and (2.2) graphs in appendix E.

From these graphs the inner region extends between

$36 < \left(\frac{y u_o}{\nu}\right) < 90$ and the logarithmic overlap would seem to extend from $90 < \left(\frac{y u_o}{\nu}\right) < 270$.

The outer layer turns upwards and extends from $\left(\frac{y u_o}{\nu}\right) > 270$, whereby for traverse (2.2) a strong adverse pressure gradient exists.

8.9 Law of the Wake.

With reference to the graphs E5 and E6 in appendix E the profiles clearly differ in their outer behaviour for probe traverse (2.1) the profile is fairly linear, whereas (2.2) indicates strong adverse gradients.

Clauser noticed that the outer law should be modified to include pressure gradient, dP/dx, and he also replaced δ , by δ^* , arriving at the parameter,

$$\beta = \frac{\delta^*}{\tau_0} \frac{dP}{dx} \qquad (8.28)$$

After considerable experimental procedure, Clauser showed that a boundary layer with variable pressure gradient but with β constant is in turbulent equilibrium in the sense that all the gross properties of that boundary layer can be scaled with a single parameter.

Clauser determined the most relevent thickness parameter for equilibrium to be the defect thickness, Δ

where, $$\Delta = \int_0^\infty \frac{U-u}{U_0} dy = \delta^* \lambda \qquad (8.29)$$

where, $\lambda = \sqrt{2/C_f}$ is a measure of the local skin friction.

Since the skin friction varies with x it follows that H is not constant in an equilibrium boundary layer. This can be seen from the previous calculations,

probe traverse (2.1) $H = 1.39795$

probe traverse (2.2) $H = 1.386264$

From further work by Alber(1968) G was adopted as a form factor rather than H and a curve-fit relation proposed by Nash (1965) related G to the Clauser parameter β , thus the shape factor was related approximately to the pressure gradient.

One of the major weaknesses to Clauser approach was that curves produced by him were not easily readable, however, Coles (1956) noted that deviations of the velocity above the overlap layer when normalised by the maximum velocity deviation (at $y = \delta$) would be a single wake-like function of y/δ only.

Coles therfore proposed the following deviation,

$$\frac{u^+ - 2.5 \ln y^+ - 5.5}{U^+ - 2.5 \ln \delta^+ - 5.5} \approx \tfrac{1}{2} W(y/\delta) \qquad (8.30)$$

where $u^+ = u/u_\tau$ (8.31)

$y^+ = y u_\tau/\nu$ (8.32)

and $U^+ = U/u_\tau$ (8.33)

W is known as the wake function and is normalised to be zero at the wall and have a value of 2 at $y = \delta$. Thus Coles proposed the following curve-fit approximation for the wake function:

$$W(y/\delta) \approx 2\sin^2 (\pi/2 \cdot y/\delta) \qquad (8.34)$$

Therefore the equation (8.25) was modified to include this function resulting in

$$\frac{u}{u_\tau} = \frac{1}{K} \log_e \left(\frac{y u_\tau}{\nu}\right) + B + \frac{\Pi}{K} W(y/\delta) \qquad (8.35)$$

When Π is called the wake parameter and is related to the outer-variable overlap constant of (8.26) by $\Pi = KA/2$ where for a flat plate $\Pi \approx 0.5$.

Coles wake function $W(y/\delta)$ has since been modified to the empirical modified version.

$$W(y/\delta) = \left[6(y/\delta)^2 - 4(y/\delta)^3\right] + \frac{1}{\Pi}(y/\delta)^2(1 - y/\delta) \qquad (8.36)$$

However, as previously stated at $y = \delta$ this function has the value 2, and at $y = 0$, equals 0. Therefore near to the wall, e.g. y = 0.004m. the wake function has the value 0.045 for probe traverse (2.1) and 0.029 for probe traverse (2.2). Therefore, due to its rela-

tive magnitude it is possible to neglect it when considering the equation (8.35).

8.10 Roughness.

The preceding computations are valid only for smooth-walled channels. Roughness of the surface has very little effect in laminar flow but influences turbulent flow due to the laminar region being fairly thin.

In laminar flow the viscous region extends all the way to the edge of the boundary layer.

The average roughness height k is such that $k = \frac{k u_o}{\nu}$ and will effect the inner law but not the outer law. Therefore, from the graphs E_3 and E_4 appendix E for slopes plotted with different values of u_o then the graph which compares to the smooth wall profile is displaced an amount ΔB therefore equation (8.35) can be rewritten to take into account this shift,

$$\frac{u}{u_o} = \frac{1}{k} \log_e \left(\frac{y u_o}{\nu}\right) + 5.0 - \Delta B + \frac{\Pi}{k} W(y/\delta) \qquad (8.37)$$

For probe traverse (2.1) the graph which lies parallel to that for a smooth plate is plotted using $u_o = 0.0241$ the displacement $\Delta B = 1.658$.

$$\frac{u}{u_o} = \frac{1}{k} \log_e \left(\frac{y u_o}{\nu}\right) + 5.0 - 1.658 + \frac{\Pi}{k} W(y/\delta) \qquad (8.38)$$

For probe traverse (2.2) the graph plotted using $u_o = 0.024$ gives best agreement with that of the smooth plate and the displacement $\Delta\beta = 2.118$.

$$\frac{u}{u_o} = \frac{1}{K}\log_e\left(\frac{y u_o}{\nu}\right) + 5.0 - 2.118 + \frac{\Pi}{K} W(y/\delta) \qquad (8.39)$$

Therefore the displacement $\Delta\beta$ would have been zero had the plate been smooth, thus this value can be related to the roughness of the surface.

Prandtl and Schlichting[3] analysed various compiled roughness configurations obtained by Clauser and evolved the approximate roughness representation,

$$\Delta\beta \approx \frac{1}{K}\log_e k^+ - 3.0 \qquad (8.40)$$

$$\Delta\beta \approx \frac{1}{K}\log_e\left(\frac{k u_o}{\nu}\right) - 3.0 \qquad (8.41)$$

$$\Delta\beta \approx \frac{1}{K}\log_e 0.3\left(\frac{k u_o}{\nu}\right) \qquad (8.42)$$

8.11 Calculation of C_f using the Inner Law.

From the previous section using equation (8.38) for probe traverse (2.1),

$$\frac{u}{u_o} = \frac{1}{K}\log_e\left(\frac{yu_o}{\nu}\right) + 5.0 - 1.658$$

neglecting the wake function.

the value of u_o that satisfies this equation is 0.0241, therefore, from equation (8.14).

$$u_o = \sqrt{\frac{\tau_o}{\rho}} \quad m/s$$

$$\tau_o = (0.0241)^2 \times \rho$$

$$C_f = \frac{\tau_o}{\frac{1}{2}\rho U^2}$$

$$C_f = \frac{(0.0241)^2}{\frac{1}{2} \times U^2} = \underline{0.00364}$$

using equation (8.42) and relating ΔB to the roughness height

$$\Delta B = \frac{1}{K}\log_e 0.3\left(\frac{k u_o}{\nu}\right)$$

$$1.658 = 2.439 \log_e 0.3\left(\frac{k u_o}{\nu}\right)$$

therefore the value of k which satisfies the above equation

$$= \underline{0.000355m}$$

For probe traverse (2.2)

$$\frac{u}{u_0} = \frac{1}{K} \log_e \left(\frac{y u_0}{\nu} \right) + 5.0 - 2.118$$

and $u_0 = 0.024$ m/s

$$C_f = \frac{(0.024)^2}{\frac{1}{2} U^2} = \underline{0.00361}$$

as previous,

$$\Delta B = 2.439 \log_e 0.3 \left(\frac{k u_0}{\nu} \right)$$

$$2.118 = 2.439 \log_e 0.3 \left(\frac{k u_0}{\nu} \right)$$

therefore the value of k which satisfies this value is

$$= \underline{0.00043 \text{m.}}$$

OPERATION OF LDA SYSTEM.

9.1 Connecting Up Of Laser Electrical Equipment.

Once the three units,(laser, beam-splitter and photo-multiplier) are attached to the support system they can be connected up electrically by following the procedure as laid down below.

1) Connect the High Voltage cable supplied to the rear of the High Voltage supply Unit (55L15) and Photomultiplier (55L10) respectively.

2) Connect the 'signal out' on the photomultiplier to the 'in' socket on the high voltage supply unit.

3) Connect the 'out' socket on the high voltage supply unit to the 'in' socket on the front of the 55L30 Preamplifier.

4) Connect one of the output sockets on the 55L40 Meter unit to a dc digital voltmeter. (If possible the digital voltmeter should have the facility of an exponential time constant variation, this will allow the Doppler frequency to be averaged over a particular time interval).

5) The equipment can now be switched on as it is ready for use.

6) Note: the laser should not be switched on until measurements are to be taken.

7) The photomultiplier shutter must be kept closed so as not to damage the photo-tube.

9.2.

Adjusting LDA Equipment to Obtain Doppler Frequency.

As soon as the position of the laser/beam-splitter, relative to the side of the channel, has been established by consideration of section 7 (laws of refraction) the photomultiplier can be adjusted for maximum scattered light entering the lens. This is done by looking down the view finder and adjusting the two screws on the Pin-hole aperture for maximum effectiveness. The shutter on the photomultiplier can now be opened using the knob placed on the end of the housing, whereby this allows the scattered light to hit the PM tube.

The high voltage control knob should be increased until the Anode Current Meter reads approximately 50 μA, this should be at about 400 Volts, depending on the amount of scattering.

Now the SET LEVEL knob on the Preamplifier should be adjusted so the meter reads approx. mid-scale, which can be readjusted when the correct Doppler frequency range has been found.

The tuning selector switch on the Frequency tracker should be set to MAN and the tuning knob turned fully

clockwise. Adjust the SET LEVEL and ADJUST THRESHOLD to the middle positions and also set the IF bandwidth at 2% of frequency range, the drop out detector can now be adjusted and frequency range set at 15 MHz. The Doppler frequency meter should show full scale deflection.

Now turn the tuning knob slowly anti-clockwise until the IF level meter indicates a peak, if no peak is obtained, then adjust the Frequency range to the next lower value. The tuning procedure should now be repeated.

The frequency selector should be decreased until the IF level meter peaks and the Doppler frequency meter indicates the Doppler frequency of the signal. This will be indicated on the dc voltmeter whereby 0-10V indicates meter full scale deflection in all frequencies.

If however, the IF level meter does not peak, this may mean that:

a) the flow velocity is zero.

b) there is poor beam intersection.

c) scattering of the particles is too low.

d) Photomultiplier has been incorrectly

focused on the measuring volume.

e) the flow may be highly turbulent.

After manual setting, set the tuning selector to AUTO and the Doppler frequency is automatically tracked. The SET LEVEL knob can now be readjusted so the IF level meter reads mid-scale.

If the velocity range varies quite considerably over the measuring volume, then the Doppler frequency may go out of frequency range, the tracker will drop out of lock and resetting is required.

If the velocity of the fluid is known approximately, then the correct frequency range can be set initially. By traversing across the flowing regime the Doppler frequencies can be obtained at various positions from the surface and hence, using equation (7.10), the velocity can be calculated.

However, due to the late arrival of the equipment, no time was available to complete this work.

Plates 7 and 8 indicate the intersection of the two laser beams as they pass through the channel for measurements in the vertical and horizontal plane respectively.

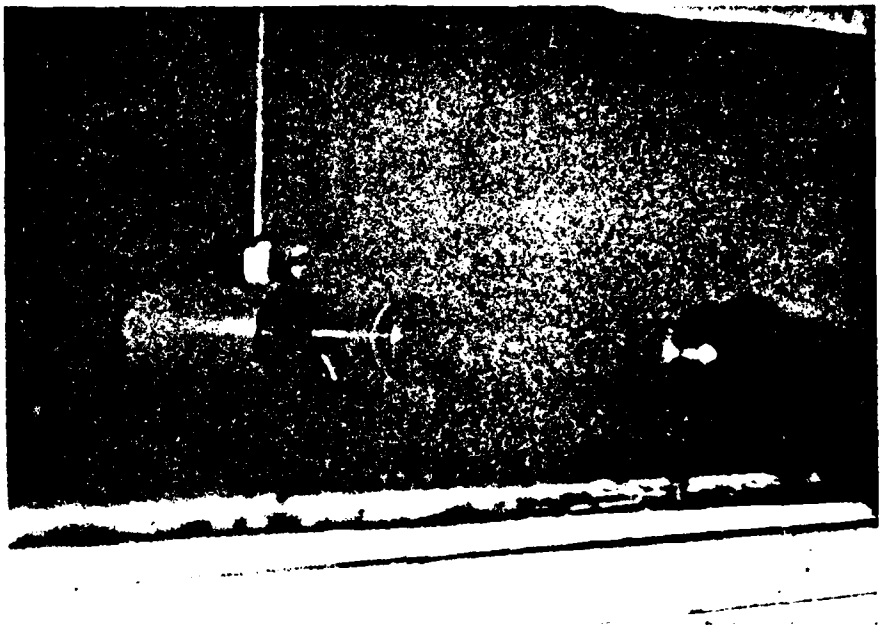

PLATE 7.

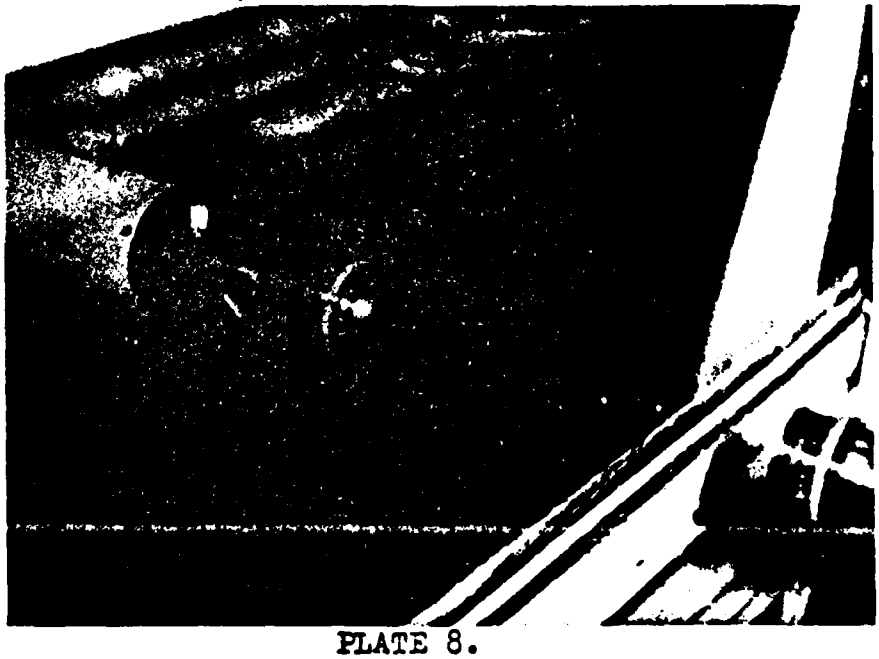

PLATE 8.

9.3 Safety Precautions.

Because of the light source being what it is, that of a laser, it is extremely important that certain safety precautions are taken.

Firstly, the laser beam must never be directly looked into because the harmful radiation will damage the delicate cells in the eye.

Secondly, if the beam hits the eye directly, then due to the eyes focusing ability this magnifies the power of the laser approximately 100000 times over a minute area killing the sensitive cells that the focused beam hits. This magnified power is of the order of 600 Watts.

Therefore, because the working region is at approximately eye level, it would be beneficial to provide some form of 'platform' along the working region of the channel ensuring that any future operators are at least working above the line of action of the laser.

Due to the two laser beams passing in and out of the channel, this means that there are four possible reflective surfaces to which the beams pass through. When operating the unit it was noticed that due to

reflection, there was a region approx. 12inches either side of the initial entry point of the two beams, whereby reflected laser light emitted.

Therefore, to prevent the author being hit in the eye, a timber screen was attached to the beam-splitter which extended this spread and shielded him from the stray beams.

9.4 Future Developments.

It is envisaged that this project, using the LDA will be continued. However, the support system designed was only that of a temporary set up in order to verify the CTA results, and it is hoped that a future sophisticated support system, incorporating automatic traversing etc. will be built. This future support will allow the laser/beam-splitter and photomultiplier to be positioned at various angles whereby the two laser beams can be focused on the surface, hence accurate velocities at the surface can be obtained.

With the present system, the closest one can measure from the surface is approx. 0.5mm. However, there are certain set-backs using the existing channel, and these are:

1) Because the existing glass sides are plate glass then there is quite a large amount of refraction of the two laser beams at inlet and entry.

2) If the beam-splitter is to be set at various angles, then alignment of the two glass sides will be critical.

3) Because of the beam-splitter set at an angle, then this may mean that one beam enters the channel

before the other, this will result in the two beams being out of alignment which may be out of the range of the beam adjusters.

4) If the units are to be used other than in the horizontal plane, then a working region in the channel will have to be decided upon, and the existing glass sides should be replaced with Schlieren glass to obtain best possible results.

DISCUSSION.

10.1 Equipment Used.

From the previous sections, 3.1.1 to 3.1.4, it is quite evident that there are only two types of equipment suitable for close boundary layer work. These are the Constant Temperature Anemometer and the Laser Doppler Anemometer.

All other types of equipment cause large scale disturbance to the flow invalidating any results.

The Propeller type current meter, however, is a very useful piece of equipment because it does give a quick indication of the velocity in a freestream. This was used to establish that there is a central core within the channel where the flow is uniform potential. The proof of this can be seen from appendix D FIG. D1.

10.2 Difficulties Observed Using the CTA.

This equipment, because of its relative size, makes it ideal for close boundary layer work, there is a minimum flow disturbance, both between the probe and the surface and around the probe. However, there is some disturbance no matter how slight, which therefore causes the validity of results obtained very close to the surface, to be treat with caution.

The CTA relies upon the amount of heat conducted away from the sensing element, therefore when working very close to steel surfaces there will be a higher conduction rate than when working close to plastic surfaces, thus again results obtained depending on the environment must be treat with suspicion.

It should be remembered that the concept of the boundary layer probe being so minute, is that velocities can be obtained as near to the surface as possible.

During the velocity traverse using probes 1 and 2 the linearizer was constantly connected to an oscilloscope so that the turbulence fluctuations could be observed. From the results for probe 1 and 2 calibration, the voltage results, although taken through a varying range of flow rates with Re varying between 10615 to

2840 for probe 1 and 13530 to 3438 for probe 2 are fairly steady with no large scale fluctuations. However, upon observation of results obtained for the various probe traverses where Re is in the region 1.79×10^6 to 2.053×10^6 there are large voltage fluctuations. The Re transition range for a flat plate is approx. 2×10^6 depending upon roughness, therefore it has been assumed that the values above are within the Re transition range. This turbulence intensity was observed on the oscilloscope and it was also noticed that the voltage recording equipment did not seem to keep pace with the response from the probe. Therefore it was decided to build a small RC integrator with a time constant of approx. 10 seconds using solid state resistors and capacitors. When connected to a standard type ac/dc digital voltmeter this then integrated the voltage signals from the linearizer giving a single value of mean integrated voltage and not a fluctuating one. After comparing the results from this unit with that obtained from the data logging system the two sets of voltage did compare quite favourably. Also a Solartron digital voltmeter was used with the facility for varying the exponential time constant and the results obtained from that compared with the results from the data logger. One other possibility however exists, and that is, the probes recording equipment cannot keep pace with the frequency response from the probe due to the turbulent intensity. If this is so then improvements in the response of the unit will be

required. It should be noted that all voltage readings recorded on the data logger during a test were accepted as being required by the bridge for balance even though some readings seemed either too high or too low compared with the rest. As mentioned in section 4.10, Probe Contamination, before being used the probe was gently brushed using a dilute solution of acetic acid. This was to remove impurities from the probes operating surface. However, it was also observed that if the probe was submerged and set to operate, the recorded voltages could only be guaranteed for a period of some 20 seconds, whereby the probes sensing characteristics would start to reduce thereby giving slowly decreasing voltage results. The wandering of the probes voltage would eventually end up at zero after about 45-60 seconds. Therefore, it was necessary to limit the test time to approx. 10 seconds, whereby 30 voltage readings were recorded. If the probe was now withdrawn from the flow and brushed with clean water, re-submerged and switched to operate, the probe would once again be operating satisfactorily. Therefore, it is quite evident that some form of insulation was building up on the probe, which was most probably due to air bubbles forming on the surface caused by nucleation effects due to the operating temperature of the probe. The perpetual brushing of the delicate probes sensing element inevitably meant that the odds against damaging the probe were reducing. Probe 1 was however, damaged

in this way. Before Probe 2 could be used this meant resetting of the probes operating resistance and frequency response was necessary, and then recallibration thus reducing the overall efficiency in the method of velocity measurements. As mentioned in section 2.3, the system incorporates a filtration system.This system cannot, however, be guaranteed to filter all the water in the system and particles of rust and debris still pass through the channel. Probe 2 was damaged at probe traverse (2.3) by one such deposit hitting the probe.

The calibration of the probes was carried out in a glass tube, where the flow was such that the Re numbers indicated fully turbulent flow. If however, the probes had then been used to obtain velocity measurements whereby the Re numbers indicated laminar flow the equations (4.8) and (4.9) could not have been used with accuracy. Therefore this presents another problem using the CTA, and that is that it must only be used in the same type of flow it is calibrated in, otherwise results would be suspect.

Therefore, from these observations and the difficulties encountered, it would indicate that the hot film probe is not very suitable a method for velocity measurements in a substance that has such large conductivity changes, and varying flow regimes unless calibration in the flow types has been carried out.

10.3 Velocity Profiles.

The graphs as plotted for probe traverses (1.1), (2.1), (2.2) and (2.3) do however give fairly good interpreted velocity profiles. To establish the thickness of the boundary layer this has been taken as to extend to 98% of the freestream velocity, and for probe traverses (2.1) and (2.2) was 52mm and 65mm respectively.

10.4 Evaluation of C_f.

Initially C_f was calculated from the Ludwieg - Tillman empirical equation (8.11), but first it was necessary to calculate the displacement thickness δ^*, and the momentum thickness Θ. For the calculation of δ^* and Θ the Prandtl power law was used wherby $u/U = (y/\delta)^n$ where n is some power (usually 1/7 for smooth surfaces).

The results table E1 and E2 are for probe traverses (2.1) and (2.2) respectively and indicates that the best values of n which satisfy $(y/\delta)^n = u/U$.

For rough surfaces the value of n reduces to less than 1/7 and these results illustrate that this is so, the value of n varies from 1/4 to 1/5.6 for the profiles (2.1) and (2.2).

Once the shape of the velocity profile was obtained the equations (8.4) and (8.6) could be evaluated and Cf obtained directly. The calculations of which are in sections 8.7.

The equation (8.11) is an empirical equation and is formerly accepted as an addition to boundary layer computation. However, its accuracy is only of the order of $\pm$ 10%, due to the fact that the power law does not give a good approximation. However, from these calculations, one power law was not used and the values of Θ and δ^* were calculated from an addition of power laws that gave the best profile, therefore the accuracy of these results should be well within $\pm$ 10%.

The next method of calculating Cf was using the logarithmic inner law. By plotting graphs FIG. E1 and E2 of velocity Vs $\log_e y$ we can see that there is a small region where the graph is straight. However, this particular point is not so well defined.

Equation (8.27) is the inner law equation for a smooth flat plate and graphs, FIG. E3, E4, E5 and E6 appendix E illustrate the inner regions of probe traverse (2.1) and (2.2). FIG. E1 and E2 were plotted using different values of friction velocity u_τ.

The values of Cf obtained using the Ludwieg - Tillman equation for probe traverses (2.1) and (2.2) were 0.00334 and 0.00323 respectively. Therefore by calculating τ_o from equation (8.9), u_o the friction velocity can be calculated from (8.14), therefore an indication as to the range of u_o could be obtained for traverse (2.1) and (2.2), u_o was calculated to be 0.023 and 0.0227 respectively.

From FIG. E3 and E4 the value of u_o whereby when the inner region velocities and distance y are plotted u/u_o Vs $\log_e(yu_o/\nu)$, that gives the best parallel line to that for a smooth flat plate is $u_o = 0.0241$ and $u_o = 0.024$ for traverse (2.1) and (2.2) respectively.

The resulting calculated values of Cf are therefore, 0.00364 and 0.00361 as noted in section (8.11). These values, obtained using the inner region do however differ approximately 10% from those obtained from the Ludwieg - Tillman equation, but the two sets of results are however comparable.

FIG. E5 and E6 indicate 3 sets of plotted points with u_o varying from 0.022 to 0.026. Each profile plotted is for y varying from 0 to δ .

From these plotted profiles it is easier to distinguish the inner and outer region showing the overlap region inbetween.

The profiles plotted with $u_\circ = 0.0241$ for (2.1) and $u_\circ = 0.024$ for (2.2) are however, displaced downward and amount ΔB which is as suggested by Scholz (1955).[3] This downward shift increases for larger values of roughness k.

Coles modified his original smooth plate equation to take account of this downward shift whereby ΔB was called the roughness function. This roughness function can only be obtained from experiment and modifies the equation for the inner law to that of (8.38) and (8.39) for (2.1) and (2.2) respectively.

The value of ΔB , the roughness function has also been designated $\Delta u/u_\circ$[22] where Δu is the difference in velocity between a rough and smooth surface, at the surface, due to the roughness profile.

Had the surface been smooth then ΔB or $(\Delta u/u_\circ)$ would have been zero.

The wake function has been ignored due to it having very little effect because of the closeness of the inner region to the surface in question.

The inner region extends between $36 < (yu_\bullet/\nu) < 90$ and the logarithmic overlap would seem to extend from $90 < (yu_\bullet/\nu) < 270$.

Various interpretations of this region have been used and Miller[25] used the inner law for a flat plate Eq.(8.27) and using the region $100 < (yu_\bullet/\nu) < 300$ for his calculation. He then wrote a computer program that, for each experimental point within that region computed a value of u that gave least residual to the equation (8.27). Results for u from each experimental point in the defined range 100 - 300 were then averaged to give their arithmetic mean value.

In these investigations it would seem that the region 100 - 300 is outside the inner region, but does correspond to the logarithmic overlap. From FIG. E3, E4, E5 and E6 we can see that the profiles plotted for increasing $u_\bullet$ rotate in a clockwise manner. Therefore, for the overlap region to be parallel to that for a smooth plate would have resulted in $u_\bullet$ being in the order of 0.032 which would have increased Cf to 0.006, whereby this

value is approximately 100% greater than that calculated from the Ludwieg - Tillman equation.
Therefore it must be assumed that the inner region, shown in FIG. E5 and E6 is that relating to this particular profile.

The average roughness height, k, has been calculated using the Prandtl - Schlichting[3] approx. solution and was found to be 0.000355m and 0.00043m for probe traverse (2.1) and (2.2) respectively.

These results could however be verified using surface measurement techniques.
One difficulty in obtaining surface friction coefficients is that the surface is not a constant roughness. Therefore due to the flow regime being that of tranquil mode the flow as it passes over the surface is influenced by the flow that is in front of it. Therefore, it would be more beneficial if the surface in question was that of a constant roughness which would ensure that effects due to uneven roughness were alleviated.

One of the major problems associated with the LDA is that equation (7.10) depends upon the wavelength of laser light in the flowing medium. This however, is governed by the refractive index which is temperature

dependant. Therefore, if correct velocity measurements are to be obtained, then it must be ensured that the correct value of wavelength is calculated at the correct water temperature.

CONCLUSION

11.1 Conclusion.

One of the major problems in obtaining the surface friction coefficient during this project, was accurately recording the velocity in the boundary layer. The problems and disadvantages have been discussed in the preceding sections in detail. However, had the time been available then these could have been checked using the Laser Doppler Anemometer.

Evaluation of Cf from the inner law does require that measurements of velocity are made as accurately as possible.

APPENDIX A

VOLTAGE RESULTS PROBE (1) CALIBRATION.

(1)

+0275 +0273 +0272 +0270 +0268 +0275 +0270 +0273 +0270
+0271 +0274 +0273 +0271 +0268 +0264 +0271 +0272 +0270
+0269 +0264 +0258 +0263 +0260 +0259 +0258 +0259 +0261
+0262 +0260 +0256 +0253 +0253 +0254 +0249 +0256 +0252
+0249 +0255 +0254 +0255
(Average Value = 2.616 Volts.)

+0202 +0269 +0267 +0273 +0271 +0272 +0273 +0271 +0266
+0266 +0268 +0268 +0267 +0269 +0268 +0264 +0269 +0268
+0274 +0272 +0268 +0264 +0264 +0269 +0272 +0269 +0266
+0266 +0268 +0267 +0267 +0269 +0269 +0269 +0268 +0271
+0270 +0269 +0264 +0260
(Average Value = 2.6665 Volts.)

+0064 +0266 +0266 +0264 +0262 +0265 +0265 +0267 +0262
+0260 +0261 +0264 +0264 +0265 +0263 +0261 +0263 +0265
+0265 +0262 +0263 +0262 +0267 +0262 +0262 +0261 +0260
+0261 +0260 +0265 +0267 +0263 +0261 +0261 +0259 +0261
+0261 +0261 +0263 +00
(Average Value = 2.6289 Volts.)

(2)

+0226 +0229 +0225 +0227 +0223 +0226 +0228 +0227 +0227
+0221 +0219 +0224 +0223 +0227 +0224 +0225 +0225 +0221
+0227 +0227 +0220 +0223 +0226 +0223 +0222 +0225 +0226
+0221 +0223 +0224 +0225 +0201 +0201 +0199 +0097 +0198
+0199 +0195 +0197 +0200 +0196
(Average Value = 2.1863 Volts.)

+0201 +0231 +0227 +0228 +0223 +0228 +0228 +0226 +0227
+0228 +0228 +0226 +0226 +0226 +0224 +0229 +0227 +0220
+0226 +0223 +0224 +0228 +0226 +0222 +0228 +0227 +0224
+0228 +0226 +0226 +0222 +0224 +0225 +0223 +0221 +0222
+0218 +0217 +0219 +001
(Average Value = 2.2441 Volts.)

+022 +0228 +0224 +0224 +0225 +0230 +0228 +0220 +0222
+0226 +0224 +0224 +0224 +0221 +0225 +0228 +0224 +0228
+0224 +0217 +0223 +0220 +0223 +0222 +0228 +0225 +0223
+0223 +0224 +0223 +0225 +0225 +0227 +0223 +0225 +0224
+0223 +0225 +000
(Average Value = 2.2424 Volts.)

(3)

+0005 +0183 +0183 +0183 +0178 +0177 +0178 +0180 +0179
+0179 +0181 +0183 +0176 +0181 +0180 +0180 +0183 +0180
+0182 +0181 +0179 +0179 +0182 +0182 +0178 +0182 +0181
+0182 +0178 +0181 +0178 +0179 +0175 +0181 +0176 +0179
+0178 +0179 +0178 +0001
(Average Value = 1.7503 Volts.)

+0007 +0186 +0186 +0188 +0185 +0186 +0189 +0185 +0183
+0189 +0186 +0189 +0183 +0189 +0186 +0186 +0183 +0184
+0186 +0187 +0185 +0187 +0187 +0182 +0183 +0182 +0181
+0187 +0187 +0186 +0183 +0184 +0184 +0188 +0181 +0186
+0186 +0181 +0181 +0180
(Average Value = 1.8505 Volts.)

+0186 +0187 +0186 +0189 +0186 +0186 +0186 +0186 +0186
+0187 +0187 +0187 +0188 +0186 +0185 +0187 +0187 +0186
+0187 +0189 +0188 +0190 +0190 +0186 +0186 +0188 +0192
+0187 +0188 +0188 +0186 +0186 +0187 +0188 +0188 +0185
+0183 +0182 +0186 +0001
(Average Value = 1.869 Volts.)

(4)

+0139 +0140 +0142 +0137 +0141 +0141 +0141 +0141 +0144
+0141 +0140 +0142 +0137 +0140 +0140 +0139 +0142 +0138
+0141 +0137 +0141 +0137 +0139 +0142 +0140 +0139 +0135
+0137 +0142 +0135 +0133 +0135 +0142 +0138 +0139 +0141
+0140 +0142 +0137 +0100
(Average Value = 1.374 Volts.)

+0043 +0142 +0144 +0141 +0138 +0140 +0139 +0136 +0137
+0141 +0137 +0137 +0136 +0138 +0139 +0135 +0136 +0137
+0137 +0129 +0138 +0138 +0131 +0140 +0133 +0134 +0135
+0139 +0137 +0138 +0140 +0138 +0138 +0137 +0136 +0136
+0138 +0137 +0138 +0001
(Average Value = 1.3737 Volts.)

+0137 +0137 +0139 +0141 +0138 +0136 +0138 +0139 +0136
+0136 +0137 +0137 +0140 +0138 +0138 +0136 +0134 +0138
+0137 +0136 +0139 +0138 +0137 +0139 +0140 +0139 +0138
+0138 +0138 +0135 +0139 +0139 +0138 +0137 +0137 +0138
+0136 +0137 +0138 +0000

(Average Value = 1.3764 Volts.)

(5)

+2080 +0080 +0081 +0076 +0079 +0080 +0080 +0080 +0077
+0078 +0078 +0080 +0080 +0079 +0079 +0079 +0078 +0077
+0083 +0079 +0081 +0080 +0078 +0080 +0079 +0082 +0080
+0078 +0080 +0078 +0078 +0081 +0078 +0077 +0080 +0078
+0076 +0077 +0082 +000
(Average Value = 0.791 Volts.)

+006 +0078 +0080 +0081 +0076 +0080 +0078 +0081 +0078
+0080 +0078 +0075 +0081 +0082 +0079 +0079 +0079 +0078
+0079 +0080 +0078 +0078 +0079 +0077 +0075 +0078 +0079
+0077 +0078 +0078 +0080 +0078 +0074 +0077 +0079 +0078
+0080 +0080 +0078 +0000
(Average Value = 0.785 Volts.)

+000 +0081 +0080 +0077 +0082 +0078 +0081 +0076 +0078
+0081 +0078 +0078 +0078 +0078 +0076 +0078 +0080 +0079
+0079 +0079 +0077 +0078 +0077 +0076 +0079 +0080 +0079
+0079 +0078 +0076 +0075 +0077 +0078 +0079 +0079 +0078
+0077 +0080 +0079 +20
(Average Value = 0.784 Volts.)

(6)

+0049 +0051 +0050 +0050 +0051 +0049 +0049 +0049 +0051
+0047 +0048 +0052 +3050 +0050 +0052 +0053 +0050 +0049
+0051 +0050 +0048 +0046 +0049 +0047 +0050 +0051 +0052
+0050 +0048 +080
(Average Value = 0.497 Volts.)

+0040 +0047 +0047 +0047 +0049 +0049 +0051 +0047 +0049
+0050 +0048 +0048 +0048 +0052 +0050 +0050 +0049 +0052
+0049 +0050 +0050 +0048 +0049 +0050 +0053 +3048 +0052
+0049 +0046 +0048 +0050 +0048 +0053 +0047 +0049 +0048
+0049 +0048 +0049 +0051
(Average Value = 0.489 Volts.)

+3849 +0048 +0047 +0049 +0050 +0049 +0047 +0046 +0048
+0049 +0049 +0049 +0050 +0050 +0051 +0048 +0049 +0049
+0051 +0050 +0049 +0048 +0049 +0049 +0049 +0051 +0048
+0049 +0049 +0049 +00494+0047 +0050 +0050 +0050 +0051
+0049 +0049 +0049 +0800
(Average Value = 0.490 Volts.)

BOUNDARY LAYER PROBE (1) CALIBRATION				
POSITION OF GLOBE VALVE	FLOW RATE cc	TIME sec	AVERAGE FLOW RATE cc /s	MEAN VELOCITY m/s
1	2950 2960 2990	10.9 11.1 11.1	268.893	0.74055
2	2848 2485 1765	12.3 10.9 7.7	229.582	0.63228
3	1555 1795 1590	8.0 9.2 8.1	195.26	0.53776
4	1595 1865 1714	10.2 12.0 11.1	155.41	0.42798
5	1455 1555 1490	14.2 15.1 14.4	102.973	0.28359
6	1280 1320 1400	17.7 18.4 19.5	71.95	0.19816

TABLE A1.

CALCULATIONS FOR CALIBRATION OF PROBE 1.

SET (1)

(1) $\frac{2950}{10.9}$ = 270.642 cc /s

(2) $\frac{2960}{11.1}$ = 266.667 cc /s

(3) $\frac{2990}{11.1}$ = 269.369 cc /s

Average value of (1),(2),(3)= 268.893 cc /s

Diameter of calibration tube= 2.15 cm
= 0.0215 m

$$\text{Area} = \frac{\pi D^2}{4} = \frac{3.1415927 \times 2.15 \times 2.15}{4}$$
$$= 3.631 \text{ cm}^2$$

$$\text{Average mean velocity} = \frac{\text{Average value of flow rate}}{\text{Area}}$$
$$= \frac{268.893}{3.631}$$
$$= 74.055 \text{ cm/s}$$
$$= 0.74055 \text{ m/s}$$

Reynolds No. (Re)= $\frac{\rho v_a l}{\mu} = \frac{v_a l}{\nu}$

Where l = diameter of calibration tube.

From fig. 4.3 at 8°C ν= 0.0000015 m^2/s

$$Re = \frac{v_a \times 0.0215}{0.0000015} = 14333.333\ v_a$$

From above v_a = 0.74055 m/s

Re = 14333.333 x 0.74055 = 10614.55

From fig. 4.2 with Re= 10614.55

$$\text{Ratio of } \frac{\text{Average Velocity}}{\text{Centre-Line-Velocity}} = 0.7915$$

$$\text{Centre-Line-Velocity} = \frac{0.74055}{0.7915} = 0.936 \text{ m/s}$$

SET (2)

(1) $\frac{2848}{12.3}$ = 270.642 cc /s

(2) $\frac{2485}{10.9}$ = 227.982 cc /s

(3) $\frac{1765}{7.7}$ = 229.221 cc /s

Average value of (1),(2) and (3) = 229.582 cm^3/s

Average mean velocity va = $\frac{229.582}{3.631}$

= 63.228 cm /s

va = 0.63228 m/s

Reynolds Number (Re) = 14333.333 va

= 9062.74

From FIG. 4.2 with Re = 9062.74

ratio of va/vc = 0.7865

Centre-line velocity vc = $\frac{0.63228}{0.78650}$

vc = 0.8039 m/s.

SET (3)

(1) $\frac{1555}{8.0}$ = 194.375 cc /s

(2) $\frac{1795}{9.2}$ = 195.109 cc /s

(3) $\frac{1590}{8.1}$ = 196.296 cc /s

Average value of (1),(2) and (3) = 195.26 cm^3 /s

Average means velocity va = $\frac{195.26}{3.631}$

= 53.776 cm /s

va = 0.53776 m/s

Reynolds Number (Re) = 14333.333 x va

= 7707.87

From FIG. 4.2 with Re = 7707.87

ratio of va/vc = 0.7835

Centre-line velocity vc = $\frac{0.53776}{0.7835}$

vc = 0.6864 m/s.

SET (4)

(1) $\frac{1595}{10.2}$ = 156.373 cc /s

(2) $\frac{1865}{12.0}$ = 155.417 cc /s

(3) $\frac{1714}{11.1}$ = 154.415 cc /s

Average value of (1),(2) and (3) = 155.41 cm^3/s

Average means velocity va = $\frac{155.41}{3.631}$

= 42.798 cm /s

va = 0.42798 m/s

Reynolds Number (Re) = 14333.333 x va

= 6134.45

From FIG. 4.1 with Re = 6134.45

ratio of va/vc = 0.7645

Centre-line velocity vc = $\frac{0.42798}{0.7645}$

vc = 0.5598 m/s

SET (5)

(1) $\frac{1455}{14.2}$ = 102.465 cc /s

(2) $\frac{1555}{15.1}$ = 102.980 cc /s

(3) $\frac{1490}{14.4}$ = 103.472 cc /s

Average value of (1),(2) and (3) = 102.973 cm^3/s

Average mean velocity va = $\frac{102.973}{3.631}$

= 28.359 cm /s

va = 0.28359 m/s

Reynolds Number (Re) = 14333.333 x va

= 4064.824

From FIG. 4.1 with Re = 4064.824

ratio of va/vc = 0.745

Centre-line velocity vc = $\frac{0.28359}{0.745}$

vc = 0.3807 m/s

SET (6)

(1) $\frac{1280}{17.7}$ = 72.316 cc /s

(2) $\frac{1320}{18.4}$ = 71.739 cc /s

(3) $\frac{1400}{19.5}$ = 71795 cc /s

Average value of (1),(2) and (3) = 71.95 cm^3/s

Average mean velocity va = $\frac{71.95}{3.631}$

= 19.816

va = 0.19816 m/s

Reynolds Number (Re) = 14333.333 x va

= 2840.22

From FIG. 4.1 with Re = 2840.22

ratio of va/vc = 0.7025

Centre-line velocity vc = $\frac{0.19816}{0.7025}$

= 0.282 m/s.

CALCULATIONS FOR PROBE 1 CALIBRATION GRAPH.

Using the Method of Least Squares as described in section 4.8 and using equations (4.5), (4.6) and (4.7).

X	X^2	Y	Y^2	XY
0.9360	0.87609600	2.6371	6.95429610	2.46832560
0.8039	0.64625521	2.2243	4.94751049	1.78811477
0.6864	0.47114496	1.8233	3.32442289	1.25151312
0.5598	0.31337604	1.3747	1.88980009	0.76955106
0.3807	0.14493249	0.7870	0.61936900	0.29961090
0.2820	0.07952400	0.4920	0.24206400	0.13874400
3.6488	2.53132870	9.3384	17.97746288	6.71586545

$$6a + 3.6488b = 9.3384 \qquad (4.5.1)$$

$$3.6488a + 2.5313287b = 6.71586545 \qquad (4.6.1)$$

(4.5.1) x 3.6488 AND (4.6.1) x 6

$$21.8928a + 13.31374144b = 34.07395392 \qquad (4.5.2)$$

$$21.8928a + 15.18797220b = 40.2951927 \qquad (4.6.2)$$

(4.6.2) - (4.5.2)

$$b = 3.319355819$$

$$\underline{b = 3.319356}$$

Substitute b into equation (4.5.1)

$$6a = 9.3384 - 3.6488 \times 3.319356$$

$$\underline{a = -0.462211}$$

Equation for the best straight line is:

$$V = 3.319356v - 0.462211$$

therefore

$$\underline{v = 0.301263V + 0.1392472}$$

where v = velocity
and V = voltage.

To check whether or not statistically the equation gives a good fit to the experimental data:

$$(4.7) = \frac{n\Sigma XY - \Sigma X\Sigma Y}{\sqrt{(n\Sigma X^2 - (\Sigma X)^2)(n\Sigma Y^2 - (\Sigma Y)^2)}}$$

$$= \underline{0.999793}$$

Therefore the above equation does give a good fit to the experimental data.

GRAPH OF CENTRE-LINE-VELOCITY Vs VOLTAGE READING.

PROBE CALIBRATION 1.

FIG. A1.

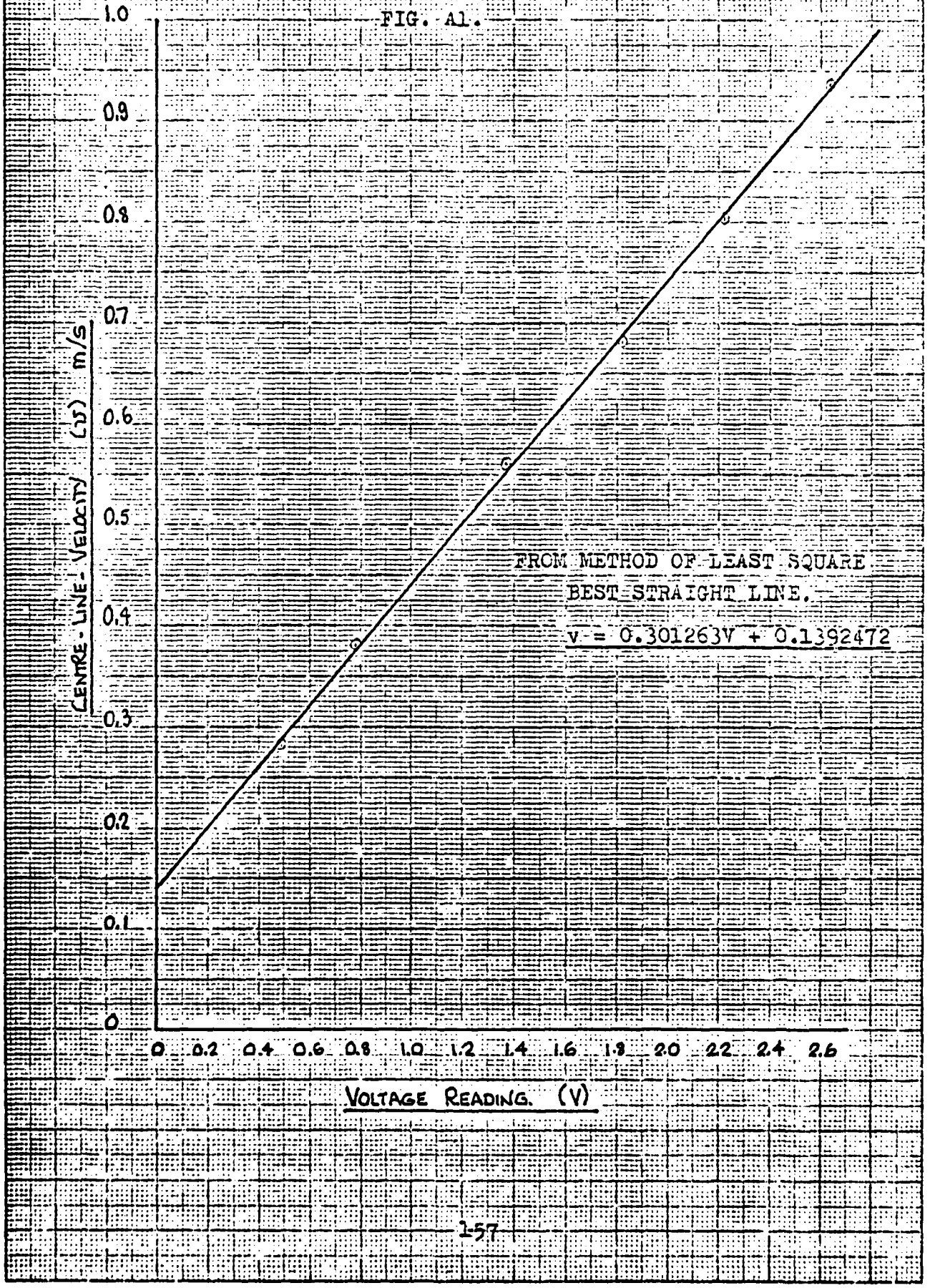

VOLTAGE RESULTS PROBE (2) CALIBRATION.

(A)

+004 +0334 +0335 +0333 +0336 +0331 +0331 +0327 +0328
+0329 +0329 +0327 +0331 +0334 +0328 +0327 +0327 +0330
+0330 +0329 +0331 +0326 +0325 +0326 +0326 +0329 +0328
+0328 +0329 +001

+0334 +0335 +0336 +0335 +0333 +0330 +0332 +0335 +0333
+0331 +0333 +0332 +0332 +0334 +0334 +0331 +0332 +0330
+0332 +0331 +0327 +0328 +0325 +0329 +0328 +0329 +0328
+0327 +0330 +0328 +000

+0329 +0329 +0327 +0325 +0321 +0326 +0319 +0319 +0319
+0317 +0319 +0319 +0318 +0316 +0309 +0308 +0309 +0307
+0303 +0302 +0305 +0305 +0313 +0319 +0320 +0318 +0319
+0315 +0315 +0316 +C01
(Average Value = 3.255 Volts.)

(B)

+0208 +0204 +0205 +0206 +0203 +0205 +0208 +0202 +0207
+0205 +0204 +0202 +0205 +0204 +0202 +0202 +0204 +0199
+0200 +0202 +0197 +0198 +0199 +0202 +0195 +0194 +0198
+0201 +0199 +0000

+0210 +0211 +0205 +0210 +0210 +0211 +0204 +0208 +0203
+0204 +0206 +0203 +0206 +0205 +0204 +0209 +0207 +0205
+0205 +0207 +0206 +0206 +0206 +0201 +0204 +0202 +0204
+0198 +0201 +0200

+000 +0204 +0208 +0205 +0200 +0208 +0207 +0207 +0205
+0207 +0204 +0206 +0202 +0207 +0204 +0203 +0204 +0204
+0207 +0206 +0205 +0204 +0205 +0207 +0204 +0201 +0206
+0205 +0205 +0000
(Average Value = 2.042 Volts.)

(C)

+015 +0153 +0156 +0152 +0151 +0149 +0149 +0147 +0150
+0149 +0150 +0149 +0150 +0151 +0149 +0148 +0146 +0146
+0147 +0149 +0149 +0151 +0152 +0150 +0152 +0152 +0146
+0146 +0147 +0001

+0005 +0154 +0152 +0150 +0150 +0151 +0152 +0156 +0150
+0154 +0151 +0148 +0147 +0145 +0151 +0155 +0148 +0146
+0148 +0154 +0150 +0150 +0146 +0150 +0146 +0147 +0147
+0146 +0147 +000

+0148 +0152 +0150 +0150 +0151 +0151 +0149 +0150 +0147
+0150 +0148 +0150 +0145 +0148 +0147 +0146 +0151 +0149
+0150 +0149 +0152 +0150 +0148 +0148 +0149 +0152 +0144
+0147 +0150 +0000
(Average Value = 1.494 Volts.)

(D)

+0127 +0124 +0127 +0122 +0112 +0113 +0111 +0109 +0109
+0111 +0111 +0113 +0113 +0109 +0112 +0111 +0112 +0111
+0114 +0108 +0110 +0113 +0114 +0110 +0113 +0111 +0109
+0113 +0113 +0100

+0124 +0124 +0124 +0123 +0120 +0123 +0123 +0120 +0120
+0123 +0127 +0121 +0120 +0121 +0120 +0123 +0119 +0118
+0124 +0118 +0121 +0121 +0117 +0120 +0121 +0123 +0123
+0122 +0119 +002

+0123 +0119 +0126 +0126 +0121 +0127 +0124 +0124 +0125
+0126 +0124 +0120 +0122 +0122 +0119 +0120 +0124 +0121
+0120 +0123 +0126 +0127 +0123 +0123 +0122 +0122 +0126
+0123 +0121 +0100
(Average Value = 1.188 Volts.)

(E)

+208 +0080 +0083 +0081 +0081 +0082 +0083 +0078 +0080
+0084 +0084 +0079 +0083 +0079 +0082 +0083 +0082 +0078
+0081 +0081 +0080 +0079 +0077 +0081 +0084 +0082 +0081
+0080 +0078 +000

+0080 +0078 +0080 +0080 +0082 +0079 +0080 +0082 +0082
+0080 +0079 +0080 +0079 +0078 +0077 +0079 +0081 +0078
+0081 +0080 +0080 +0081 +0079 +0081 +0082 +0081 +0078
+0083 +0080 +001

+2083 +0083 +0083 +0084 +0084 +0082 +0083 +0078 +0082
+0081 +0080 +0080 +0082 +0079 +0083 +0079 +0081 +0082
+0082 +0081 +0079 +0080 +0080 +0079 +0079 +0081 +0082
+0080 +0081 +001
(Average Value = 0.807 Volts.)

(F)

+0806 +0037 +0036 +00354+0036 +0037 +0036 +0038 +0035
+0033 +0037 +0034 +0036 +0036 +0036 +0038 +0036 +0035
+0036 +0035 +0034 +0036 +0035 +0036 +0037 +0037 +0034
+0037 +0036 +0800

+003 +0038 +0035 +0038 +0034 +0036 +0035 +0037 +0037
+0035 +0038 +0035 +0036 +0035 +0035 +0039 +0036 +0035
+0036 +0036 +0036 +0034 +0033 +0035 +0036 +0036 +0034
+0036 +0034 +0030

+0037 +0035 +0036 +0037 +0036 +0034 +0035 +0035 +0039
+0035 +0036 +0037 +0034 +0035 +0036 +0034 +0036 +0037
+0036 +0035 +0035 +0037 +0035 +0038 +0035 +0037 +0034
+0035 +0036 +080
(Average Value = 0.356 Volts.)

BOUNDARY LAYER PROBE (2) CALIBRATION				
POSITION OF GLOBE VALVE	FLOW RATE cc	TIME sec	AVERAGE FLOW RATE cc /s	MEAN VELOCITY m/s
A	2570 2852 2770	7.6 8.2 8.1	342.646	0.9438
B	2210 1750 1680	8.4 6.3 6.5	273.112	0.75227
C	1755 1790 1755	8.4 8.5 8.4	209.284	0.57646
D	1650 1590 1605	8.75 8.65 8.6	186.338	0.513257
E	1315 1355 1315	9.3 9.5 9.3	141.809	0.39061
F	890 1155 1270	10.1 13.5 14.5	87.087	0.23988

TABLE A2.

CALCULATIONS FOR CALIBRATION OF PROBE 2.

SET (A) (1) $\frac{2570}{7.6}$ = 338.158 cc /s

(2) $\frac{2852}{8.2}$ = 347.805 cc /s

(3) $\frac{2770}{8.1}$ = 341.975 cc /s

Average value of (1),(2) and (3) = 342.646 cc /s

Area of calibration tube = 3.631 cm

Average mean velocity = $\frac{342.646}{3.631}$

= 94.38 cm /s

= 0.9438 m/s

Reynolds No. (Re) = $\frac{\rho V_a l}{\mu} = \frac{V_a l}{\nu}$

From FIG. 4.3 at 8° C ν = 0.0000015 m^2/s

Re = 14333.333 Va

From above Va = 0.9438 m/s

Re = 13527.79

From FIG. 4.2 with Re = 13527.79

Ratio of Va/Vc = 0.795

Centre-line velocity = $\frac{0.9438}{0.795}$ = 1.187 m/s

Calculations for (B),(C),(D),(E) and (F) are similar to the above, results of which are in table A4.

AD-A081 394 TEESSIDE POLYTECHNIC MIDDLESBROUGH (ENGLAND) DEPT O--ETC F/G 13/10
DETERMINATION OF SURFACE FRICTION COEFFICIENT OF A REPLICA OF S--ETC(U)
APR 79 D C AUGUSTSON N00014-78-G-0059

UNCLASSIFIED NL

3 OF 3
AD
A081 394

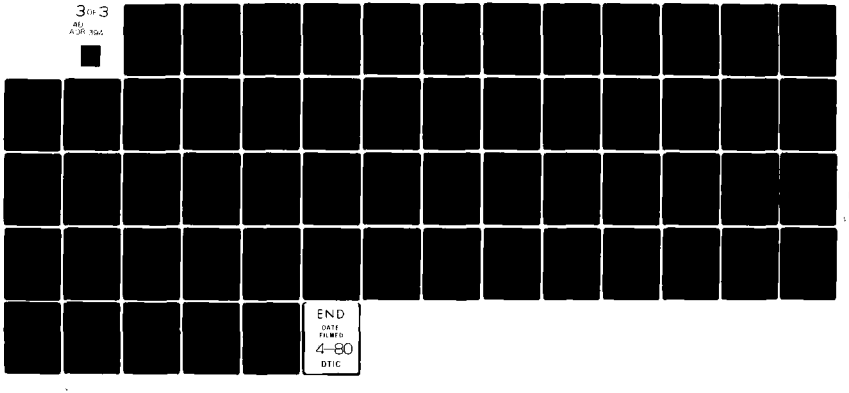

END
DATE FILMED
4-80
DTIC

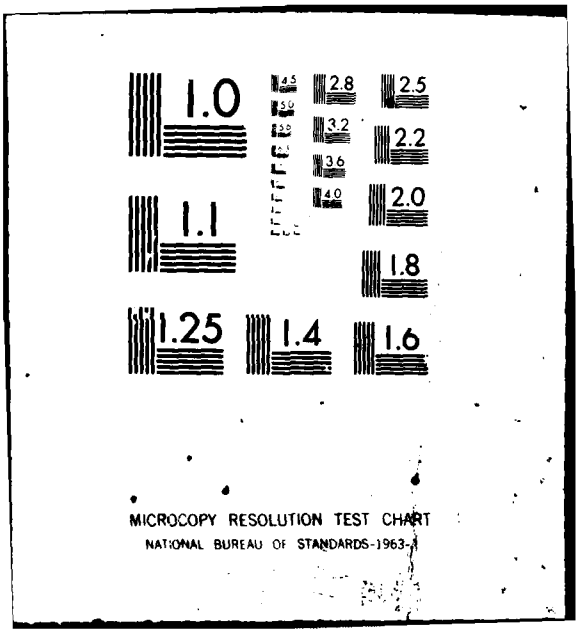
1.0
1.1
1.25
1.4
1.6
1.8
2.0
2.2
2.5
2.8
3.2
3.6
4.0
MICROCOPY RESOLUTION TEST CHART
NATIONAL BUREAU OF STANDARDS-1963-A

CALCULATIONS FOR PROBE 2 CALIBRATION GRAPH.

Using the Method of Least Squares as described in section 4.8 and using equations (4.5), (4.6) and (4.7).

X	X^2	Y	Y^2	XY
1.1870	1.40896900	3.255	10.595025	3.8636850
0.9490	0.90060100	2.042	4.169764	1.9378580
0.7329	0.53714241	1.494	2.232036	1.0949526
0.6567	0.43125489	1.188	1.411344	0.7801596
0.5100	0.26010000	0.807	0.651249	0.4115700
0.3268	0.10679824	0.356	0.126736	0.1163408
4.3624	3.64486554	9.142	19.186154	8.2045660

$$6a + 4.3624b = 9.142 \qquad (4.5.3)$$

$$4.3624a + 3.64486554b = 8.204566 \qquad (4.6.3)$$

(4.6.3) x 4.3624 AND (4.6.3) x 6

$$26.1744a + 19.03053376b = 39.8810608 \qquad (4.5.4)$$

$$26.1744a + 21.86919324b = 49.227396 \qquad (4.6.4)$$

(4.6.4) - (4.5.4)

$$2.83865948b = 9.3463352$$

$$b = 3.292517213$$

$$\underline{b = 3.292517}$$

Substitute (b) into equation (4.5.3)

$$6a + 4.3624 \times 3.292517213 = 9.142$$

$$a = -0.8702128484$$

$$\underline{a = -0.870213}$$

Equation for the best straight line is:

$$V = 3.292517v - 0.870213$$

therefore

$$\underline{v = 0.303719V + 0.2643}$$

where v = velocity
and V = voltage.

To check whether or not statistically the equation gives a good fit to the experimental data:

$$(4.7) = \frac{n\Sigma XY - \Sigma X\Sigma Y}{\sqrt{(n\Sigma X^2 - (\Sigma X)^2)(n\Sigma Y^2 - (\Sigma Y)^2)}}$$

$$= \underline{0.9895}$$

Therefore the line obtained is a good fit to the experimental data.

GRAPH OF CENTRE-LINE-VELOCITY Vs VOLTAGE READING.

PROBE CALIBRATION 2.

FIG A2.

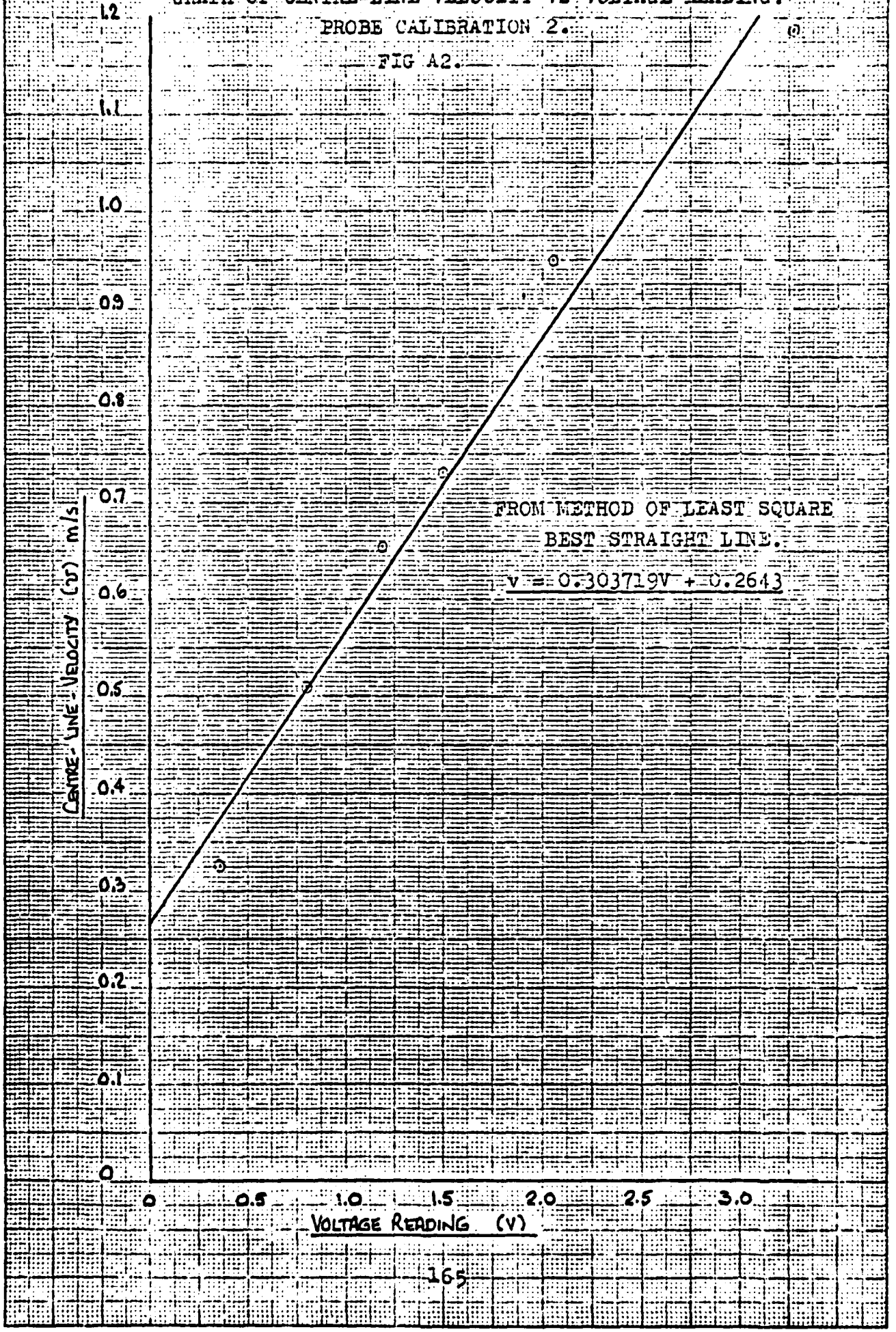

FROM METHOD OF LEAST SQUARE BEST STRAIGHT LINE.

$v = 0.303719V + 0.2643$

BOUNDARY LAYER PROBE (1) CALIBRATION					
POS-ITION OF VALVE	AVERAGE MEAN VELOCITY m/s	REYNOLDS NUMBER (Re)	va/vc	CENTRE LINE VELCCITY m/s	AVERAGE VCLTAGE READING (V)
1	0.74055	10614.55	0.7915	0.936	2.6371
2	0.63228	9062.74	0.7865	0.8039	2.2243
3	0.53776	7707.87	0.7835	0.6864	1.8233
4	0.42798	6134.45	0.7645	0.5598	1.3747
5	0.28359	4064.82	0.745	0.3807	0.787
6	0.19816	2840.22	0.7025	0.282	0.492

TABLE A3.

BOUNDARY LAYER PROBE (2) CALIBRATION					
POS-ITION OF VALVE	AVERAGE MEAN VELOCITY m/s	REYNOLDS NUMBER (Re)	va/vc	CENTRE LINE VELCCITY m/s	AVERAGE VCLTAGE READING (V)
A	0.9438	13527.79	0.795	1.187	3.255
B	0.75227	10782.54	0.792	0.949	2.042
C	0.57646	8262.59	0.7865	0.7329	1.494
D	0.513257	7356.68	0.7815	0.6567	1.188
E	0.39061	5598.74	0.766	0.51	0.807
F	0.23988	3438.28	0.734	0.3268	0.356

TABLE A4.

APPENDIX B

VOLTAGE READINGS PROBE TRAVERSE (1.1)

+0072 +0081 +0071 +0063 +0079 +0073 +0081 +0085 +0068
+0071 +0069 +0082 +0089 +0069 +0063 +0073 +0072 +0081
+0060 +0092 +0093 +0070 +0075 +0070 +0071 +0089 +0095
+0083 +0078 +0088 +0090 +0084 +000

+0075 +0048 +0057 +0074 +0084 +0058 +0082 +0088 +0080
+0057 +0077 +0067 +0088 +0077 +0079 +0073 +0083 +0080
+0084 +0079 +0085 +0070 +0064 +0078 +0067 +0087 +0073
+0092 +0074

+0087 +0090 +0082 +0064 +0069 +0081 +0084 +0074 +0086
+0080 +0083 +0064 +0065 +0087 +0067 +0076 +0072 +0082
+0087 +0087 +0074 +0065 +0080 +0102 +0091 +0071 +0075
+0093 +0087 +0079
(Average Value = 0.7741 Volts.)

+2080 +0098 +0097 +0076 +0063 +0075 +0087 +0095 +0080
+0084 +0090 +0102 +0089 +0093 +0078 +0084 +0079 +0075
+0082 +0079 +0074 +0081 +0088 +0082 +0078 +0089 +0080
+0068 +0081 +001
(Average Value = 0.83 Volts.)

+0085 +0070 +0067 +0070 +0086 +0091 +0093 +0084 +0083
+0084 +0081 +0088 +0063 +0087 +0081 +0096 +0078 +0071
+0087 +0092 +0085 +0085 +0086 +0081 +0062 +0076 +0078
+0069 +0082 +001
(Average Value = 0.8072 Volts.)

+0087 +0087 +0077 +0089 +0084 +0088 +0073 +0090 +0084
+0079 +0091 +0091 +0087 +0090 +0066 +0092 +0092 +0087
+0090 +0085 +0087 +0080 +0066 +0073 +0078 +0069 +0082
+0089 +0078 +0073 +0093 +0090 +0086 +0088 +0075 +0072
+0085 +0086 +0093 +0002
(Average Value = 0.8351 Volts.)

+0070 000+0007 +0088 +0030 +0084 +0079 +0089 +0086 +0092
+0087 +0091 +0088 +0084 +0073 +0082 +0081 +0067 +0067
+0085 +0095 +0091 +0091 +0075 +0082 +0083 +0089 +0080
+0079 +0088 +0079 +0091 +0091 +0097 +0089 +0081 +0093
+0087 +0085 +000
(Average Value = 0.8430 Volts.)

0091 +0085 +0087 +0095 +0085 +0078 +0083 +0097 +0085
+0090 +0088 +0091 +0096 +0096 +0092 +0087 +0101 +0098
+0093 +0084 +0087 +0081 +0091 +0082 +0077 +0098 +0089
+0091 +0086 +0092 +0000
(Average Value = 0.891 Volts.)

+0070 +0082 +0088 +0083 +0081 +0086 +0079 +0094 +0086
+0079 +0086 +0087 +0079 +0065 +0085 +0084 +0075 +0094
+0090 +0087 +0076 +0087 +0088 +0082 +0090 +0088 +0083
+0088 +0094 +0002
(Average Value = 0.84 Volts.)

+0077 +0082 +0098 +0094 +0087 +0094 +0096 +0091 +0082
+0088 +0093 +0088 +0102 +0087 +0093 +0095 +0097 +0093
+0096 +0092 +0100 +0092 +0083 +0089 +0099 +0094 +0090
+0096 +0094 +0096 +0001
(Average Value = 0.9194 Volts.)

+0096 +0094 +0087 +0088 +0091 +0091 +0096 +0099 +0094
+0097 +0094 +0094 +0097 +0089 +0094 +0092 +0100 +0090
+0094 +0092 +0092 +0093 +0104 +0096 +0097 +0087 +0085
+0100 +0088 +0089 +0085 +0086 +0090 +0091 +002
(Average Value = 0.9271 Volts.)

+2090 +0103 +0102 +0101 +0102 +0096 +0097 +0090 +0092
+0102 +0102 +0098 +0104 +0102 +0100 +0099 +0095 +0089
+0091 +0096 +0098 +0102 +0092 +0090 +0083 +0092 +0092
+0102 +0099 +0092 +0093 +0100 +0098 +0097 +0089 +0095
+0091 +0093 +0091 +0000
(Average Value = 0.9590 Volts.)

+0097 +0100 +0096 +0092 +0089 +0095 +0097 +0092 +0101
+0099 +0098 +0101 +0097 +0090 +0093 +0095 +0096 +0102
+0100 +0099 +0088 +0091 +0087 +0098 +0098 +0098 +0097
+0097 +0098 +0094 +0092 +0098 +0106 +0106 +0099 +2001
(Average Value = 0.9646 Volts.)

+2000 +0095 +0097 +0106 +0097 +0102 +0094 +0096 +0101
+0103 +0103 +0094 +0098 +0090 +0096 +0093 +0092 +0086
+0097 +0090 +0090 +0090 +0084 +0090 +0099 +0093 +0079
+0091 +0096 +0092 +0095 +0089 +0094 +0092 +0091 +0088
+0091 +0091 +0090
(Average Value = 0.9356 Volts.)

+0109 +0102 +0109 +0106 +0110 +0108 +0104 +0104 +0103
+0102 +0103 +0103 +0090 +0091 +0094 +0096 +0105 +0112
+0108 +0106 +0104 +0105 +0101 +0098 +0106 +0108 +0105
+0100 +0104 +0102 +0103 +0103 +0102 +0105 +0103 +0105
+0108 +0105 +0105 +000
(Average Value = 1.0351 Volts.)

+0108 +0109 +0108 +0112 +0110 +0107 +0109 +0106 +0103
+0105 +0105 +0105 +0106 +0108 +0108 +0108 +0109 +0110
+0114 +0112 +0111 +0110 +0113 +0111 +0113 +0112 +0111
+0111 +0112 +0113 +0112 +0115 +0115 +0115 +0116 +0113
+0113 +0114 +0115 +0000
(Average Value = 1.1044 Volts.)

+0002 +0105 +0105 +0101 +0100 +0102 +0105 +0112 +0111
+0109 +0108 +0105 +0109 +0110 +0106 +0105 +0105 +0105
+0103 +0105 +0108 +0107 +0108 +0105 +0105 +0109 +0104
+0106 +0104 +0103 +0105 +0107 +0107 +0106 +0105 +0106
+0107 +0104 +0102 +0104 +0000
(Average Value = 1.0572 Volts.)

+0000 +0109 +0108 +0111 +0107 +0109 +0111 +0108 +0108
+0106 +0108 +0108 +0107 +0110 +0108 +0110 +0107 +0111
+0110 +0113 +0110 +0109 +0107 +0110 +0109 +0109 +0110
+0114 +0111 +0109 +0107 +0109 +0108 +0106 +0104 +0108
+0112 +0109 +0110 +0000
(Average Value = 1.0892 Volts.)

+0109 +0108 +0108 +0108 +0109 +0104 +0102 +0101 +0107
+0107 +0105 +0109 +0107 +0105 +0103 +0107 +0108 +0107
+0110 +0111 +0108 +0108 +0107 +0109 +0107 +0106 +0104
+0107 +0108 +0110 +0109 +0109 +0110 +0100
(Average Value = 1.0697 Volts.)

+007 +0108 +0113 +0107 +0106 +0108 +0107 +0110 +0112
+0109 +0111 +0109 +0107 +0106 +0107 +0111 +0114 +0112
+0109 +0110 +0106 +0107 +0114 +0110 +0109 +0107 +0112
+0109 +0107 +0107 +0110 +2000
(Average Value = 1.0914 Volts.)

+0002 +0110 +0111 +0115 +0113 +0114 +0111 +0109 +0116
+0105 +0105 +0108 +0112 +0113 +0119 +0111 +0109 +0108
+0109 +0106 +0107 +0110 +0115 +0111 +0108 +0109 +0107
+0109 +0111 +0114 +0110 +0113 +0108 +0107 +0109 +0108
+0105 +0111 +0113 +0111
(Average Value = 1.1026 Volts.)

+0102 +0099 +0104 +0100 +0108 +0105 +0103 +0106 +0106
+0106 +0101 +0101 +0101 +0104 +0103 +0105 +0102 +0106
+0112 +0108 +0110 +0107 +0109 +0108 +0108 +0113 +0105
+0108 +0106 +0110 +0104 +0110 +0102 +0099 +0104 +0104
+0102 +0103 +0110 +0110
(Average Value = 1.0535 Volts.)

+2009 +0107 +0103 +0105 +0108 +0105 +0101 +0103 +0110
+0108 +0115 +0110 +0100 +0103 +0100 +0106 +0111 +0110
+0105 +0105 +0111 +0106 +0105 +0109 +0106 +0106 +0103
+0108 +0107 +0105 +0111 +0109 +0112 +0105 +0102 +0105
+0100
(Average Value = 1.0621 Volts.)

+0111 +0112 +0120 +0118 +0117 +0113 +0114 +0114 +0114
+0115 +0116 +0113 +0121 +0118 +0113 +0120 +0120 +0111
+0108 +0108 +0107 +0109 +0110 +0111 +0112 +0112 +0115
+0113 +0110 +0114 +0112 +0112 +0111 +0113 +0111 +0113
+0110 +0110 +0112 +0100
(Average Value = 1.1283 Volts.)

+0008 +0132 +0124 +0134 +0130 +0130 +0123 +0118 +0130
+0140 +0133 +0127 +0124 +0124 +0129 +0127 +0119 +0116
+0127 +0121 +0121 +0123 +0129 +0121 +0120 +0120 +0125
+0120 +0119 +0119 +0116 +0114 +0119 +0117 +0116 +0118
+0117 +0116 +0117 +0100
(Average Value = 1.2566 Volts.)

PROBE TRAVERSE (1.1)

NOTES :

START OF TRAVERSE WATER TEMP. 12 CENTIGRADE.

END OF TRAVERSE WATER TEMP. 12.5 CENTIGRADE.

CHANNEL SLOPE 0.3 inches.

DALL FLOW TUBE VERTICAL MANOMETER READING 3Ft.
WATER-ON-MERCURY.

HEIGHT OF WATER IN CHANNEL 205mm.

PROBE RESISTANCE READING 6.63 Ohms.

PRECEDING VOLTAGE READINGS TAKEN AT, 0,1,2,3,4,
5,6,7,8,9,10,15,20,25,30,35,40,45,50,75,100,150,
200 mm ABOVE MODEL SURFACE.

PROBE POSITION - CENTRE LINE MODEL, OFt FROM
LEADING EDGE.

VOLTAGE READINGS PROBE TRAVERSE (2.1)

+3859 +0064 +0043 +0047 +0052 +0046 +0041 +0045 +0058
+0067 +0063 +0070 +0051 +0027 +0047 +0047 +0053 +0055
+0031 +0066 +0034 +0045 +0059 +0022 +0061 +0044 +0051
+0031 +0061 +000
(Average Value = 0.493 Volts.)

+0075 +0058 +0075 +0047 +0098 +0077 +0078 +0066 +0101
+0100 +0092 +0082 +0076 +0081 +0072 +0096 +0092 +0071
+0109 +0098 +0096 +0097 +0119 +0082 +0070 +0083 +0088
+0103 +0097 +000
(Average Value = 0.879 Volts.)

+0094 +0110 +0074 +0098 +0090 +0094 +0100 +0104 +0113
+0072 +0110 +0081 +0075 +0119 +0080 +0103 +0095 +0084
+0078 +0118 +0103 +0111 +0099 +0099 +0103 +0089 +0097
+0109 +0120 +0100
(Average Value = 0.974 Volts.)

+007 +0103 +0091 +0106 +0107 +0110 +0111 +0120 +0108
+0119 +0095 +0107 +0108 +0116 +0103 +0084 +0099 +0125
+0110 +0125 +0105 +0109 +0121 +0120 +0113 +0108 +0100
+0073 +0091 +0000
(Average Value = 1.043 Volts.)

+0092 +0107 +0116 +0102 +0090 +0085 +0107 +0111 +0120
+0124 +0092 +0089 +0092 +0108 +0087 +0115 +0093 +0098
+0117 +0095 +0105 +0115 +0113 +0088 +0115 +0112 +0099
+0115 +0110 +0100
(Average Value = 1.03733 Volts.)

+0096 +0117 +0141 +0132 +0116 +0120 +0124 +0130 +0126
+0111 +0109 +0127 +0095 +0122 +0108 +0109 +0125 +0113
+0111 +0125 +0117 +0132 +0147 +0118 +0127 +0149 +0133
+0108 +0135 +0100
(Average Value = 1.02077 Volts.)

+0130 +0126 +0130 +0121 +0126 +0124 +0116 +0120 +0097
+0112 +0115 +0130 +0105 +0098 +0111 +0115 +0117 +0114
+0100 +0125 +0121 +0108 +0133 +0142 +0134 +0129 +0104
+0135 +0137 +0000
(Average Value = 1.1886 Volts.)

+0132 +0128 +0100 +0095 +0094 +0107 +0105 +0088 +0117
+0120 +0120 +0123 +0106 +0110 +0116 +0129 +0121 +0129
+0130 +0121 +0091 +0119 +0134 +0117 +0125 +0124 +0115
+0120 +0121 +0101
(Average Value = 1.1526 Volts.)

+0135 +0131 +0120 +0121 +0115 +0111 +0116 +0114 +0115
+0091 +0100 +0115 +0129 +0106 +0105 +0105 +0120 +0117
+0116 +0112 +0113 +0088 +0101 +0113 +0127 +0126 +0116
+0136 +0117 +0102
(Average Value = 1.1443 Volts.)

+0133 +0129 +0135 +0126 +0115 +0143 +0102 +0105 +0130
+0137 +0134 +0129 +0118 +0109 +0106 +0098 +0129 +0105
+0120 +0105 +0108 +0099 +0119 +0108 +0114 +0105 +0093
+0119 +0107 +0101
(Average Value = 1.1603 Volts.)

+0137 +0114 +0116 +0128 +0119 +0123 +0120 +0117 +0152
+0128 +0111 +0124 +0115 +0113 +0121 +0126 +0127 +0125
+0109 +0107 +0134 +0109 +0126 +0150 +0143 +0143 +0129
+0142 +0131 +0130
(Average Value = 1.25633 Volts.)

+0151 +0138 +0140 +0132 +0133 +0158 +0127 +0129 +0132
+0148 +0154 +0137 +0143 +0154 +0160 +0156 +0162 +0166
+0154 +0134 +0149 +0161 +0128 +0155 +0142 +0147 +0143
+0162 +0155 +0000
(Average Value = 1.4655 Volts.)

+0158 +0152 +0156 +0160 +0139 +0160 +0150 +0156 +0151
+0154 +0154 +0134 +0157 +0157 +0161 +0146 +0160 +0157
+0155 +0149 +0153 +0149 +0129 +0136 +0164 +0150 +0131
+0123 +0122 +0000
(Average Value = 1.4365 Volts.)

+0178 +0156 +0179 +0172 +0168 +0162 +0163 +0174 +0182
+0158 +0157 +0154 +0172 +0163 +0165 +0167 +0163 +0162
+0152 +0182 +0166 +0155 +0152 +0155 +0160 +0170 +0169
+0173 +0166 +0170
(Average Value = 1.6543 Volts.)

+0156 +0161 +0171 +0159 +0158 +0157 +0152 +0164 +0154
+0161 +0164 +0166 +0157 +0154 +0158 +0139 +0130 +0158
+0156 +0157 +0156 +0148 +0145 +0154 +0144 +0139 +0163
+0161 +0144 +016
(Average Value = 1.5486 Volts.)

+0102 +0170 +0162 +0170 +0167 +0172 +0164 +0173 +0180
+0171 +0178 +0166 +0161 +0167 +0158 +0181 +0173 +0171
+0182 +0177 +0180 +0165 +0157 +0166 +0176 +0173 +0171
+0177 +0179 +0102
(Average Value = 1.664 Volts.)

+0183 +0176 +0167 +0175 +0185 +0188 +0182 +0170 +0178
+0185 +0175 +0174 +0173 +0180 +0183 +0184 +0168 +0165
+0166 +0172 +0162 +0160 +0165 +0167 +0173 +0167 +0166
+0170 +0167 +0161
(Average Value = 1.729 Volts.)

+0176 +0177 +0173 +0174 +0165 +0176 +0170 +0178 +0188
+0177 +0192 +0193 +0188 +0187 +0179 +0182 +0180 +0176
+0171 +0178 +0166 +0177 +0178 +0183 +0189 +0188 +0183
+0178 +0174 +0101
(Average Value = 1.7917 Volts.)

+010 +0182 +0183 +0178 +0175 +0183 +0187 +0181 +0176
+0189 +0193 +0185 +0182 +0175 +0177 +0177 +0172 +0176
+0171 +0170 +0174 +0178 +0180 +0175 +0175 +0175 +0175
+0176 +0172 +0171 +0174
(Average Value = 1.779 Volts.)

+0177 +0180 +0178 +0180 +0178 +0178 +0176 +0182 +0176
+0176 +0175 +0177 +0182 +0180 +0174 +0172 +0177 +0181
+0173 +0172 +0167 +0170 +0176 +0177 +0186 +0180 +0178
+0179 +0182 +0177 +0174 +0171 +0172 +0101
(Average Value = 1.7676 Volts.)

+0001 +0180 +0177 +0190 +0185 +0171 +0183 +0184 +0196
+0184 +0185 +0187 +0187 +0185 +0187 +0183 +0189 +0185
+0180 +0183 +0186 +0188 +0187 +0179 +0184 +0186 +0187
+0184 +0185 +0001
(Average Value = 1.8454 Volts.)

+0101 +0187 +0186 +0187 +0191 +0191 +0183 +0193 +0190
+0192 +0183 +0190 +0196 +0195 +0189 +0194 +0189 +0187
+0195 +0206 +0197 +0201 +0200 +0195 +0185 +0188 +0193
+0197 +0001

(Average Value = 1.9185 Volts.)

+0093 +0192 +0189 +0191 +0187 +0192 +0200 +0197 +0204
+0190 +0186 +0190 +0186 +0193 +0202 +0190 +0197 +0194
+0204 +0189 +0186 +0186 +0194 +0166 +0148 +0146 +0148
+0153 +0152 +000

(Average Value = 1.84 Volts.)

NOTES :

START OF TRAVERSE WATER TEMP. 10° CENTIGRADE.

END OF TRAVERSE WATER TEMP. 10.5° CENTIGRADE.

CHANNEL SLOPE 0.3inches.

DALL FLOW TUBE VERTICAL MANOMETER READING 7Ft.

WATER-ON-MERCURY.

HEIGHT OF WATER IN CHANNEL 240mm.

PROBE RESISTANCE READING 6.73 Ohms.

PRECEDING VOLTAGE READINGS TAKEN AT, 0,1,2,3,4,
5,6,7,8,9,10,15,20,25,30,35,40,45,50,75,100,150,
200 mm above model surface.

PROBE POSITION - CENTRE LINE MODEL, 2Ft FROM
LEADING EDGE.

VOLTAGE READINGS PROBE TRAVERSE (2.2)

+0000 +0093 +0073 +0068 +0070 +0086 +0049 +0057 +0039
+0061 +0063 +0059 +0050 +0074 +0060 +0056 +0058 +0054
+0049 +0044 +0052 +0039 +0070 +0055 +0070 +0056 +0043
+0057 +0044 +000
(Average Value = 0.589 Volts.)

+0090 +0084 +0079 +0066 +0112 +0089 +0082 +0096 +0101
+0084 +0083 +0105 +0090 +0087 +0106 +0088 +0104 +0076
+0079 +0072 +0106 +0071 +0086 +0081 +0084 +0078 +0099
+0086 +0102 +000
(Average Value = 0.885 Volts.)

+0002 +0111 +0115 +0088 +0093 +0086 +0103 +0107 +0123
+0102 +0082 +0094 +0078 +0093 +0088 +0110 +0103 +0086
+0087 +0086 +0096 +0085 +0113 +0099 +0089 +0083 +0098
+0073 +0092 +201
(Average Value = 0.948 Volts.)

+0100 +0125 +0091 +0104 +0083 +0098 +0108 +0094 +0089
+0115 +0120 +0113 +0121 +0112 +0109 +0117 +0100 +0107
+0105 +0097 +0102 +0069 +0113 +0108 +0087 +0103 +0112
+0105 +0097 +0000
(Average Value = 0.999 Volts.)

+0101 +0106 +0116 +0105 +0098 +0090 +0117 +0115 +0124
+0111 +0104 +0098 +0119 +0095 +0099 +0112 +0127 +0103
+0098 +0118 +0106 +0091 +0083 +0114 +0095 +0119 +0117
+0097 +0091 +0100
(Average Value = 1.056 Volts.)

+0116 +0076 +0120 +0092 +0121 +0096 +0117 +0122 +0114
+0088 +0107 +0095 +0088 +0108 +0102 +0097 +0083 +0120
+0111 +0106 +0103 +0114 +0120 +0115 +0090 +0107 +0102
+0125 +0132 +01
(Average Value = 1.065 Volts.)

+0118 +0114 +0112 +0127 +0136 +0122 +0126 +0134 +0113
+0117 +0115 +0114 +0140 +0113 +0118 +0104 +0136 +0101
+0099 +0114 +0104 +0143 +0117 +0103 +0105 +0113 +0126
+0140 +0130 +0136
(Average Value = 1.197 Volts.)

1 0130 ; 108 +0121 +0084 +0136 +0126 +0126 +0119 +0132
+0116 +0111 +0124 +0116 +0117 +0121 +0113 +0119 +0110
+0106 +0101 +0117 +0115 +0134 +0112 +0121 +0136 +0138
+0113 +0101
(Average Value = 1.1804 Volts.)

+0121 +0107 +0117 +0131 +0133 +0128 +0108 +0130 +0107
+0121 +0091 +0129 +0119 +0101 +0108 +0123 +0134 +0131
+0134 +0147 +0124 +0121 +0116 +0116 +0130 +0112 +0104
+0118 +0100 +000
(Average Value = 1.1935 Volts.)

+0004 +0116 +0124 +0141 +0137 +0140 +0129 +0123 +0093
+0132 +0146 +0147 +0138 +0122 +0117 +0123 +0116 +0144
+0127 +0139 +0132 +0117 +0113 +0117 +0133 +0110 +0123
+0086 +0110 +200
(Average Value = 1.2482 Volts.)

+0112 +0122 +0141 +0134 +0130 +0093 +0087 +0146 +0126
+0107 +0105 +0111 +0136 +0126 +0133 +0115 +0099 +0109
+0106 +0115 +0098 +0105 +0122 +0133 +0140 +0134 +0123
+0125 +0148 +0000
(Average Value = 1.2004 Volts.)

+0154 +0134 +0146 +0164 +0148 +0152 +0137 +0136 +0145
+0134 +0146 +0154 +0117 +0136 +0147 +0140 +0164 +0130
+0136 +0153 +0139 +0136 +0127 +0120 +0125 +0143 +0129
+0152 +0143 +0101
(Average Value = 1.396 Volts.)

+0176 +0170 +0154 +0165 +0143 +0158 +0141 +0143 +0150
+0144 +0155 +0163 +0146 +0145 +0137 +0169 +0164 +0135
+0162 +0171 +0158 +0156 +0151 +0131 +0128 +0151 +0146
+0158 +0159 +0133 +0129 +0100
(Average Value = 1.5133 Volts.)

+0141 +0137 +0149 +0176 +0165 +0169 +0155 +0157 +0161
+0156 +0158 +0165 +0165 +0142 +0138 +0158 +0145+0142
+0164 +0159 +0162 +0168 +0168 +0155 +0160 +0165 +0160
+0152 +0156 +0001
(Average Value = 1.5683 Volts.)

+0101 +0153 +0160 +0164 +0170 +0169 +0158 +0153 +0160
+0155 +0148 +0153 +0160 +0160 +0161 +0157 +0144 +0165
+0172 +0159 +0148 +0171 +0157 +0150 +0156 +0169 +0157
+0153 +0161 +0000

(Average Value = 1.5669 Volts.)

+0173 +0173 +0164 +0176 +0180 +0173 +0161 +0174 +0167
+0162 +0169 +0146 +0174 +0183 +0175 +0178 +0173 +0175
+0179 +0163 +0168 +0164 +0154 +0145 +0171 +0163 +0170
+0162 +0164 +0001

(Average Value = 1.6824 Volts.)

+0000 +0164 +0164 +0165 +0160 +0161 +0159 +0175 +0163
+0167 +0162 +0172 +0170 +0164 +0164 +0164 +0154 +0169
+0167 +0165 +0163 +0163 +0165 +0166 +0156 +0159 +0152
+0163 +0162 +0000

(Average Value = 1.635 Volts.)

+0161 +0163 +0161 +0167 +0164 +0180 +0168 +0164 +0167
+0169 +0173 +0166 +0160 +0167 +0171 +0174 +0178 +0170
+0175 +0165 +0171 +0168 +0169 +0173 +0168 +0175 +0172
+0171 +0178 +0174 +0182 +0166 +0173 +0161 +0100

(Average Value = 1.7015 Volts.)

+0101 +0176 +0175 +0179 +0181 +0183 +0180 +0181 +0185
+0172 +0163 +0170 +0155 +0177 +0170 +0158 +0177 +0179
+0178 +0168 +0170 +0173 +0176 +0181 +0179 +0178 +0175
+0171 +0183 +013

(Average Value = 1.722 Volts.)

+0177 +0180 +0183 +0185 +0177 +0176 +0182 +0185 +0185
+0185 +0179 +0178 +0183 +0180 +0182 +0185 +0182 +0179
+0182 +0182 +0181 +0177 +0171 +0171 +0176 +0176 +0180
+0176 +0180 +0101

(Average Value = 1.772 Volts.)

+0190 +0185 +0186 +0184 +0186 +0188 +0194 +0191 +0195
+0191 +0196 +0191 +0189 +0183 +0182 +0194 +0192 +0182
+0183 +0188 +0185 +0193 +0192 +0190 +0179 +0193 +0191
+0190 +0190 +0002

(Average Value = 1.8873 Volts.)

+0096 +0196 +0193 +0207 +0204 +0189 +0195 +0196 +0193
+0186 +0184 +0192 +0195 +0195 +0194 +0194 +0198 +0196
+0195 +0191 +0181 +0194 +0189 +0202 +0193 +0193 +0193
+0189 +0195 +0100
(Average Value = 1.8727 Volts.)

+0211 +0212 +0210 +0204 +0205 +0212 +0213 +0205 +0200
+0195 +0202 +0200 +0197 +0187 +0192 +0210 +0201 +0190
+0199 +0201 +0193 +0197 +0203 +0204 +0208 +0201 +0219
+0210 +0209 +0200
(Average Value = 2.03 Volts.)

NOTES :

START OF TRAVERSE WATER TEMP. 11 CENTIGRADE.

END OF TRAVERSE WATER TEMP. 12 CENTIGRADE.

CHANNEL SLOPE 0.3 inches.

DALL FLOW TUBE VERTICAL MANOMETER READING 7 Ft.

WATER-ON-MERCURY.

HEIGHT OF WATER IN CHANNEL 240mm.

PROBE RESISTANCE READING 6.76 Ohms.

PRECEDING VOLTAGE READINGS TAKEN AT, 0,1,2,3,4,
5,6,7,8,9,10,15,20,25,30,35,40,45,50,75,100,150,
200 mm above model surface.

PROBE POSITION - CENTRE LINE OF MODEL, 4 Ft. FROM
LEADING EDGE.

VOLTAGE READING PROBE TRAVERSE (2.3)

+0042 +0071 +0062 +0065 +0058 +0079 +0042 +0054 +0047
+0071 +0047 +0041 +0034 +0057 +0071 +0054 +0016 +0065
+0076 +0034 +0075 +0068 +0053 +0052 +0077 +0072 +0049
+0046 +0045 +0059 +000

(Average Value = 0.5607 Volts.)

+0075 +0083 +0070 +0113 +0091 +0075 +0094 +0121 +0096
+0079 +0074 +0083 +0064 +0094 +0083 +0103 +0094 +0107
+0106 +0087 +0084 +0092 +0074 +0092 +0122 +0111 +0095
+0097 +0102 +00

(Average Value = 0.9176 Volts.)

+0130 +0104 +0116 +0084 +0075 +0102 +0082 +0131 +0121
+0130 +0113 +0106 +0128 +0125 +0140 +0128 +0110 +0127
+0118 +0135 +0094 +0101 +0133 +0100 +0094 +0123 +0116
+0121 +0084 +0118

(Average Value = 1.1297 Volts.)

+0094 +0101 +0112 +0125 +0121 +0104 +0138 +0105 +0098
+0120 +0129 +0125 +0124 +0141 +0115 +0139 +0088 +0086
+0095 +0116 +0114 +0130 +0117 +0112 +0131 +0148 +0120
+0112 +0095 +0001

(Average Value = 1.1569 Volts.)

+0130 +0144 +0146 +0129 +0093 +0139 +0127 +0144 +0159
+0114 +0114 +0103 +0116 +0152 +0129 +0110 +0120 +0130
+0114 +0168 +0139 +0125 +0134 +0133 +0165 +0122 +0139
+0144 +0115 +00

(Average Value = 1.3093 Volts.)

+0126 +0113 +0122 +0126 +0126 +0130 +0109 +0156 +0131
+0113 +0116 +0112 +0151 +0128 +0136 +0106 +0116 +0125
+0118 +0110 +0082 +0134 +0118 +0132 +0119 +0120 +0145
+0132 +0107 +0000

(Average Value = 1.2273 Volts.)

+0001 +0107 +0126 +0121 +0151 +0149 +0119 +0129 +0150
+0145 +0123 +0121 +0125 +0129 +0097 +0144 +0117 +0115
+0134 +0137 +0111 +0149 +0151 +0147 +0121 +0131 +0140
+0130 +0120 +0141

(Average Value = 1.3035 Volts.)

+0141 +0138 +0130 +0129 +0115 +0120 +0130 +0130 +0126
+0141 +0143 +0128 +0121 +0135 +0129 +0117 +0127 +0125
+0135 +0130 +0152 +0144 +0127 +0151 +0135 +0140 +0150
+0118 +0138 +001

(Average Value = 1.3259 Volts.)

+040 +0148 +0124 +0137 +0129 +0172 +0159 +0164 +0147
+0125 +0136 +0124 +0139 +0117 +0134 +0156 +0126 +0128
+0144 +0145 +0139 +0128 +0152 +0162 +0115 +0122 +0152
+0174 +0135 +0101

(Average Value = 1.3910 Volts.)

+0141 +0116 +0129 +0160 +0148 +0166 +0146 +0139 +0150
+0165 +0141 +0154 +0132 +0161 +0136 +0147 +0131 +0178
+0154 +0127 +0146 +0149 +0140 +0153 +0159 +0143 +0149
+0157 +0184 +0100

(Average Value = 1.467 Volts.)

+0077 +0149 +0137 +0158 +0156 +0146 +0133 +0146 +0147
+0170 +0194 +0175 +0177 +0166 +0144 +0150 +0169 +0155
+0147 +0170 +0186 +0175 +0143 +0134 +0169 +0169 +0172
+0168 +0141 +0100

(Average Value = 1.541 Volts.)

+003 +0172 +0146 +0176 +0169 +0168 +0164 +0170 +0189
+0185 +0186 +0187 +0156 +0160 +0151 +0157 +0164 +0151
+0155 +0181 +0161 +0170 +0161 +0176 +0156 +0180 +0183
+0182 +0160 +0001

(Average Value = 1.6843 Volts.)

+0190 +0183 +0171 +0180 +0164 +0162 +0183 +0195 +0165
+0190 +0167 +0162 +0171 +0182 +0186 +0167 +0165 +0165
+0175 +0160 +0173 +0185 +0190 +0188 +0177 +0186 +0177
+0180 +0179 +0167 +0172 +0161

(Average Value = 1.7557 Volts.)

+0197 +0196 +0203 +0214 +0197 +0190 +0210 +0186 +0155
+0176 +0161 +0174 +0192 +0193 +0189 +0194 +0183 +0189
+0164 +0170 +0199 +0211 +0203 +0202 +0196 +0188 +0194
+0187 +0192 +0180 +0171 +0100

(Average Value = 1.8890 Volts.)

PROBE TRAVERSE (2.3)

NOTES :

START OF TRAVERSE WATER TEMP. 13 CENTIGRADE.

END OF TRAVERSE WATER TEMP. 13.5 CENTIGRADE.

CHANNEL SLOPE 0.3 inches.

DALL FLOW TUBE VERTICAL MANOMETER READING 7 Ft.

WATER-ON-MERCURY.

HEIGHT OF WATER ABOVE SURFACE IN CHANNEL 236 mm.

PROBE RESISTANCE READING 6.76 Ohms.

PRECEDING VOLTAGE READINGS TAKEN AT, 4,5,6,7,8,

9,10,11,12,13,14,19,24,29 mm above surface of model.

PROBE DAMAGED AT 34 mm.

PROBE POSITION - CENTRE LINE OF MODEL, 6 Ft.

FROM LEADING EDGE.

APPENDIX C

CALCULATED VELOCITIES FOR PROBE TRAVERSE (1.1)

POSITION FROM LEADING EDGE 0 Ft.

POSITION OF PROBE ABOVE SURFACE (mm)	AVERAGE VOLTAGE READING (Volts)	CALCULATED VELOCITY (USING EQ.4.8) (m/s)	TRUE FLUID VELOCITY (m/s)
0	0.7741	0.3725	0.2332
1	0.8300	0.3893	0.2500
2	0.8072	0.3825	0.2432
3	0.8351	0.3908	0.2516
4	0.8430	0.3932	0.2540
5	0.8910	0.4077	0.2684
6	0.8400	0.3923	0.2531
7	0.9194	0.4163	0.2770
8	0.9271	0.4186	0.2793
9	0.9590	0.4282	0.2890
10	0.9646	0.4299	0.2906
15	0.9356	0.4211	0.2819
20	1.0351	0.4511	0.3118
25	1.1044	0.4720	0.3327
30	1.0572	0.4578	0.3185
35	1.0892	0.4674	0.3281
40	1.0697	0.4615	0.3223
45	1.0914	0.4681	0.3288
50	1.1026	0.4714	0.3322
75	1.0535	0.4566	0.3174
100	1.0621	0.4593	0.3200
150	1.1283	0.4792	0.3400
200	1.2566	0.5178	0.3786

TABLE C1.

CALCULATED VELOCITIES FOR PROBE TRAVERSE (2.1)

POSITION FROM LEADING EDGE 2 Ft.

POSITION OF PROBE ABOVE SURFACE (mm)	AVERAGE VOLTAGE READING (Volts)	CALCULATED VELOCITY (USING EQ.4.9) (m/s)	TRUE FLUID VELOCITY (m/s)
0	0.493	0.4140	0.1500
1	0.879	0.5313	0.2670
2	0.974	0.5601	0.2958
3	1.043	0.5811	0.3168
4	1.037	0.5793	0.3150
5	1.208	0.6312	0.3669
6	1.189	0.6254	0.3611
7	1.153	0.6145	0.3502
8	1.144	0.6118	0.3475
9	1.160	0.6166	0.3523
10	1.256	0.6458	0.3815
15	1.466	0.7096	0.4453
20	1.437	0.7008	0.4365
25	1.654	0.7667	0.5024
30	1.549	0.7348	0.4705
35	1.664	0.7697	0.5054
40	1.729	0.7894	0.5251
45	1.792	0.8086	0.5443
50	1.779	0.8046	0.5403
75	1.768	0.8013	0.5370
100	1.846	0.8250	0.5607
150	1.919	0.8472	0.5828
200	1.840	0.8232	0.5588

TABLE C2.

CALCULATED VELOCITIES FOR PROBE TRAVERSE (2.2)

POSITION FROM LEADING EDGE 4 Ft.

POSITION OF PROBE ABOVE SURFACE (mm)	AVERAGE VOLTAGE READING (Volts)	CALCULATED VELOCITY (USING EQ.4.9) (m/s)	TRUE FLUID VELOCITY (m/s)
0	0.5890	0.4432	0.1789
1	0.8850	0.5331	0.2688
2	0.9480	0.5522	0.2879
3	0.9990	0.5677	0.3034
4	1.0560	0.5850	0.3207
5	1.0650	0.5878	0.3235
6	1.1970	0.6279	0.3636
7	1.1804	0.6228	0.3585
8	1.1935	0.6268	0.3625
9	1.2482	0.6434	0.3791
10	1.2004	0.6289	0.3646
15	1.3960	0.6883	0.4240
20	1.5133	0.7239	0.4596
25	1.5683	0.7406	0.4763
30	1.5669	0.7402	0.4759
35	1.6824	0.7753	0.5110
40	1.6350	0.7609	0.4966
45	1.7015	0.7811	0.5168
50	1.7220	0.7873	0.5230
75	1.7220	0.7873	0.5230
100	1.8873	0.8375	0.5732
150	1.8727	0.8331	0.5688
200	2.0300	0.8809	0.6165

TABLE C3.

CALCULATED VELOCITIES FOR PROBE TRAVERSE (2.3)

POSITION FROM LEADING EDGE 6 Ft.

POSITION OF PROBE ABOVE SURFACE (mm)	AVERAGE VOLTAGE READING (Volts)	CALCULATED VELOCITY (USING EQ.4.9) (m/s)	TRUE FLUID VELOCITY (m/s)
4	0.5607	0.4346	0.1703
5	0.9176	0.5430	0.2787
6	1.1297	0.6074	0.3431
7	1.1569	0.6157	0.3514
8	1.3093	0.6620	0.3977
9	1.2273	0.6370	0.3728
10	1.3035	0.6602	0.3959
11	1.3259	0.6670	0.4027
12	1.3910	0.6868	0.4225
13	1.4670	0.7099	0.4456
14	1.5410	0.7324	0.4680
19	1.6843	0.7759	0.5116
24	1.7557	0.7976	0.5332
29	1.8890	0.8380	0.5737

TABLE C4.

GRAPH OF POSITION OF PROBE ABOVE SURFACE Vs FLOW VELOCITY.

PROBE TRAVERSE (1.1) POSITION FROM LEADING EDGE 0 Ft.

FIG C1.

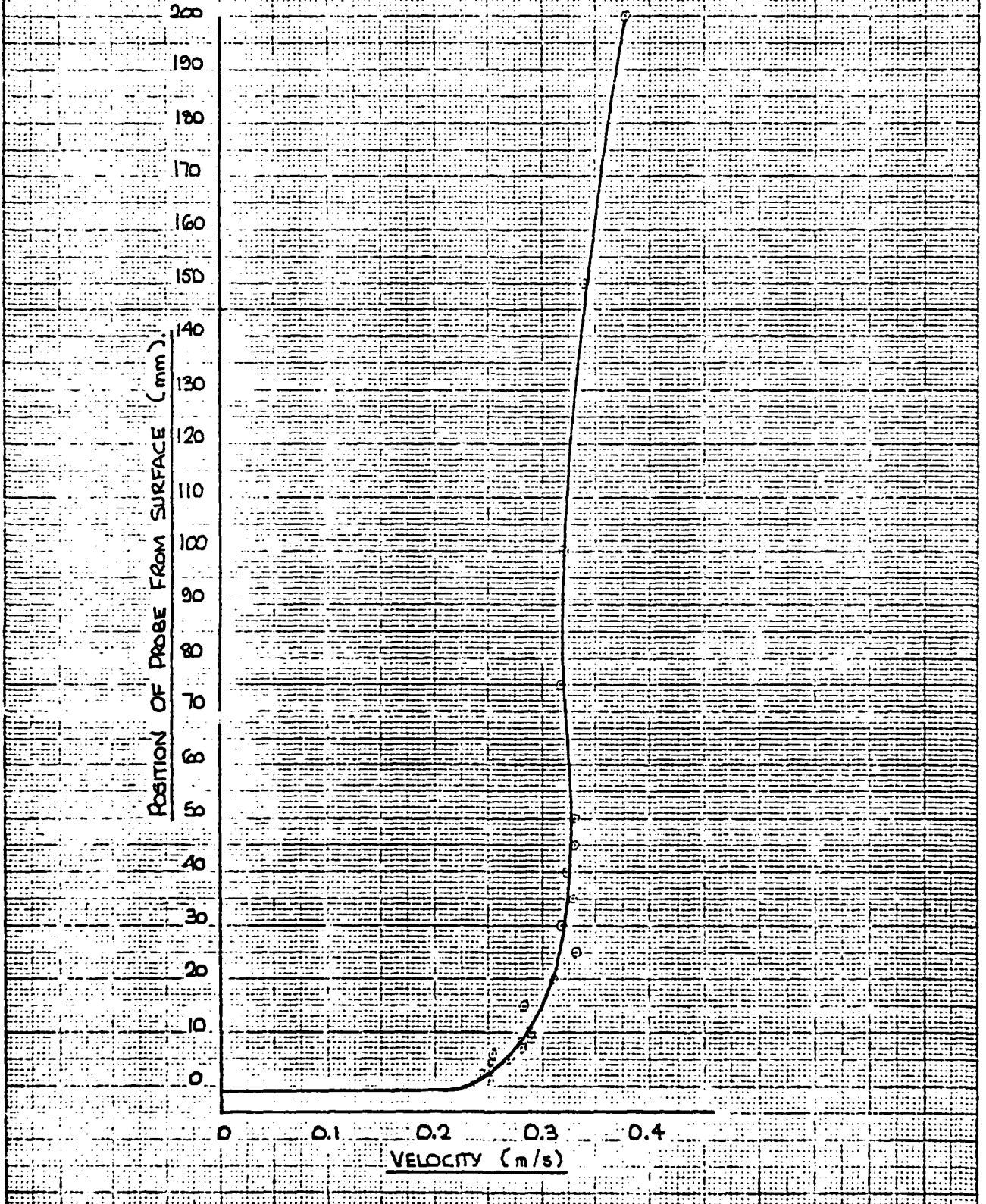

GRAPH OF POSITION OF PROBE ABOVE SURFACE Vs FLOW VELOCITY.

PROBE TRAVERSE (2.1) POSITION FROM LEADING EDGE 2 Ft.

FIG C2.

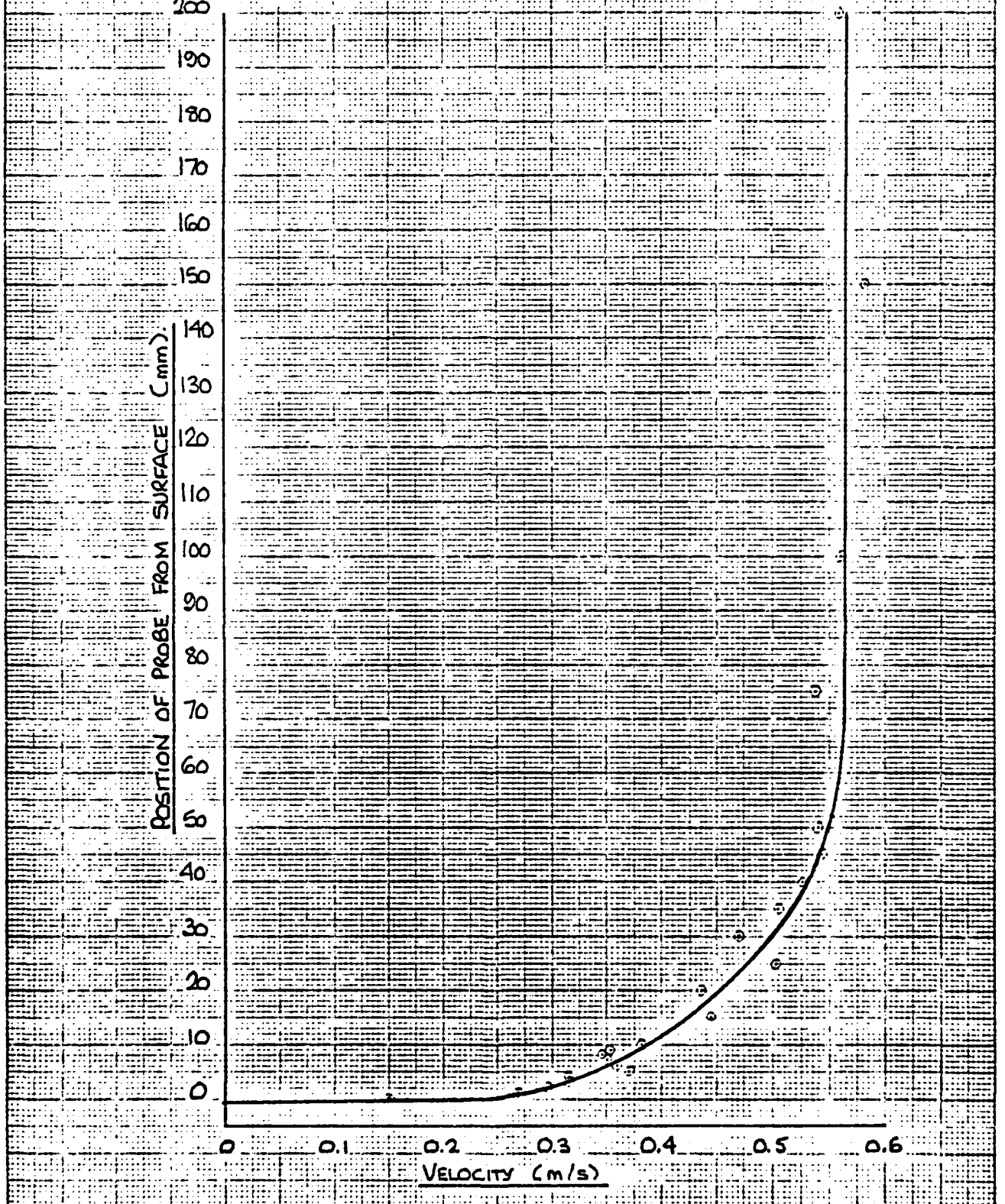

GRAPH OF POSITION OF PROBE ABOVE SURFACE Vs FLOW VELOCITY.

PROBE TRAVERSE (2.1) POSITION FROM LEADING EDGE 2 Ft.

FIG 03.

FREESTREAM VELOCITY = 0.565 m/s.

EDGE OF BOUNDARY LAYER OCCURS AT 98% FREESTREAM.

BOUNDARY LAYER VELOCITY = 0.98 x 0.565

= 0.554 m/s.

THICKNESS OF BOUNDARY LAYER = 52 mm.

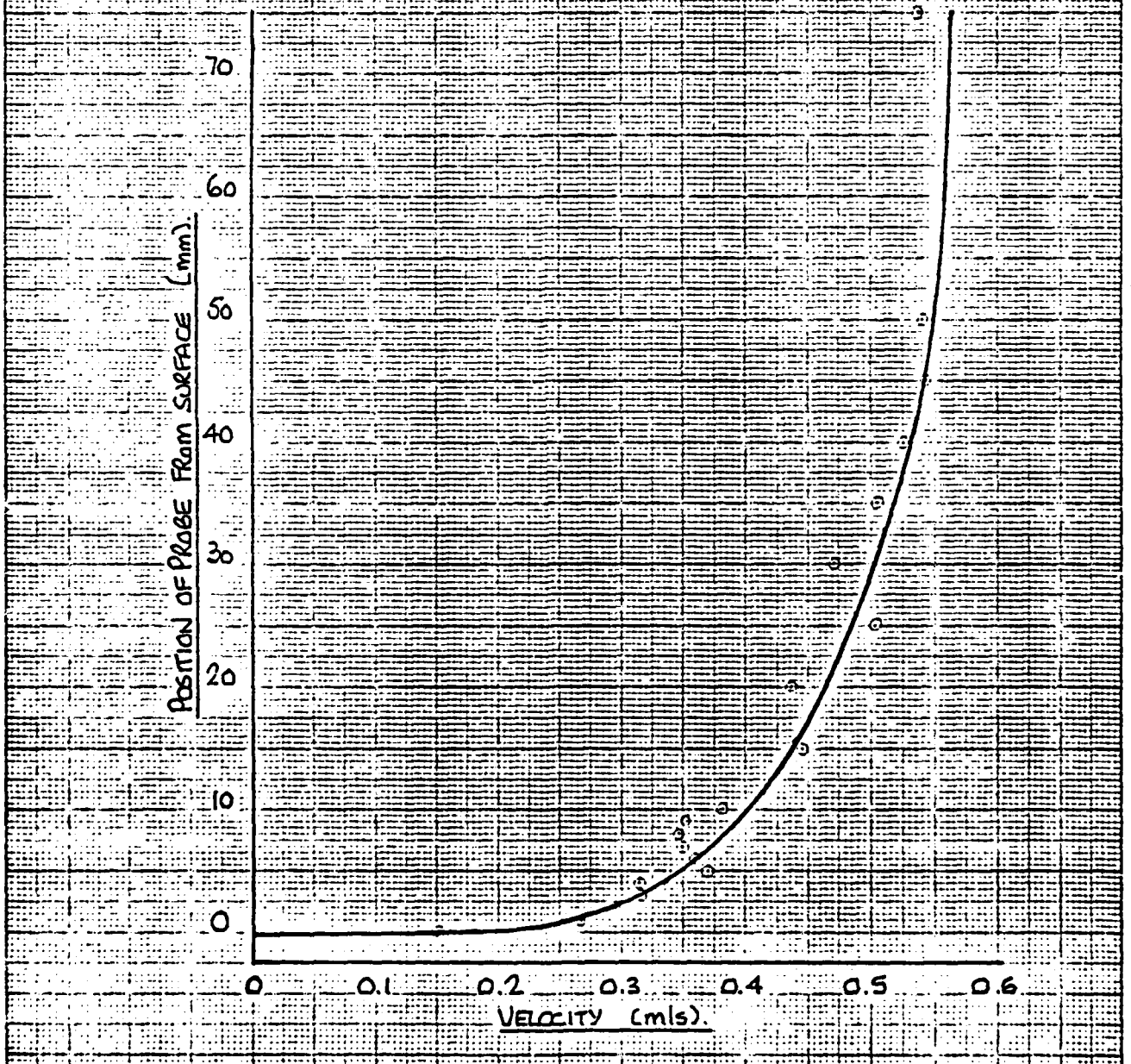

GRAPH OF POSITION OF PROBE ABOVE SURFACE Vs FLOW VELOCITY.

PROBE TRAVERSE (2.2) POSITION FROM LEADING EDGE 4 Ft.

FIG C4.

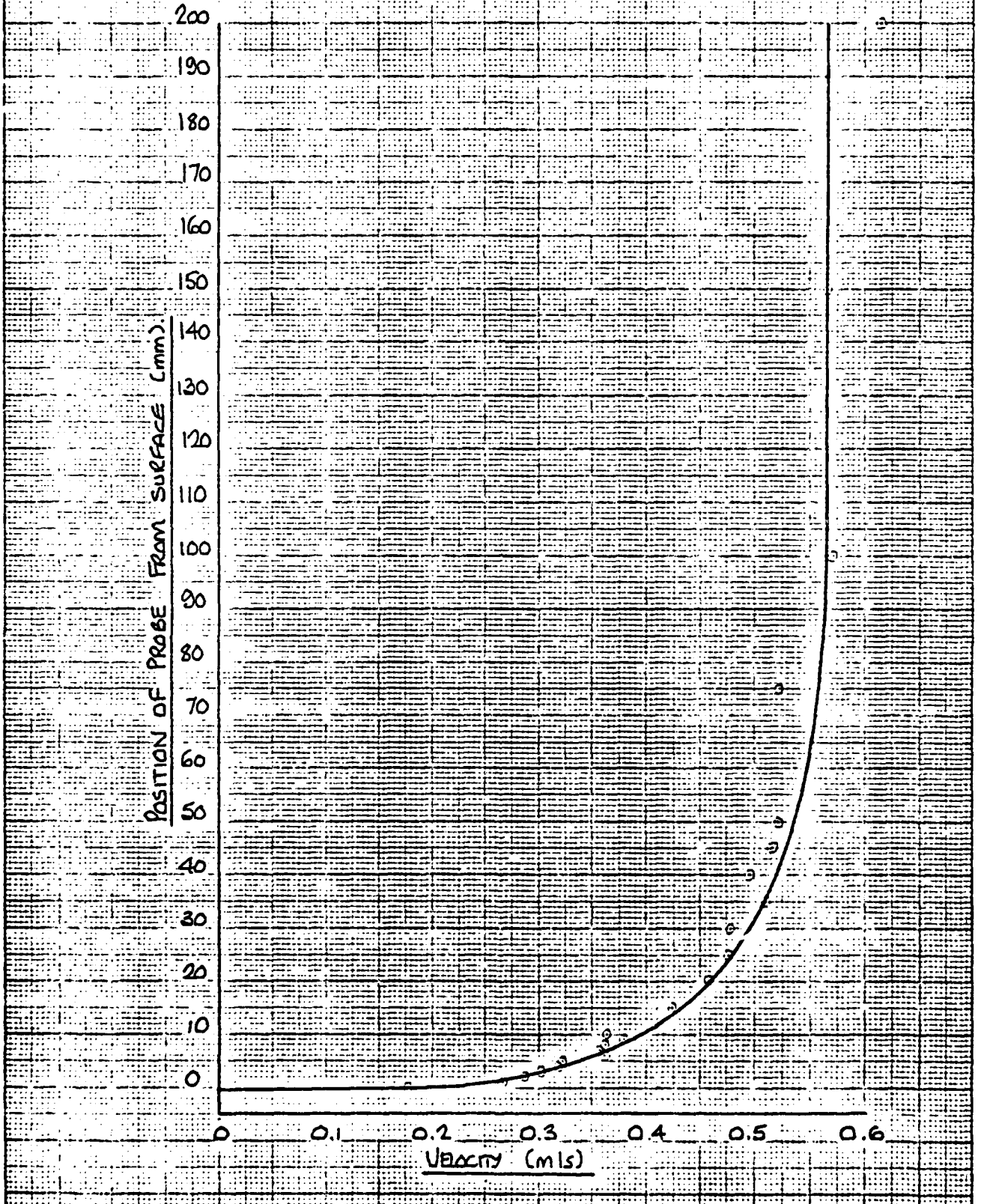

GRAPH OF POSITION OF PROBE ABOVE SURFACE Vs FLOW VELOCITY.

PROBE TRAVERSE (2.2) POSITION FROM LEADING EDGE 4 Ft.

FIG C5.

FREESTREAM VELOCITY = 0.565 m/s.

EDGE OF BOUNDARY LAYER OCCURS AT 98% FREESTREAM.

BOUNDARY LAYER VELOCITY = 0.98 x 0.565

= 0.554 m/s.

THICKNESS OF BOUNDARY LAYER = 65 mm.

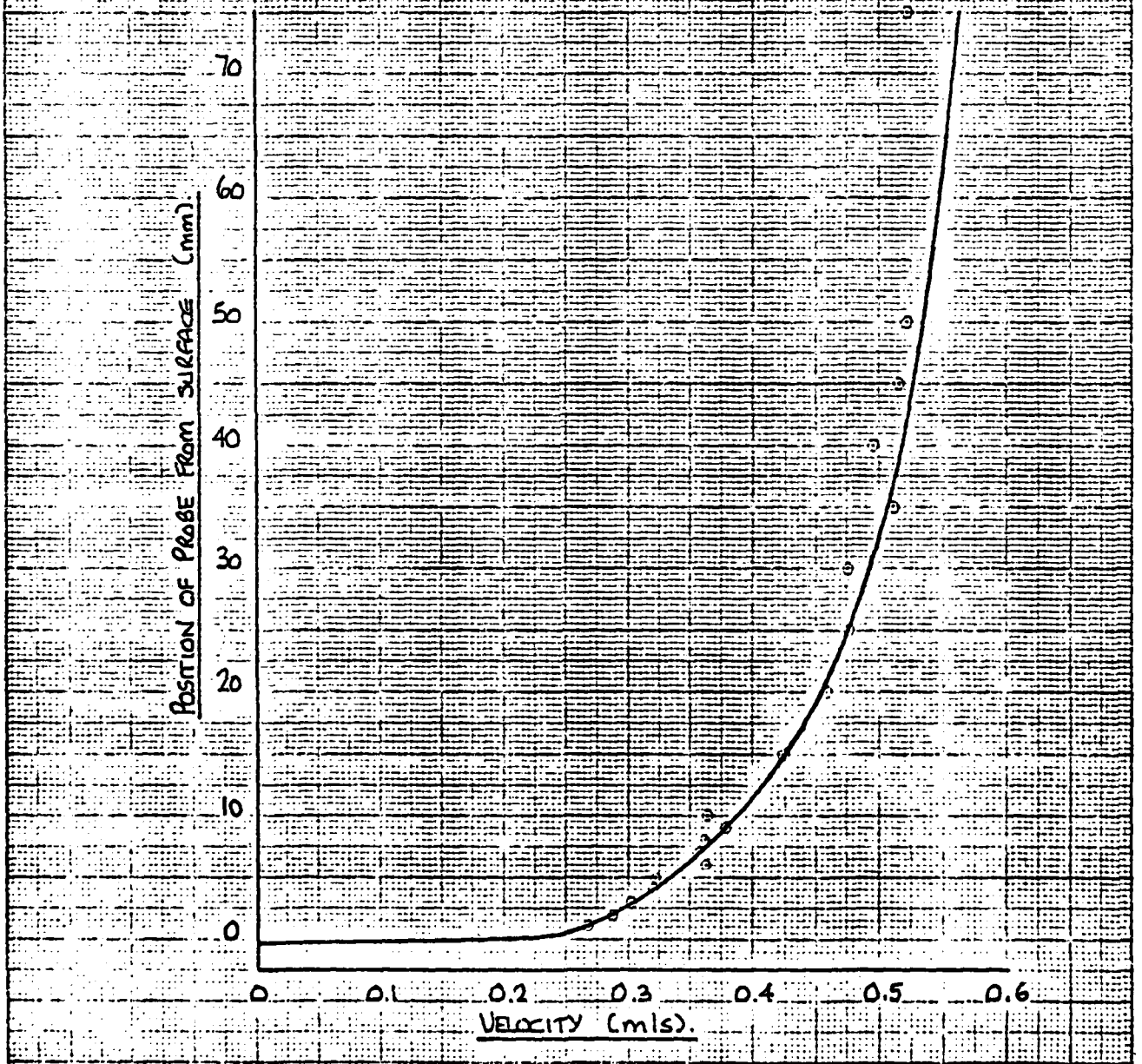

GRAPH OF POSITION OF PROBE ABOVE SURFACE Vs FLOW VELOCITY.
PROBE TRAVERSE (2.3) POSITION FROM LEADING EDGE 6 Ft.

FIG C6.

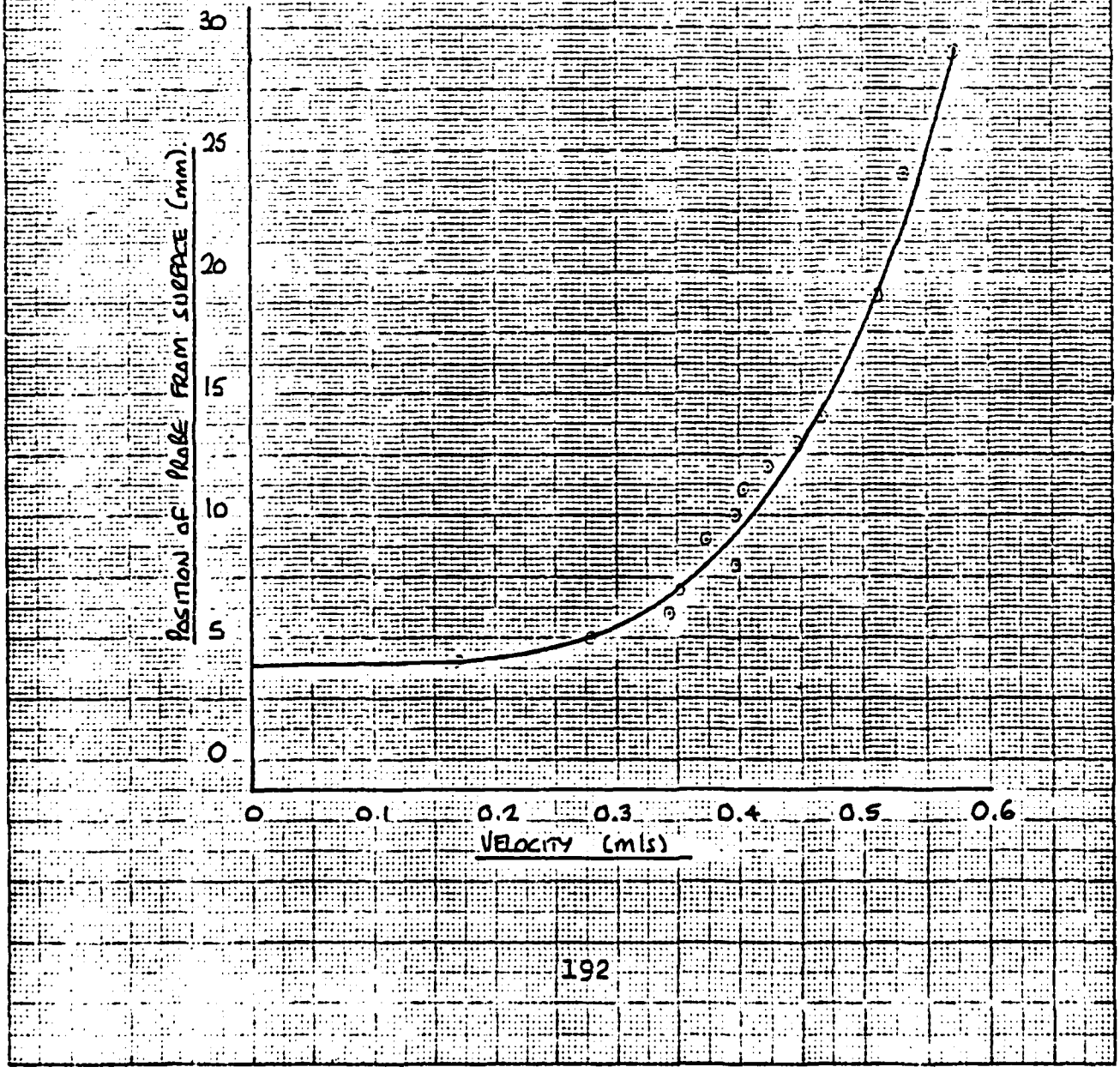

APPENDIX D

PROPELLOR TYPE CURRENT METER.

CROSS CHANNEL VELOCITY MEASUREMENTS.

FLOW DIRECTION ——●

POSITION FROM LEADING EDGE 2 Ft.

TOTAL DISTANCE ALONG CHANNEL 11 Ft 6 ins.

DALL TUBE VERTICAL MANOMETER READING (Ft)	DEPTH OF PROPELLOR (mm)	POSITION OF PROPELLOR ACROSS CHANNEL (mm)	PERIOD OF TEST (sec)	TOTAL REVS/ TEST	REVS PER SEC (n)	VELOCITY USING EQUATION (3.2) (m/s)
3	100	80	60	242	4.04	0.4324
		60	60	248	4.14	0.4426
		40	60	249	4.15	0.4443
		20	60	250	4.17	0.4460
		C/L	60	249	4.15	0.4443
		20	60	249	4.15	0.4443
		40	60	248	4.14	0.4426
		60	60	248	4.14	0.4426
		80	60	234	3.90	0.4188
7	120	100	60	296	4.94	0.5243
		80	60	310	5.17	0.5481
		60	60	320	5.34	0.5651
		40	60	320	5.34	0.5651
		20	60	322	5.37	0.5685
		C/L	60	320	5.34	0.5651
		20	60	321	5.35	0.5668
		40	60	320	5.34	0.5651
		60	60	320	5.34	0.5651
		80	60	309	5.15	0.5464
		100	60	296	4.94	0.5243
10	120	100	60	328	5.47	0.5789
		80	60	343	5.72	0.6043
		60	60	352	5.87	0.6196
		40	60	351	5.85	0.6179
		20	60	356	5.94	0.6264
		C/L	60	354	5.90	0.6230
		20	60	356	5.94	0.6264
		40	60	350	5.84	0.6162
		60	60	351	5.85	0.6179
		80	60	344	5.74	0.6060
		100	60	326	5.44	0.5754

TABLE D1.

GRAPH SHOWING PROPELLER TYPE CURRENT METER

CROSS CHANNEL VELOCITY MEASUREMENTS.

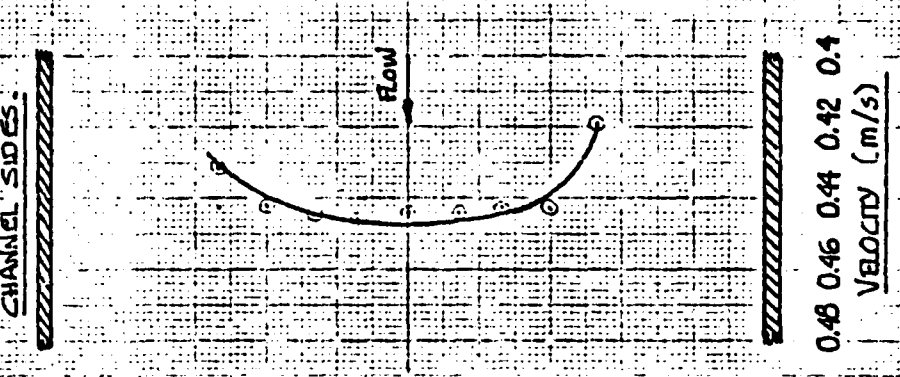

DALL FLOW TUBE VERTICAL MANOMETER READING

3 Ft WATER-ON-MERCURY.

DALL FLOW-TUBE VERTICAL MANOMETER READING

7 Ft WATER-ON-MERCURY.

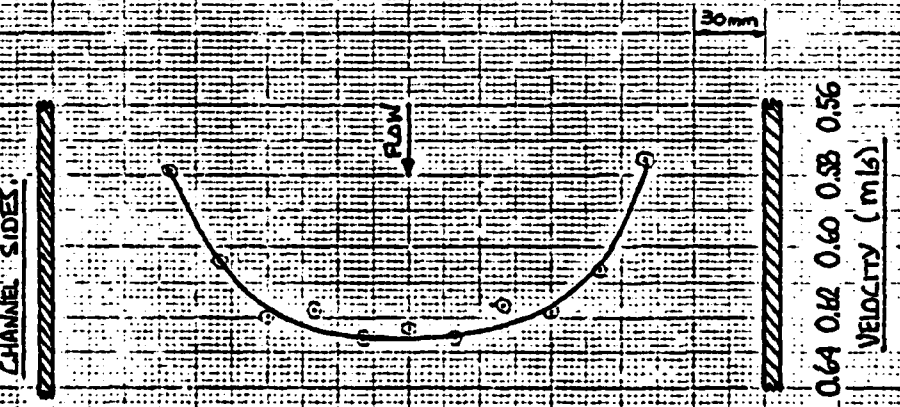

DALL FLOW TUBE VERTICAL MANOMETER READING

10 Ft WATER-ON-MERCURY.

FIG D1.

APPENDIX E

VELOCITIES OBTAINED FROM PROFILE FOR PROBE TRAVERSE

(2.1) FIG. C3 APPENDIX C.

U = 0.565 m/s			δ = 52 mm.		
DISTANCE FROM SURFACE y (mm)	VELOCITY FROM PROFILE u (m/s)	$\frac{u}{U}$	$\log_e(y)$	$(y/\delta)^{\frac{1}{5}}$	$(y/\delta)^{\frac{1}{4}}$
0	0.150	0.266	$-\infty$	0.000	-
1	0.258	0.457	0.000	0.454	-
2	0.294	0.520	0.693	0.521	-
3	0.317	0.561	1.099	0.565	-
4	0.335	0.593	1.386	0.598	-
5	0.350	0.619	1.609	0.626	-
6	0.362	0.641	1.792	0.679	-
7	0.375	0.664	1.946	0.669	-
8	0.385	0.681	2.079	0.687	-
9	0.395	0.699	2.197	0.704	-
10	0.404	0.715	2.303	0.719	-
15	0.438	0.775	2.708	0.779	-
20	0.465	0.823	2.996	0.826	-
25	0.486	0.860	3.219	0.863	-
30	0.504	0.892	3.401	0.895	-
35	0.519	0.919	3.555	0.923	-
40	0.533	0.943	3.689	0.948	-
45	0.543	0.961	3.807	0.971	0.964
50	0.550	0.973	3.912	0.992	0.990
52	0.554	0.980	3.951	1.000	-

TABLE E1.

VELOCITIES OBTAINED FROM PROFILE FOR PROBE TRAVERSE

(2.2) FIG. C5 APPENDIX C.

U = 0.565 m/s				δ = 65 mm.		
DISTANCE FROM SURFACE y (mm)	VELOCITY FROM PROFILE u (m/s)	$\frac{u}{U}$	$\log_e(y)$	$(y/\delta)^{\frac{1}{8}}$	$(y/\delta)^{\frac{1}{10}}$	$(y/\delta)^{\frac{1}{7}}$
0	0.179	0.316	$-\infty$	0.000	-	-
1	0.268	0.474	0.000	0.434	0.474	-
2	0.286	0.506	0.693	0.498	-	-
3	0.304	0.538	1.099	0.540	-	-
4	0.321	0.568	1.386	0.573	-	-
5	0.335	0.593	1.609	0.598	-	-
6	0.349	0.618	1.792	0.620	-	-
7	0.358	0.634	1.946	0.640	-	-
8	0.369	0.653	2.079	0.657	-	-
9	0.380	0.673	2.197	0.673	-	-
10	0.387	0.685	2.303	0.687	-	-
15	0.425	0.752	2.708	0.746	-	-
20	0.454	0.804	2.996	0.790	0.810	-
25	0.476	0.842	3.219	0.826	0.843	-
30	0.492	0.870	3.401	0.857	0.871	-
35	0.506	0.896	3.555	0.884	0.896	-
40	0.517	0.915	3.689	0.908	0.916	-
45	0.526	0.930	3.807	0.929	-	-
50	0.535	0.947	3.912	0.948	-	-
55	0.540	0.956	4.007	0.967	-	0.959
60	0.548	0.970	4.094	0.984	-	0.980
65	0.554	0.980	4.174	1.000	-	-

TABLE E2.

GRAPH OF VELOCITY Vs $\log_e(y)$ SHOWING

LOGARITHMIC INNER-LAW REGION

PROBE TRAVERSE (2.1)

FIG E1.

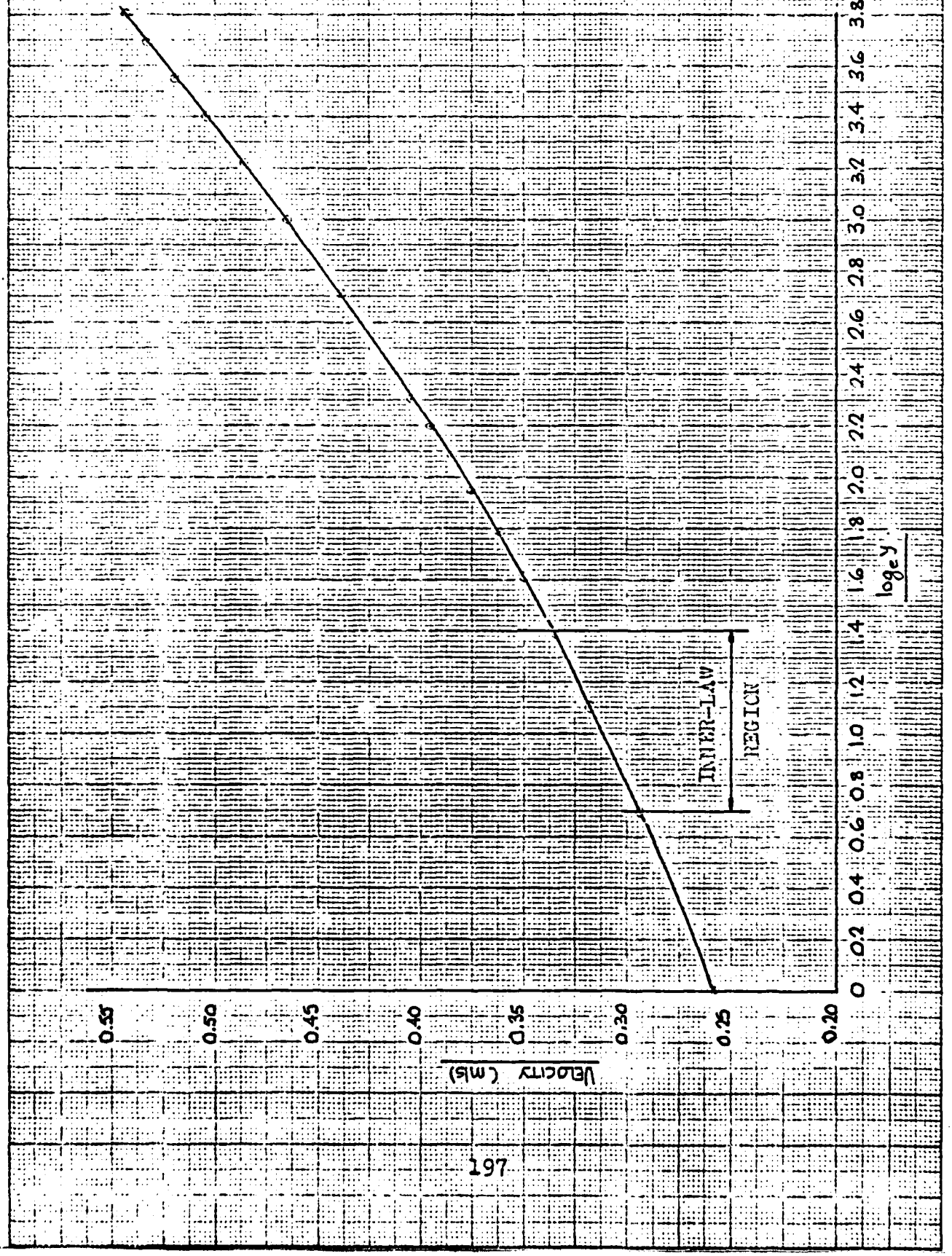

GRAPH OF VELOCITY Vs $\log_e(y)$ SHOWING
LOGARITHMIC INNER-LAW REGION
PROBE TRAVERSE (2.2)
FIG E2.

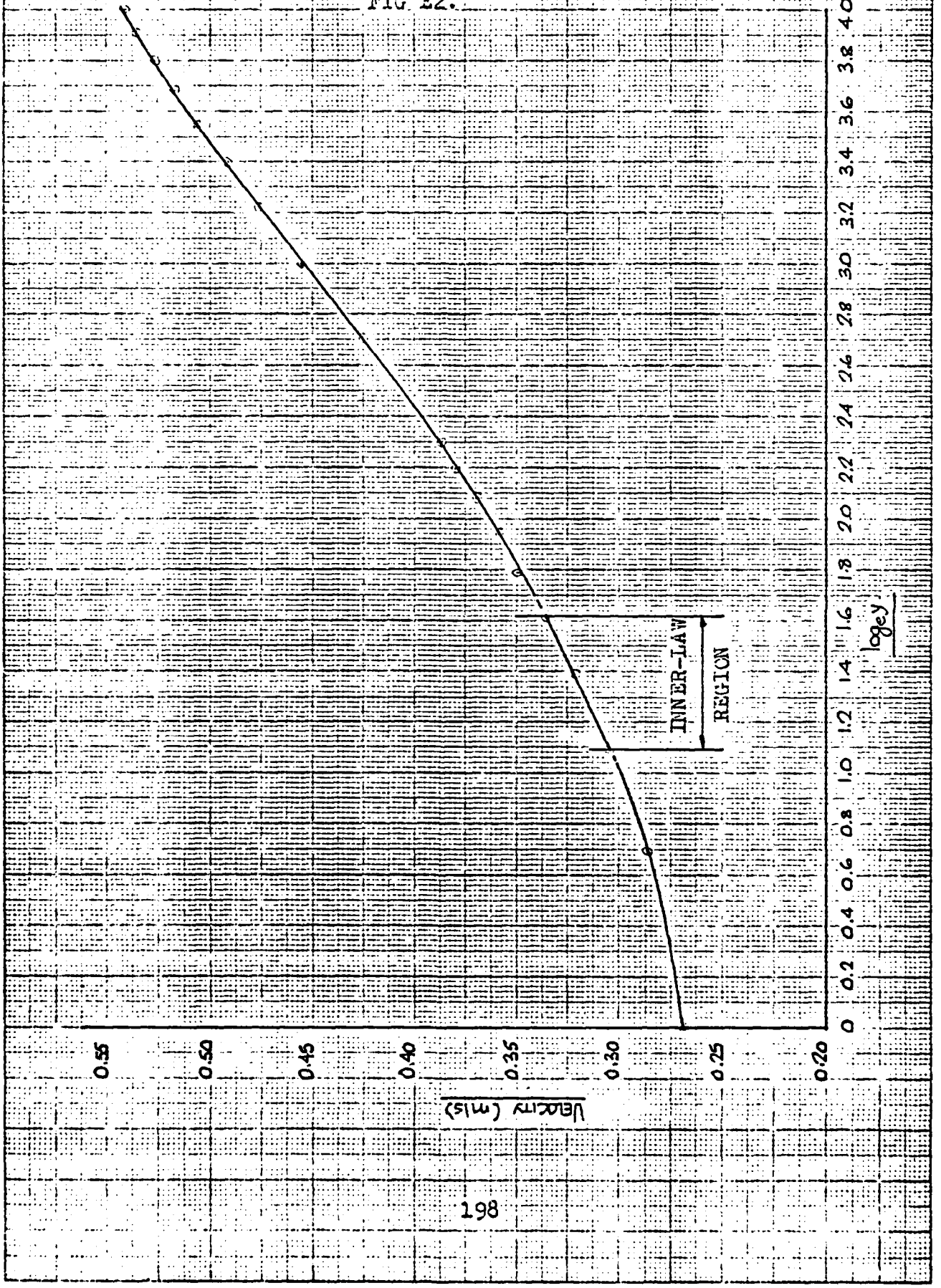

PROBE TRAVERSE (2.1).

INNER LAW REGION 2,3 and 4 mm.

$u_\circ$ (m/s)	Distance y (mm)	u (m/s)	$\frac{u}{u_\circ}$	$(yu_\circ/\nu)$	log $(yu_\circ/\nu)$
0.020	2	0.294	14.700	30.769	3.426
	3	0.317	15.850	46.153	3.832
	4	0.335	16.750	61.538	4.129
0.021	2	0.294	14.000	32.308	3.475
	3	0.317	15.095	48.462	3.881
	4	0.335	15.952	64.615	4.169
0.022	2	0.294	13.364	33.846	3.522
	3	0.317	14.409	50.769	3.927
	4	0.335	15.227	67.692	4.215
0.023	2	0.294	12.783	35.385	3.566
	3	0.317	13.783	53.077	3.972
	4	0.335	14.565	70.769	4.259
0.024	2	0.294	12.250	36.923	3.609
	3	0.317	13.208	55.385	4.014
	4	0.335	13.958	73.846	4.302
0.025	2	0.294	11.760	38.462	3.649
	3	0.317	12.680	57.692	4.055
	4	0.335	13.400	76.923	4.343
0.026	2	0.294	11.308	40.000	3.689
	3	0.317	12.192	60.000	4.094
	4	0.335	12.885	80.000	4.382

TABLE E3.

PROBE TRAVERSE (2.2).

INNER LAW REGION 3,4 and 5 mm.

u_o (m/s)	Distance y (mm)	u (m/s)	$\frac{u}{u_o}$	(yu_o/ν)	log (yu_o/ν)
0.021	3	0.304	14.476	48.462	3.881
	4	0.321	15.286	64.616	4.168
	5	0.335	15.952	80.769	4.392
0.022	3	0.304	13.818	50.769	3.927
	4	0.321	14.591	67.692	4.215
	5	0.335	15.227	84.615	4.438
0.023	3	0.304	13.217	53.077	3.972
	4	0.321	13.957	70.769	4.259
	5	0.335	14.565	88.462	4.483
0.024	3	0.304	12.667	55.385	4.014
	4	0.321	13.375	73.846	4.302
	5	0.335	13.958	92.308	4.525
0.025	3	0.304	12.160	57.692	4.055
	4	0.321	12.840	76.923	4.343
	5	0.335	13.400	96.154	4.566
0.026	3	0.304	11.692	60.000	4.094
	4	0.321	12.346	80.000	4.382
	5	0.335	12.885	100.000	4.605
0.027	3	0.304	11.259	62.308	4.132
	4	0.321	11.889	83.077	4.419
	5	0.335	12.407	103.846	4.643

TABLE E4.

GRAPH OF u/u_o Vs $\log_e(yu_o/\nu)$

PROBE TRAVERSE (2:1)

FIG E3.

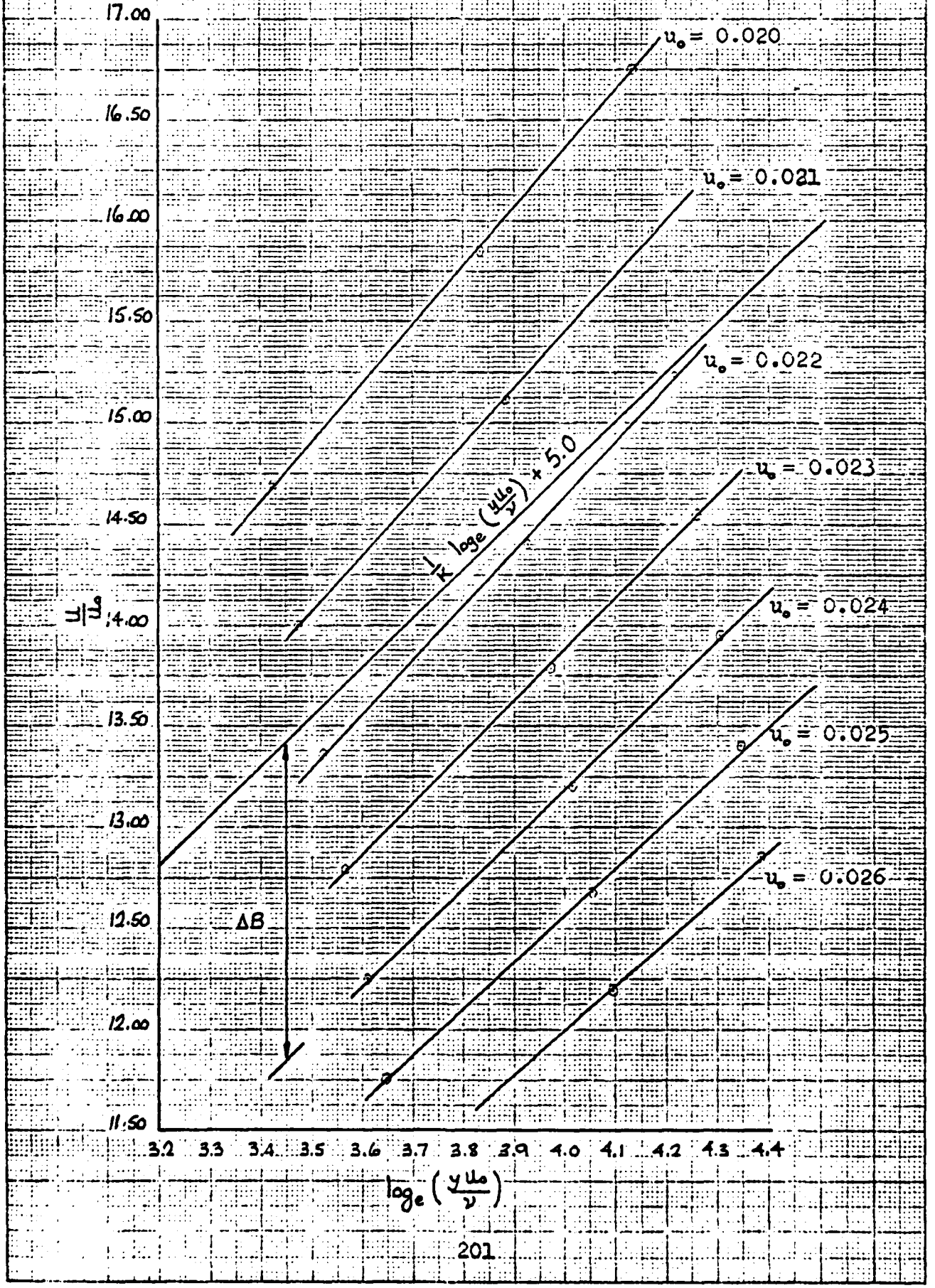

GRAPH OF u/u_o Vs $\log_e (yu_o/\nu)$

PROBE TRAVERSE (2.2)

FIG E4.

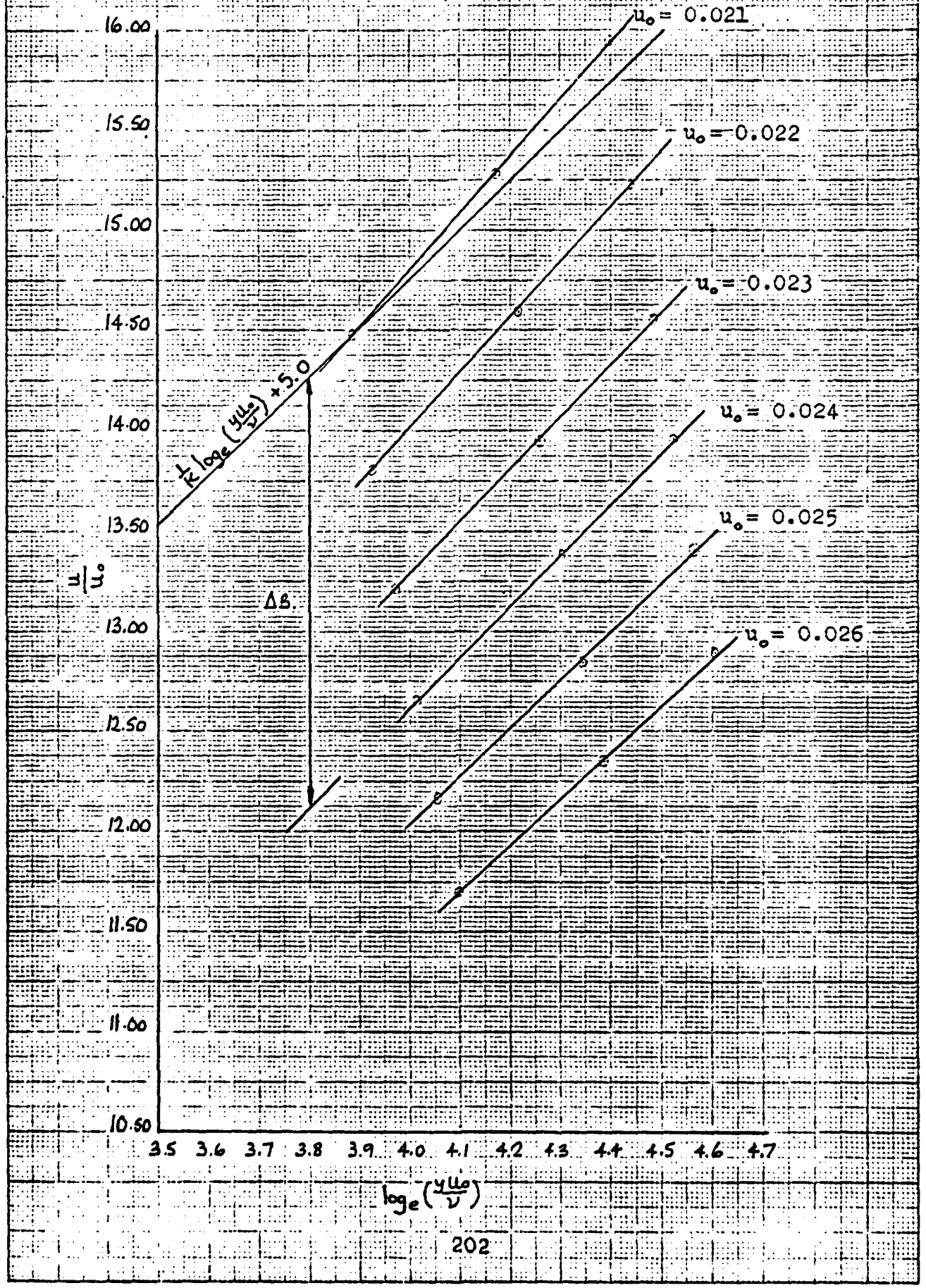

PROBE TRAVERSE (2.1).

Distance y (mm)	u_o = 0.022		u_o = 0.024		u_o = 0.026	
	$\frac{u}{u_o}$	$\log_e(\frac{yu_o}{\nu})$	$\frac{u}{u_o}$	$\log_e(\frac{yu_o}{\nu})$	$\frac{u}{u_o}$	$\log_e(\frac{yu_o}{\nu})$
1	11.727	2.829	10.750	2.916	9.923	2.996
2	13.364	3.522	12.250	3.609	11.308	3.689
3	14.409	3.927	13.208	4.014	12.192	4.094
4	15.227	4.215	13.958	4.302	12.885	4.382
5	15.909	4.438	14.583	4.525	13.462	4.605
6	16.455	4.621	15.083	4.708	13.923	4.787
7	17.045	4.775	15.625	4.862	14.423	4.942
8	17.500	4.908	16.042	4.995	14.808	5.075
9	17.955	5.026	16.458	5.113	15.192	5.193
10	18.364	5.131	16.833	5.218	15.538	5.298
15	19.909	5.537	18.250	5.624	16.846	5.704
20	21.136	5.825	19.375	5.911	17.885	5.991
25	22.091	6.048	20.250	6.135	18.692	6.215
30	22.909	6.230	21.000	6.317	19.385	6.397
35	23.591	6.384	21.625	6.471	19.962	6.551
40	24.227	6.518	22.208	6.605	20.500	6.685
45	24.682	6.635	22.625	6.722	20.885	6.803
50	25.000	6.741	22.917	6.828	21.154	6.908

TABLE E5.

PROBE TRAVERSE (2.2).

Distance y (mm)	u_o = 0.022		u_o = 0.024		u_o = 0.026	
	$\frac{u}{u_o}$	$\log_e(\frac{yu_o}{\nu})$	$\frac{u}{u_o}$	$\log_e(\frac{yu_o}{\nu})$	$\frac{u}{u_o}$	$\log_e(\frac{yu_o}{\nu})$
1	12.182	2.829	11.167	2.916	10.308	2.996
2	13.000	3.522	11.917	3.609	11.000	3.689
3	13.818	3.927	12.667	4.014	11.692	4.094
4	14.591	4.215	13.375	4.302	12.346	4.382
5	15.228	4.438	13.959	4.525	12.885	4.605
6	15.864	4.621	14.542	4.708	13.423	4.788
7	16.273	4.775	14.917	4.862	13.769	4.942
8	16.773	4.908	15.375	4.995	14.192	5.075
9	17.273	5.026	15.833	5.113	14.616	5.193
10	17.591	5.131	16.125	5.218	14.885	5.298
15	19.318	5.537	17.708	5.624	16.346	5.704
20	20.636	5.825	18.917	5.911	17.462	5.991
25	21.636	6.048	19.833	6.135	18.308	6.215
30	22.364	6.230	20.500	6.317	18.923	6.397
35	23.000	6.384	21.083	6.471	19.462	6.551
40	23.500	6.518	21.542	6.605	19.885	6.685
45	23.909	6.635	21.917	6.722	20.231	6.802
50	24.318	6.741	22.292	6.828	20.577	6.908
55	24.546	6.836	22.500	6.923	20.769	7.003
60	24.909	6.923	22.833	7.010	21.077	7.090

TABLE E6.

GRAPH OF u/u_o Vs $\log_e(yu_o/\nu)$ FOR DIFFERENT VALUES OF u_o.

PROBE TRAVERSE (2.1)

FIG E5.

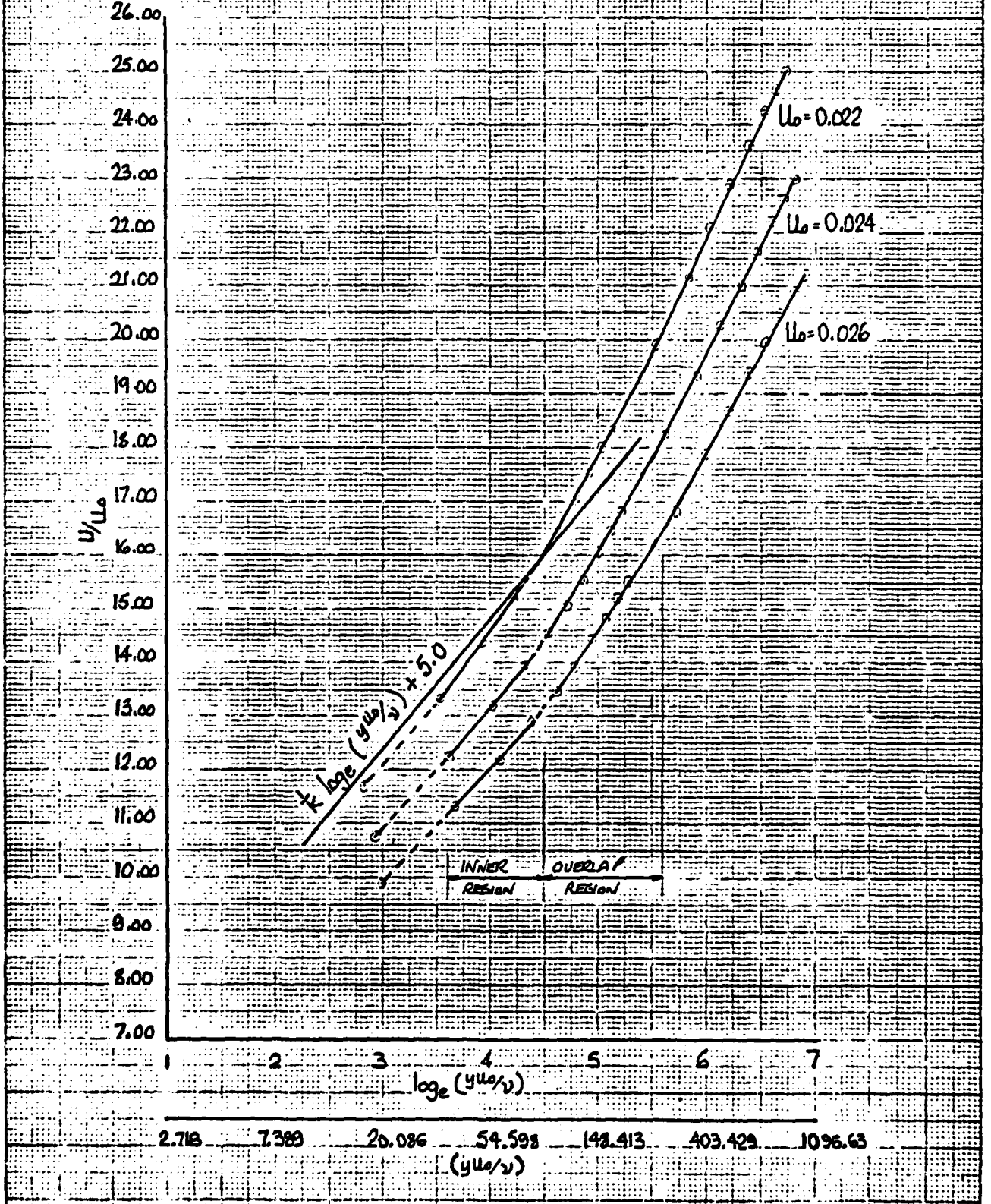

GRAPH OF u/u_o Vs $\log_e(yu_o/\nu)$ FOR DIFFERENT VALUES OF u_o.

PROBE TRAVERSE (2.2)

FIG E6.

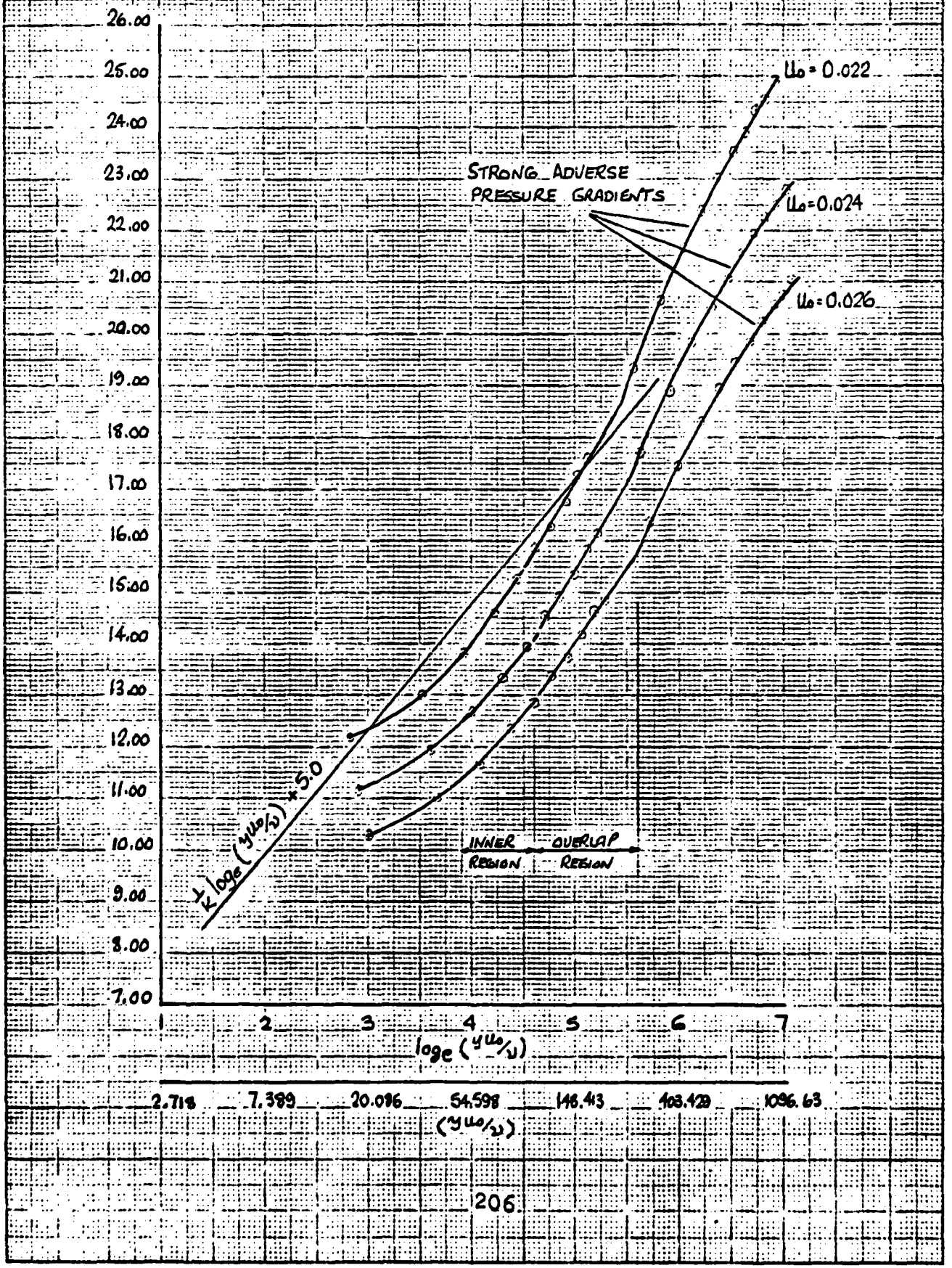

APPENDIX F

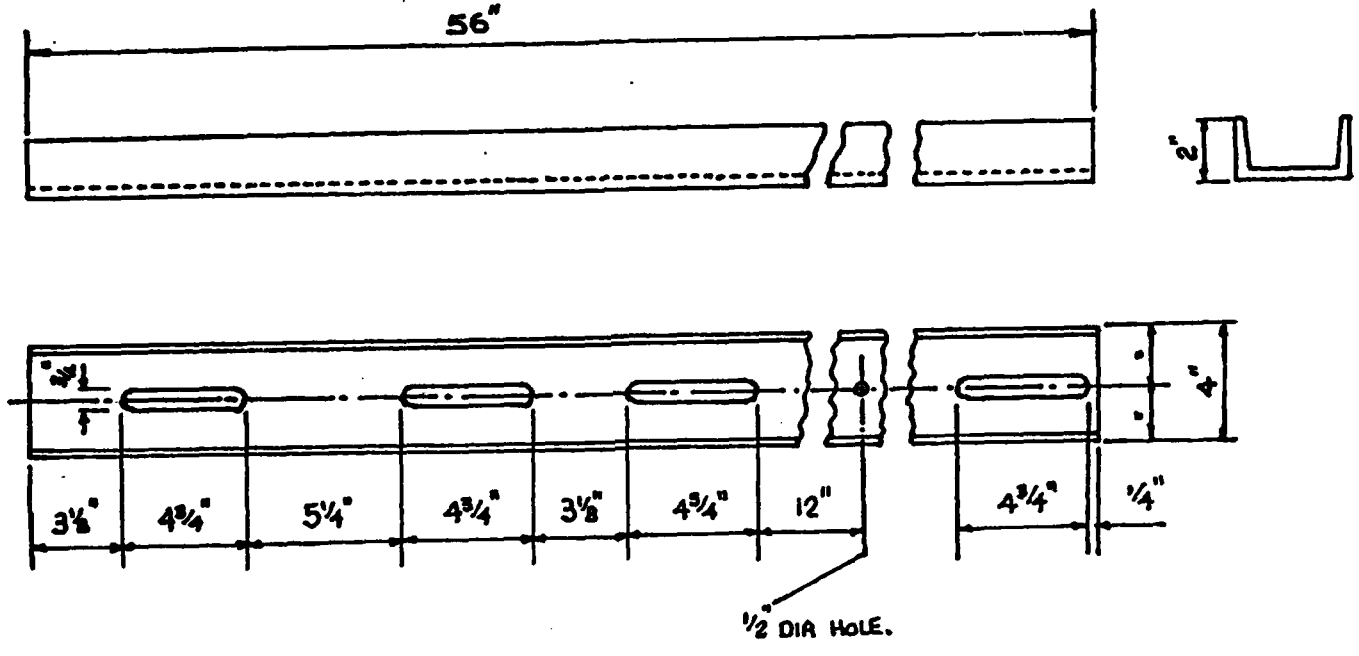

MAIN SUPPORT.

No REQ'D. 1.
Scale 4mm = 1"
MATERIAL MILD STEEL.

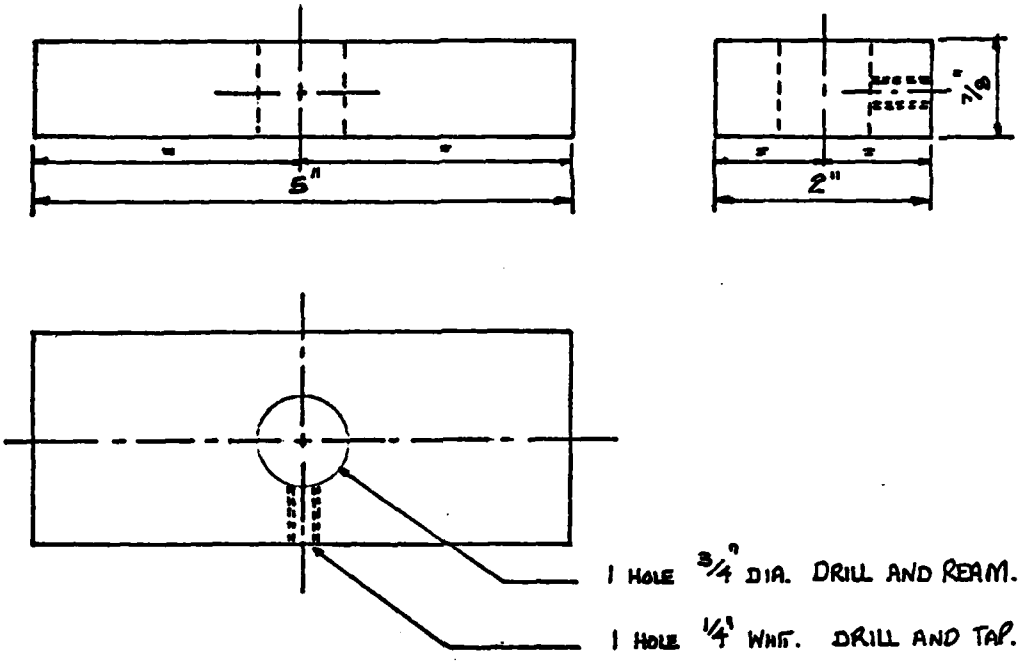

SLIDING SUPPORTS.

No REQ.D 3.
SCALE 15mm = 1"
MATERIAL MILD STEEL.

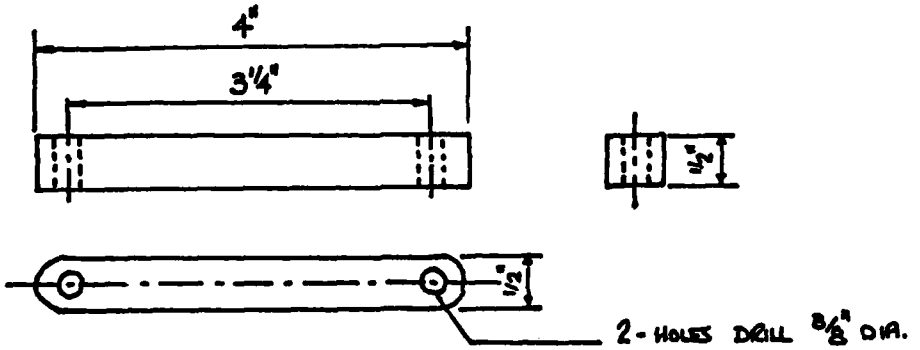

ADJUSTMENT BAR.

No REQ.D 1.
SCALE 15mm = 1"
MATERIAL ALUMINIUM.

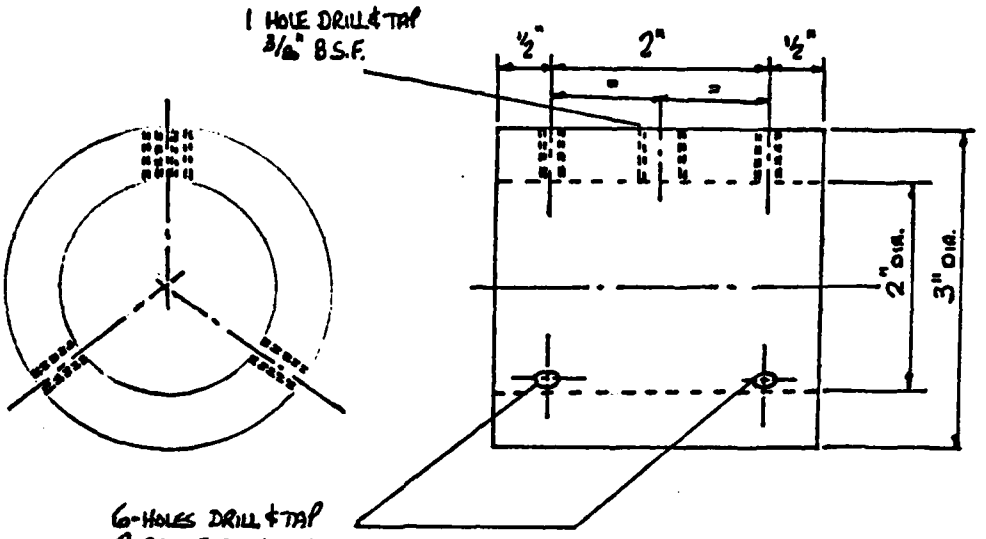

No REQ.D 1.
SCALE 15mm = 1"
MATERIAL ALUMINIUM.

LASER BARREL SUPPORT.

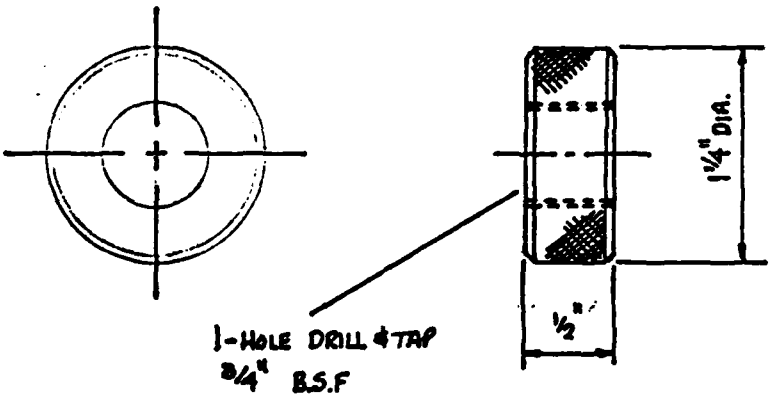

No REQ.D 6
SCALE 24mm = 1"
MATERIAL BRASS.

CLAMPING NUTS.

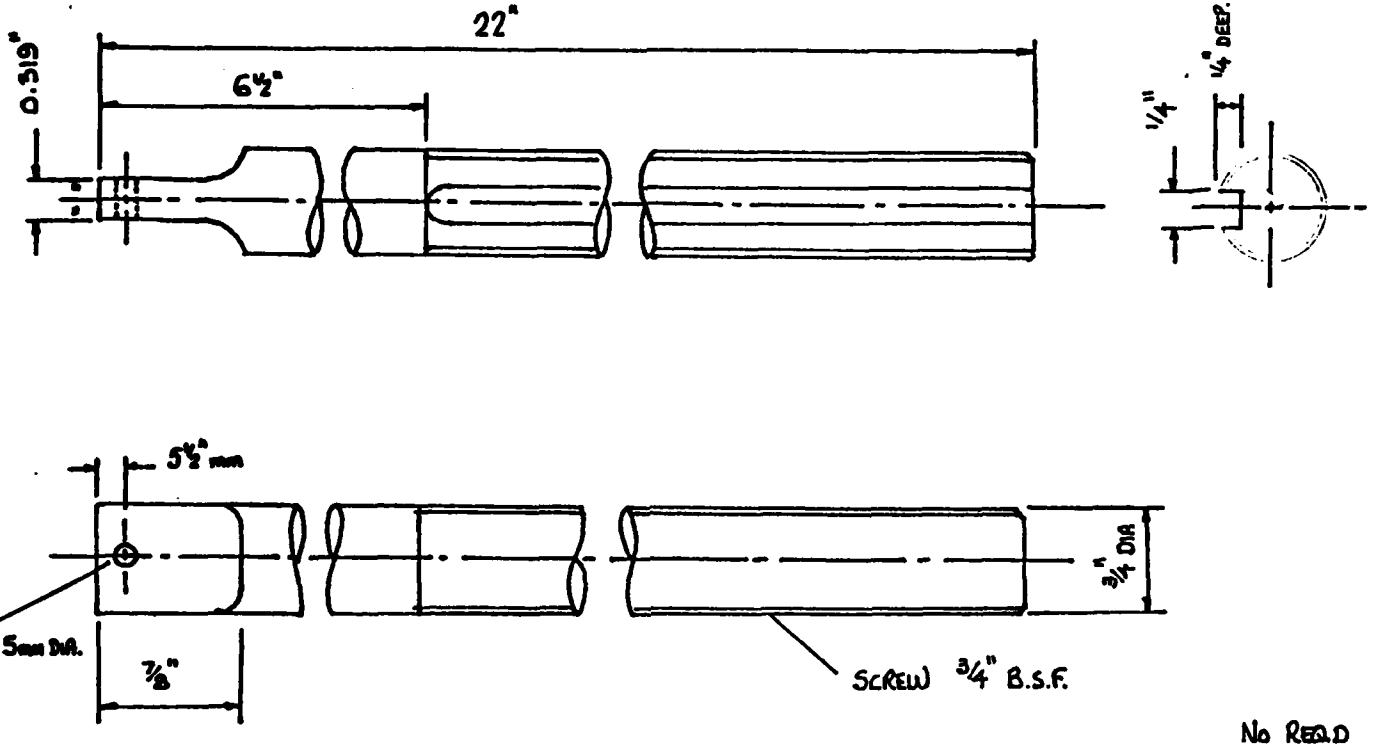

PHOTOMULTIPLIER ADJUSTING BAR.

No REQ'D 1.
SCALE 20mm = 1"
MATERIAL BRASS.

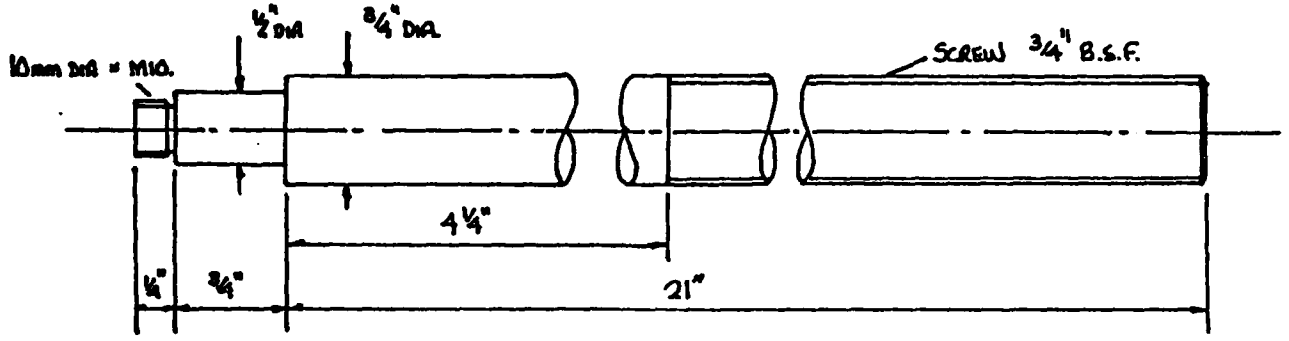

NO REQ.D. 1.
SCALE 20mm = 1"
MATERIAL BRASS.

OPTICAL UNIT ADJUSTING BAR.

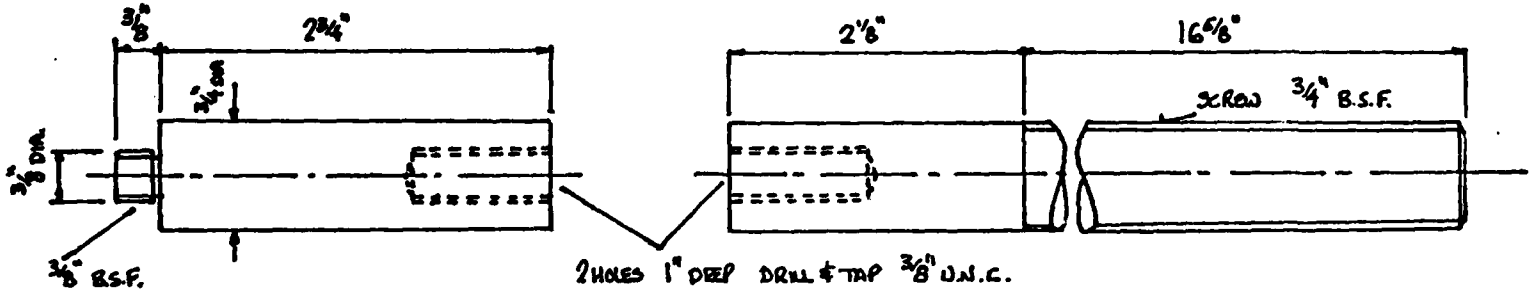

NO REQ.D 1 EACH
SCALE 20mm = 1"
MATERIAL BRASS.

LASER ADJUSTING BAR.

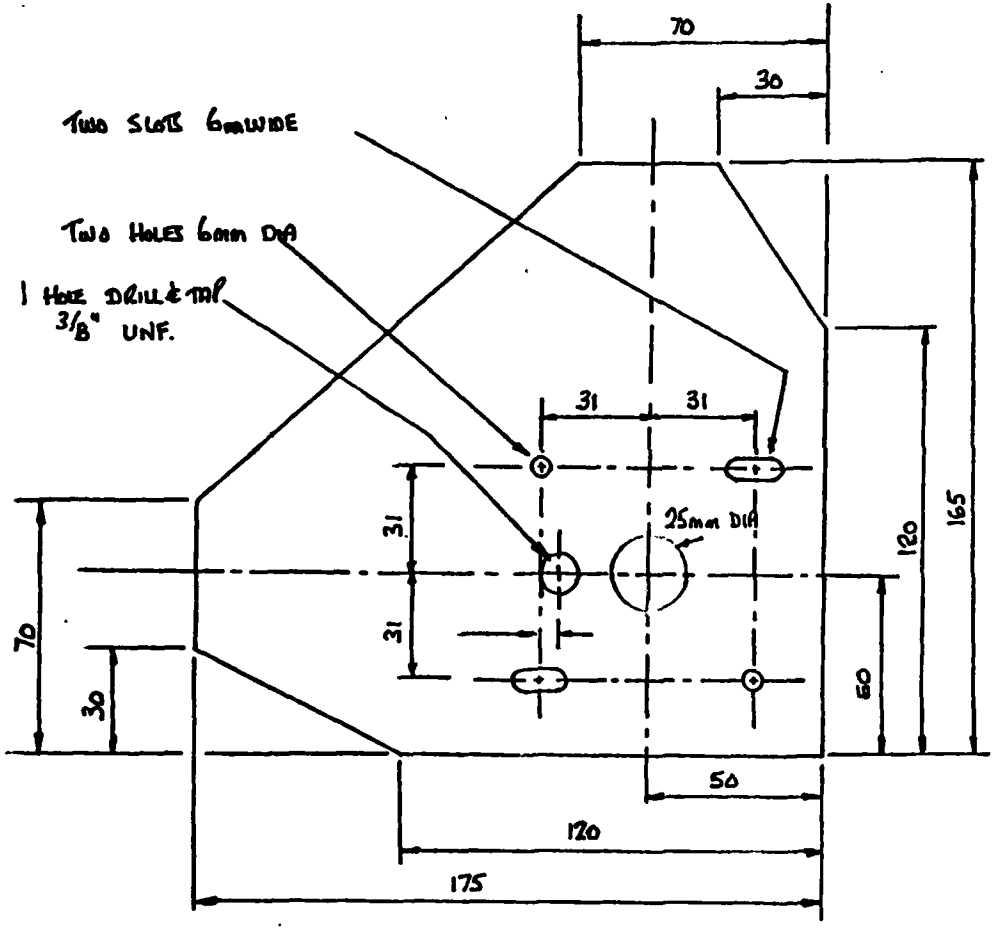

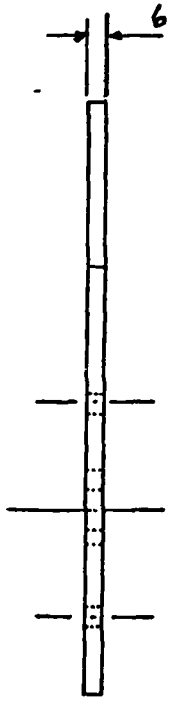

BACK PLATE.

N° REQUIRED 1

MATERIAL ALUMINIUM.

SCALE : 1 : 2

ALL DIMENSIONS mm UNLESS OTHERWISE STATED.

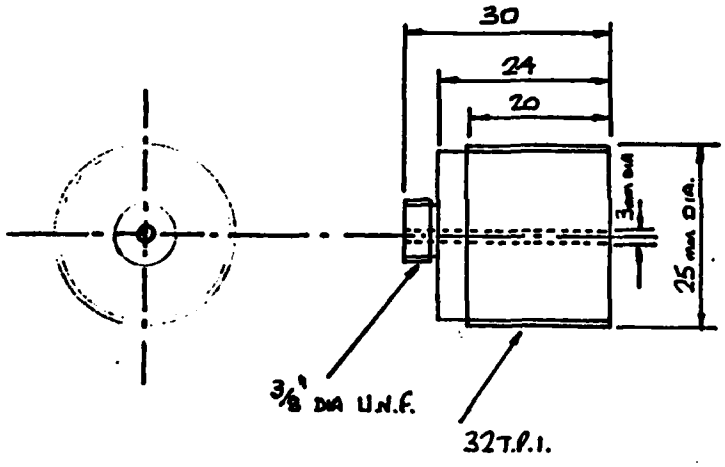

1 REQUIRED.
MATERIAL BRASS.
SCALE:- FULL SIZE.

ADAPTER.

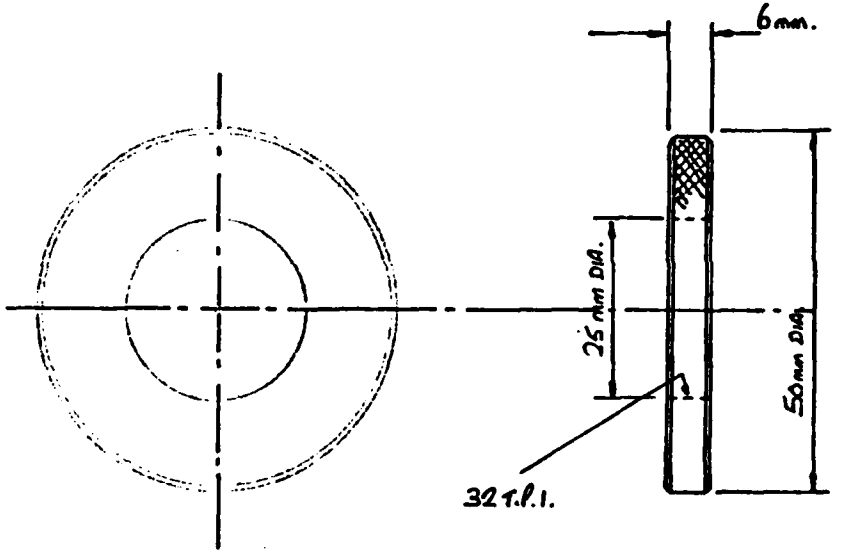

1 REQUIRED.
MATERIAL ALUMINIUM.
SCALE :- FULL SIZE.

LOCKING RING.

APPENDIX G

REFERENCES

1 Massey, B.S. Mechanics of Fluids, 2nd Edition, 1972, Van Nostrand Reinhold.

2 Binder, R.C. Advanced Fluid Mechanics, Volume 1 and 2, 1958, Prentice Hall Incorporated.

3 White, F.M. Viscous Fluid Flow, 1974, McGraw Hill Book Company.

4 Peerless, S.J. Basic Fluid Mechanics, 1967, Pergamon Press.

5 Francis, J.R.D. Fluid Mechanics, 1958, Edward Arnold Ltd.

6 Knudsen, J.G. and Katz, D.L. Fluid Dynamics and Heat Transfer, 1958, McGraw Hill Book Co.

7 Durst, F., Melling, A. and Whitelaw J.H. Journal of Fluid Mechanics, 1972, Vol. 56, Pg. 143, 160.

8 Angus, J.C., Morrow, D.L., Dunning, J.W. and French, M.J. Industrial and Engineering Chemistry, 1969, Vol 61, No.2, Pg. 9, 20.

9 Bedi, P.S. Journal of Physics E, 1971, Vol. 4, Pg. 27, 28.

10 Adrian, R.J. and Goldstein, R.J. Journal of Physics E, 1971, Vol. 4, Pg. 505, 511.

11 Forrester, A.T., Parkins, W.E. and Gerjuoy, E. ibid 72, 728 (1947)

12 Gerjuoy, E., Forrester, A.A. and Parkins, W.E. Physics, Rev. 73, 922 (1948)

13 Yeh, Y. and Cummins, H.Z. Applied Phys. Lett 4. 176 (1964)

14 Foreman, J.W.Jr., George, E.W. and Lewis, R.D. Applied Phys. Lett. 7.77 (1965)

15 Foreman, J.W.Jr., Lewis, R.D., Thornton, J.R. and Watson, H.J. Proc. IEEE, 54,424 (1966)

16 Goldstein, R.J. and Hagen, W.F. Physics. Fluids, 10,1349 (1967)

17 Goldstein, R.J. and Kreid, d.k. Trans ASME, Ser. E, J. Appl. Mech., 34, 813 (1967)

18 Blake, K.A. and Jesperser, K.J. NEL Report 510 (1972)

19 Disa Instruction Manual, Type 55L LDA, Sept. 1973.

20 Disa Instruction Manual, Type 55M10, Aug. 1977.

21 Disa Instruction Manual, Type 55L02, Dec. 1973.

22 Musker, A.J. Roughness Group Meeting at Newcastle University. March 1979.

23 Lewkowicz, A.K., Musker, A.J. The Surface Roughness and Turbulent Wall Friction on Ships-Hulls Interaction in the Viscous Sublayer SSRA (1978).

24 Kreyszig, E. Advanced Engineering Mathematics, Third Edition, 1972, Wiley International Edition.

25 Leicester University, Dept. Mechanical Engineering.